BIOPHYSICAL INSIGHTS INTO THE TRANSPORT PROPERTIES OF LYSENIN

CHANNELS

by

Andrew Merlin Bogard

A dissertation

submitted in partial fulfillment

of the requirements for the degree of

Doctor of Philosophy in Biomolecular Sciences

Boise State University

May 2022

BOISE STATE UNIVERSITY GRADUATE COLLEGE

DEFENSE COMMITTEE AND FINAL READING APPROVALS

of the dissertation submitted by

Andrew Merlin Bogard

Dissertation Title: Biophysical Insights into the Transport Properties of Lysenin Channels

Date of Final Oral Examination: 05 April 2022

The following individuals read and discussed the dissertation submitted by student Andrew Merlin Bogard, and they evaluated the student's presentation and response to questions during the final oral examination. They found that the student passed the final oral examination.

Daniel Fologea, Ph.D.   Chair, Supervisory Committee

Denise Wingett, Ph.D.   Member, Supervisory Committee

Matthew Ferguson, Ph.D.   Member, Supervisory Committee

The final reading approval of the dissertation was granted by Daniel Fologea, Ph.D., Chair of the Supervisory Committee. The dissertation was approved by the Graduate College.

DEDICATION

To my Father, Charles, for showing me the world is interesting; my Mother, Felicia, for showing me people are interesting; my Wife, Shanae, for showing me I am interesting; my Friends, for showing me being alive is interesting; my Mentor, Daniel, for showing me that being interested is joy; and my Daughter, Kia, for reminding me it's not all about me.

ACKNOWLEDGMENTS

Thank you to the Biomolecular Sciences program for the funded opportunity to learn science. I appreciate all your efforts, even those I did not take advantage of. The research presented in this dissertation was also funded by the National Science Foundation (grant number 1554166). I'd like to give a special thanks to Beth Gee and Denise Wingett for their efforts in providing and protecting my experience and those of our other students; their work, without a doubt, is likely harder and less appreciated than any of us know.

More specifically, I'd like to say thank you so much to the current and former Fologea Lab members; each of you is special to me, and without you I am diminished. Every member I've met has helped me make it here, either through friendship and support or through parallel journeys. Regardless of our relationship, this work could not exist without you. I'd like to express particular gratitude to Gamid Abatchev for being an intellectual foil and a friend, and to Rosey Whiting for being a kindred spirit when it was critical to have one. I'd also like to express a deep gratitude to Sheenah Bryant for providing her time and an affordable place to live.

Finally, I'd like to express very profound gratitude to Daniel Fologea. No one, aside from my blood and marriage family, has ever given me more than you have. I will always try to live up to your example and be someone you would respect. For my feelings here, words cannot suffice.

ABSTRACT

The defense work focused on deciphering novel functionalities of lysenin

channels with respect to adjustment of their regulation and transport properties in

response to environmental changes. Lysenin is a pore-forming toxin extracted from the

earthworm E. fetida, which self-assembles into large pores in artificial and natural lipid

membranes containing sphingomyelin. Prior investigations on their functionality

identified strong regulation by voltage and ligands as fundamental traits of lysenin,

similar to ion channels. In addition, stochastic sensing, controlled switching, and

hysteretic conductance have been added to the list of intricate biophysical properties of

lysenin channels as potential enablers of biotechnological and biomedical applications.

Our work employed electrophysiological measurements of lysenin's biophysical activity

in various environmental conditions. The first important feature we discovered is the

unusual selectivity of lysenin channels for monovalent anions and cations, which is

uncommon for pore-forming toxins. In the same line, we exploited the ability of divalent

cations to force the lysenin channels into a stable sub-conducting state and assessed how

such conformational changes modulate their selectivity. Experimental and theoretical

approaches indicated that sub-conductance is accompanied by a substantial loss of

selectivity, leading to the dissipation of the electrical gradients. Next, our work focused

on investigating the influence of Cu^{2+} ions on the functionality of lysenin channels. The

major finding of these experiments is that Cu^{2+} addition influences the hysteretic

conductance to such an extent that lysenin behaves like a memory molecule capable of

preserving information about its immediate history in the absence of any applied voltage. Also, we identified that addition of Cu^{2+} restores the voltage-induced gating of lysenin channels reconstituted in neutral lipid membranes, known to suppress the voltage regulation. In conclusion, our results identified unusual biophysical properties of lysenin channels which may be further exploited not only for understanding novel biological activities of transmembrane transporters but also for potential use in biotechnology, bioengineering, and bioelectronics.

TABLE OF CONTENTS

LIST OF TABLES

LIST OF FIGURES

LIST OF ABBREVIATIONS

α Equilibrium constant of ion-channel binding process

AC   Alternating Current

AFM   Atomic force microscopy

Ang II   Angiotensin II

Aso   Asolectin

ADP   Adenosine diphosphate

AMP   Adenosine monophosphate

ATP   Adenosine triphosphate

b Factor accounting for the linear changes in conductivity upon Me^{2+} addition

BLM   Bilayer lipid membrane

cDNA   Complementary deoxyribonucleic acid

Chol   Cholesterol

c_r Concentration ratio

Cryo-EM   Cryogenic electron microscopy

DC   Direct Current

Diphytanoyl-PC   Diphytanoyl-phosphatidylcholine

DiPhyt-PC   Diphytanoyl-phosphatidylcholine

DNA   Deoxyribonucleic acid

EDTA   Ethylenediaminetetraacetic acid

EGTA   Egtazic acid

F   Faraday's number

f   Ratio of individual channel resistances

f Ratio of individual channel conductances

G   Conductance measured after ion addition

G_0 Conductance recorded at minimal salt concentration

GHK   Goldman-Hodgkin-Katz equation

G_{min} Minimum relative conductance measured at saturation of channel

                binding

G_r Relative conductance

G_r Relative macroscopic conductance of lysenin channels

HEPES   4-(2-hydroxyethyl)-1-piperazineethanesulfonic acid

I   Current

I_B Current blockage

I_D Current blockage

I_r Relative current; I/I_t

I Current through fully open channels

I_t Current through channels after Me^{2+} addition

IC_{50} Concentration of an inhibitor where the binding or response is

                reduced by half

IC_{50} Halfway inhibitory concentration

IV   Current-voltage

I-V   Current-voltage

K	Langmuir constant
K_0	Specific conductivity of bulk solution before Me^{2+} addition
LC-MS	Liquid chromatography-mass spectrometry
Me^{2+}	Divalent metal ion
m/z	Mass-to-charge ratio
N	Total number of open and sub-conducting channels
n	Hill coefficient
n_1	Number of channels in open state
n_2	Number of channels in sub-conducting state
nt	Nucleotides
P	Permeability of ionic species
P_A^-	Permeability of anionic species
PBS	Phosphate-buffered saline
PC	Personal computer
PCR	Polymerase chain reaction
P_C^-	Permeability of cationic species
PEI	Polyethyleneimine
PFT	Pore-forming toxin
Popen	Open probability
PTFE	Polytetrafluoroethylene
R	Universal gas constant
r_1	Resistance of individual open channel
r_2	Resistance of individual sub-conducting channel

R_1	Total resistance of open channels
R_2	Total resistance of sub-conducting channels
SD	Standard deviation
SM	Sphingomyelin
ssDNA	Single-stranded deoxyribonucleic acid
T	Absolute temperature
t_D	Dwell time
T_D	Dwell time
V	Voltage source
V_m	Membrane voltage
x	Purine concentration

CHAPTER ONE: OVERVIEW

The objective of this research work was to explore the functionalities of lysenin channels originating in their transport properties. In this respect, we added a meaningful contribution to understanding their similarities with ion channels regarding selectivity; however, unlike ion channels we discovered that transition to sub-conducting states strongly adjusts their selectivity function. We also obtained novel, exciting evidence regarding their molecular memory which may lead to fruitful development in future bioelectronic applications. While some of these advancements naturally add to previous knowledge of lysenin and its exquisite biophysical features, the novel understanding gained through this work provides context for fundamental physiological insight and applications not achievable by using similar transporters.

In the second chapter, the focus of material reviewed is the ability of lysenin channels inserted into a bilayer lipid membrane to function as sensors for ions and molecules. This ability relies on the large conducting pore allowing high transport rate and translocation of biological macromolecules. It also relies on the channel's regulation and ionic selectivity properties as well as the memory function arising from interactions with those ions. Specifically, ligand- and voltage-gating, conductance changes, and hysteresis arising from channel-lipid interactions are the salient features involved with establishing the function and potential application of lysenin channels in natural and artificial membrane systems.

The exposure of multivalent ions to membrane-inserted lysenin channels in our work leads to a few different endpoints. Divalent ions generally induce a sub-conducting state in lysenin channels. This proceeds through an unknown interaction with the channels and leads to a parabolic decrease and subsequent increase in conductance of the channels (Cu^{2+} is a notable exception and is explored further later). Trivalent ions generally lead to the complete inhibition of conductance upon increasing concentrations and, in the case of Cr^{3+}, display an inhibition implying a cooperative process of ion-channel interaction. In either case we see the interaction between the ions and the channels is a ligand-gating process as evidenced by stepwise current variations, and likewise we found most ions may have their effects reversed by chelation, precipitation, or buffer exchange of the bulk solution.

With the differences in channel regulation varying amongst monovalent, divalent, and trivalent ions in mind, we explored the relationship between ligand-gating effects and ionic charge density. Use of $Fe^{2+/3+}$ cations and organic cations revealed a tendency for lower charge density to induce a sub-conducting state, but that trivalent metal ions usually induce full closure.

It may be useful, however, for lysenin applications to achieve irreversible abolishment of conductance; it was found that Cr^{3+}-induced gating was irreversible even after extended buffer exchange times. Unfortunately, the use of Cr^{3+} is not necessarily suitable for biological applications due to its range of safe concentrations. The use of cationic polymers chitosan and polyethyleneimine, on the other hand, were found to allow irreversible conductance abrogation while also being biologically inert. This allowed, in previous collaborative work, our group to successfully deliver a drug

substitute to adherent and suspended cells while maintaining a high percentage of viability.

With such detail regarding ligand-gating function available, it was logical to explore the connection, if any, between voltage-gating and ligand-gating of lysenin channels. As it is known that lysenin channels do not voltage-gate in neutral lipid bilayers, we found that use of such bilayers still allowed ligand-gating mechanisms to proceed in a qualitatively similar fashion when divalent and trivalent metal cations were employed.

Finally, in the drive to further elucidate biological applicability regarding the channels' regulation properties, our group explored the interaction between purines (i.e., adenosine mono-, di-, and tri-phosphates) and lysenin channels. We found the interaction of purines with channels was a positively cooperative binding process, with a decreasing IC_{50} and increasing Hill coefficient associated with increasing phosphate groups. The electrostatic nature of this binding process was confirmed through ionic screening experiments, but interestingly there was no significant change in Hill coefficient.

As mentioned before, the lysenin channel's large pore lumen allows high transport rate. This size allowed the exploration of biological polymer translocation. It was found that lysenin channels are capable of translocating both the octameric peptide Angiotensin II (Ang II) and 69 nucleotide single-stranded deoxyribonucleic acid (ssDNA) test strands. While sequencing of these polymers was not attempted, examination of the current blockage and dwell times associated with current changes suggested successful translocation. These findings were confirmed by liquid

chromatography/mass spectroscopy (LC-MS) and gel electrophoresis for Ang II and the ssDNA, respectively.

We've seen that lysenin may be used as a sensor for a variety of biologically relevant ions and molecules by adjustment of its ability to conduct. This has manifested through changing conducting states, utilizing and/or modifying gating properties, and transient changes in current. These sensing mechanisms may be further expanded by chemical modifications and amino acid substitutions, but a deeper exploration of existing responses could also provide insight and utility. The remainder of this work drives forward in the direction of the latter, exploring the ionic selectivity, divalent cation responses, and modifiable memory functions of lysenin channels.

In the third chapter, due to the importance of electrochemical gradients in biological functions and previously scant data regarding the selectivity of lysenin channels, our next investigations began with an expansion addressing these topics. As both dynamic and resting membrane potentials are facilitated by ion channels, the study of lysenin as a model may prove fruitful for physiological understanding. In this line, we investigated the selectivity of lysenin channels for monovalent ions in open and Ca^{2+}-induced sub-conducting states.

Regarding monovalent ions, we created transmembrane voltages from asymmetrical concentrations of salt solutions and modeled the results. The model used was the Goldman-Hodgkin-Katz equation, and its use allowed us to show evidence supporting the clear selectivity of lysenin channels. Through the permeability ratios obtained, we found that lysenin possesses both cationic and anionic selectivity, although it is weaker than that found in ion channels.

Previous work regarding the influence of Ca^{2+} and other divalent ions provided results of lysenin channels obtaining stable sub-conducting states. The current work revealed that the sub-conducting state also nearly abolishes the selectivity function. Further than this, we derived a simple equivalent circuit and corresponding mathematical model predicting the magnitude of transmembrane voltage as it depends on Ca^{2+} concentration.

Altogether, this portion of work demonstrates selectivity, transport, and sub-conduction behaviors of lysenin channels which are favorable and relevant to the modeling of and providing insight to ion channel functions (including their poorly understood sub-conduction function), and to the expansion of utility of lysenin in both natural and artificial membrane systems.

In the fourth chapter, we return to the exploration of the unique interaction between lysenin channels and Cu^{2+} ions. Cu^{2+} not only ligand-gates lysenin but also affects the voltage-gating; channel re-opening during descending (positive to negative) voltage ramps is severely inhibited, while closing is enhanced during ascending ramps. This greatly decreases their open probability at identical voltage conditions; consequently, the resulting current hysteresis is also changed. These results draw attention to both the channel populations' general gating behaviors and their specific gating behavior at 0 mV direct current (DC) voltage.

To focus on the effect of Cu^{2+} regarding channel opening and closing, we applied single magnitude step voltages to force-close and re-open the channels outside of ramping voltage sweeps. We found the slow closing and fast reopening characteristic of +60 and -60mV applications, respectively, to qualitatively change upon exposure to Cu^{2+}.

With Cu^{2+} addition, the channels instead close faster and reopen more slowly; this behavior supports the change in hysteresis, even considering lysenin's ligand-gating properties regarding Cu^{2+}.

To investigate the channel population behavior in the presence of Cu^{2+} while at 0 mV DC, we developed, tested, and applied a combination of alternating and direct current (AC/DC) voltage stimulation where the frequency and amplitude of the AC voltage could provide a current signal amplitude proportional to the open state of the channels while not affecting their open/closed state alone. After finding our experimental method did not affect the channels' state without the addition of a DC voltage (similar to results without the AC addition), we used the combination to explore behavior at 0 mV DC. We found that with or without Cu^{2+} addition we may observe the closing and reopening of the channels, hysteretic behavior reflecting Cu^{2+}'s influence, and importantly, more detailed behavior of the channels at 0 mV. Specifically, the results show the channels, in the absence of Cu^{2+}, will reopen such that the current may eventually reach the same value regardless of previous channel state (in line with previous knowledge); however, with the addition of a small amount of Cu^{2+} the channels display behavior leading to hysteretic currents with no applied DC voltage.

Finally, due to the previously observed behavior regarding the enhanced gating of lysenin channels when exposed to Cu^{2+}, we decided to explore the behavior of Cu^{2+}-exposed channels when they are inserted into neutral lipid membranes. Typically, lysenin is inserted into anionic lipid-based membranes (i.e., asolectin) for its experimentations, and it is well-established (including in previous work in our group) that lysenin loses its voltage-gating behavior in these situations. However, with the addition of Cu^{2+} to

solutions bathing channels in Diphytanoyl-phosphatidylcholine-based lipid membranes (a neutral lipid), lysenin not only regains its voltage-gating function but also displays clear hysteresis qualitatively similar to lysenin inserted in charged lipid membranes. Importantly, this implies the mechanism of voltage-gating for lysenin in neutral membranes results from an interaction between Cu^{2+} and the channels, rather than the previously proposed hypothesis that lysenin's voltage-gating is a result of interactions between the channel and lipid membrane only. Overall, these recent results involving Cu^{2+} and lysenin channels provides an expanded toolset regarding the adjustment of the channels' regulation, hysteresis, and molecular memory properties.

This work progresses what is known about lysenin as a sensing molecule; adjustments to selectivity, voltage-gating, hysteresis, and memory function facilitate improved detection and response avenues of lysenin to multivalent ions. However, the most notable contributions of this work regard a detailed modeling of transmembrane voltage and its dependence on divalent ion-induced sub-conducting states within the channels' population and the ability to impart a memory function on a lysenin channels without the need for an external voltage supply. Regarding the former, insights into sub-conducting ion channel behaviors and selectivity adjustments are provided, and regarding the latter, a lysenin channel population is presented as a memristor. Both contributions may aid in investigations and potential applications regarding bioelectronics, bioengineering, sensing, drug delivery, and ion channels.

CHAPTER TWO: LYSENIN CHANNELS AS SENSORS FOR IONS AND

MOLECULES

Andrew Bogard [1,2], Gamid Abatchev [1,2], Zoe Hutchinson [1], Jason Ward [1], Pangaea W. Finn [1], Fulton McKinney [1], and Daniel Fologea [1,2,*]

[1] Department of Physics, Boise State University, Boise, ID 83725, USA

[2] Biomolecular Sciences Graduate Program, Boise State University, Boise, ID 83725, USA

*Correspondence: danielfologea@boisestate.edu

Abstract

Lysenin is a pore-forming protein extracted from the earthworm Eisenia fetida, which inserts large conductance pores in artificial and natural lipid membranes containing sphingomyelin. Its cytolytic and hemolytic activity is rather indicative of a pore-forming toxin; however, lysenin channels present intricate regulatory features manifested as a reduction in conductance upon exposure to multivalent ions. Lysenin pores also present a large, unobstructed channel which enables the translocation of relatively large molecules driven by electrochemical gradients. These important features of lysenin channels provide opportunities for using them as sensors for a large variety of applications. In this respect, this comprehensive review is focused on investigations aimed at the potential use of lysenin channels as analytical tools. The described explorations include interactions with multivalent inorganic and organic cations, assessments of reversibility, insights into the regulation mechanisms of lysenin channels, interactions with purines, stochastic sensing of peptides and DNA molecules, and evidence of molecular translocation. Lysenin channels present themselves as versatile sensing platforms that exploit either intrinsic regulatory features or the electric signature of molecules threading the conducting pathway, which may be further developed into analytical tools of high specificity and sensitivity or exploited for other scientific biotechnological applications.

1. Introduction

The ability of pore forming proteins and peptides to establish conducting pathways between two sides of a lipid membrane was exploited for decades for numerous analytical applications [1-9] . The most common sensing principle relies on measuring

changes in the ionic currents elicited by specific and non-specific interactions between analytes of interest and wild-type or engineered protein channels [10-17]. These tiny nano-scale analytical tools present a high electrical gain hence detection is straightforward with relatively simple amplifiers. Modulation of ionic currents may occur because of selectivity, existence of regulatory mechanisms that lead to conformational changes and conductance adjustments, and diminished ionic flows resulting from analyte binding or translocation through the pore [6, 8, 15, 18-20].

Adjustments of conductance in response to chemical stimuli are an essential biological function of canonical ion channels in living cells [18, 21, 22], and such features may be replicated in vitro for sensing purposes. However, ion channel reconstitution in artificial membrane systems is not always an easy task [23-25]. Besides not always being readily available, the channels often have narrow confinements that limit the magnitude of the ionic currents and the size of the analytes passing through. As alternatives, porins and pore-forming toxins present similar functionalities to ion channels in terms of creating transmembrane conducting pathways and ensuring high transport rates [16, 26-28]. Although they often lack selectivity and regulation, which might be an important characteristic for sensor development, they are amenable to chemical and genetic modifications aiming at introducing specific bio-recognition elements into their structure and changing their response to stimuli [5, 13, 16, 19]. Porins and pore-forming toxins often present a large conducting pathway which not only ensures greater ionic currents, but also allow passage of larger analytes for translocation-based sensing.

Numerous nanopores of biological origin were investigated for sensing applications [5, 6, 8, 29-36]. Among those biological tools, lysenin channels are attractive candidates for sensor development. Lysenin is a 297 amino acid pore-forming toxin extracted from the coelomic fluid of the earthworm *E. fetida*, which specifically interacts with sphingomyelin and oligomerizes into large conductance channels in artificial and natural lipid membrane systems [37-46]. Structural data achieved by employing X-ray crystallography, cryo-EM, and AFM indicate the existence of a large nonameric β-barrel pore (9-11 nm long, and 2-3 nm diameter) and no visible constrictions in the lumen [45-51]. This large conductance pathway introduced in the cell membranes leads to fast dissipation of the electrochemical gradients responsible for the observed hemolytic and cytolytic activity [39]. Although the toxin may play an important role in the earthworm's innate immunity and defense strategies [39], the exact physiological role of lysenin has yet to be elucidated. Nonetheless, lysenin channels present a large variety of intricate, sometimes unique features among pore-forming toxins, which make them excellent models for fundamental biological studies and applications. For example, the transitions from soluble form to fully functional transmembrane transporters and the role played by sphingomyelin and cholesterol in membrane binding, oligomerization, and pore formation are extraordinary characteristics of lysenin channels, and they have been addressed in multiple reports and reviews [37, 38, 41-44, 46, 50, 52]. In addition, lysenin channels possess some salient features commonly shared by ion channels. Like many ion channels and pore forming proteins, lysenin has a high transport rate; it also presents a certain selectivity for cations [41], but this is much less apparent compared to the selectivity of many ion channels. What is unusual and uncommon for other pore-forming

toxins is the lysenin channel's regulatory mechanisms. When reconstituted into artificial membrane systems containing anionic lipids, lysenin channels present a strong, asymmetrical voltage-induced gating well within the physiological transmembrane voltage range [40, 41]. Lysenin channels undergo massive closure at transmembrane voltages exceeding ~20 mV; however, this remarkable feature vanishes when the target membrane is exclusively composed of neutral lipids, in which case lysenin channels remain open for both positive and negative transmembrane voltages [40, 41, 53]. The voltage-induced gating is influenced not only by membrane composition but also by ionic strength and pH of the support electrolyte [53], which is expected for a gating mechanism that implies interactions between a voltage-domain sensor and electric fields. Although the voltage induced gating is reversible, return to the open states is realized through a different, invariant pathway, leading to a significant hysteresis in conductance [54]. This hysteresis manifests at large time scales, excluding a dynamic origin stemming in the slow activation/inactivation of the channels subjected to oscillatory voltage stimuli.

The requirement for sphingomyelin in the target membrane can be exploited for applications such as probing lipid rafts [52, 55-57]. However, two other salient features suggest the potential use of lysenin channels as powerful analytical tools, and these are the major focus of this informative review. Lysenin presents binding sites for multivalent cations and anions; when such compounds are used as analytes, lysenin channels respond by diminishing their conductance proportionally to the concentration of the chemical stimulus [58-63]. In most cases, the response is reversible and ligand removal leads to complete restoration of the channel's conducting properties. The mechanisms by which different chemicals modulate the channel's conductance depends on the physical

properties and chemical identities of analytes, and include simple binding and partial occlusion, conformational changes to closed or sub-conducting states (ligand-induced gating), and gating and trapping of long polymeric molecules [58-62]. In the same line of sensing capabilities, the large opening of lysenin channels and absence of vestibular constrictions recommends them as analytical tools for single molecule detection and characterization by resistive pulse techniques (stochastic sensing) [29, 51, 58].

Lysenin presents itself with intrinsic sensing capabilities that may be exploited for a large variety of scientific, biomedical, and biotechnological applications. Further channel engineering may lead to development of precise, highly sensitive and specific sensors with single molecule identification and discrimination capabilities.

2. Lysenin channels as multivalent ion sensors

A typical experimental setup for assessing the sensing capabilities of lysenin channels by employing electrophysiology approaches is detailed in Appendix A and Figure A1. This setup comprises either reconstitution of large populations of lysenin channels for determination of changes in macroscopic conductance upon interactions with multivalent ions, or single channel analyses that enable identification of regulatory mechanisms responsible for the observed changes in macroscopic currents.

2.1 Divalent metal cations modulate the macroscopic conductance of lysenin channels in a concentration dependent manner

Addition of monovalent ions to the bulk electrolyte solutions bathing lysenin channels inserted into planar lipid membranes leads to an anticipated increase of the relative macroscopic conductance in a concentration-dependent manner (Figure 1-1) [53, 62]. Given the linearity of the plot, there is no doubt that this trend originates in the

increased solution conductivity after ion addition, therefore no change in the channel's conformation and geometry is observed. Consequently, monovalent anions and cations do not modulate the channel's conductance other than by adjusting the electrolyte solution's conductivity [53, 62].

In contrast to monovalent ions, addition of divalent ions elicits a significant decrease of the channel's conductance [58, 61, 62]; earlier single channel conductance measurements show that addition of 50 mM $CaCl_2$ to the support electrolyte solutions strongly diminishes the ionic currents through lysenin channels [58]. However, this was interpreted as the channel's charge selectivity against divalent cations. While the channel
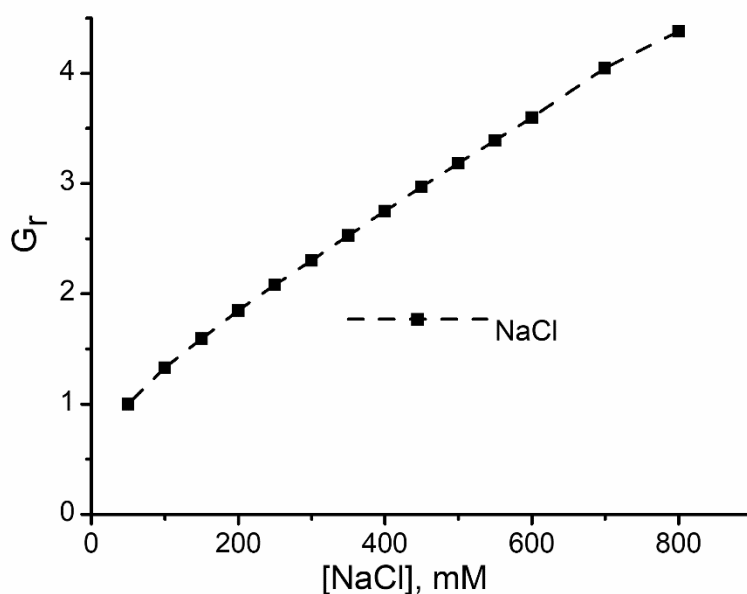
Figure 1-1.   Monovalent ion addition increases the relative conductance Gr of lysenin channels by increasing the support electrolyte solution's conductivity in a concentration dependent manner. Gr = G/G0, where G0 is the channel's conductance recorded at the minimal salt concentration (in this case, 50 mM), and G is the channel conductance measured after the addition of ions. The conductance is measured as the slope of I-V plots recorded in the negative voltage range to prevent lysenin gating. Adapted from ref. [62], with permission.

may present such selectivity, this is not the reason for the reported diminished conductance. Later systematic studies focused on investigating the changes in macroscopic conductance of lysenin channels induced upon addition of increasing concentrations of divalent metal cations showed that the magnitude of the inhibitory effects of divalent metal ions on conductance clearly depends on both electrovalence and chemical identity [61, 62]. Increasing amounts of Ca^{2+} and Mg^{2+} ions added to both reservoirs filled with the support electrolyte bathing the channels-containing membrane similarly decrease the macroscopic conductance in a concentration dependent manner; for both ions, a decrease by ~35% is observed for divalent ion concentration of 20 mM (Figure 1-2a) [62]. A different group of divalent metals, i.e. Mn^{2+}, Ni^{2+}, Cd^{2+}, and Co^{2+} shows a similar concentration dependency of inhibition but enhanced inhibitory capabilities [61] (Figure 1-2b). A third group of ions (Pb^{2+}, Fe^{2+}, and Zn^{2+}) diminish the channel's conductance by a greater extent (~80-90%) when added to the bulk at concentrations up to 25 mM (Figure 1-2c) [61]. Although the conductance modulation is dependent on the chemical identity of the divalent ions, the inhibition curves are otherwise similar and maximum effects are observed at relatively large concentrations in the bulk (i.e., ~20 mM). A notable exception is Cu^{2+}, which is a very potent conductance inhibitor (Figure 1-2d) and practically cancels the channel's conducting properties at 200 µM bulk concentration [61], which is much lower than the ~20 mM required to achieve maximum inhibition for the other divalent ions [61, 62].
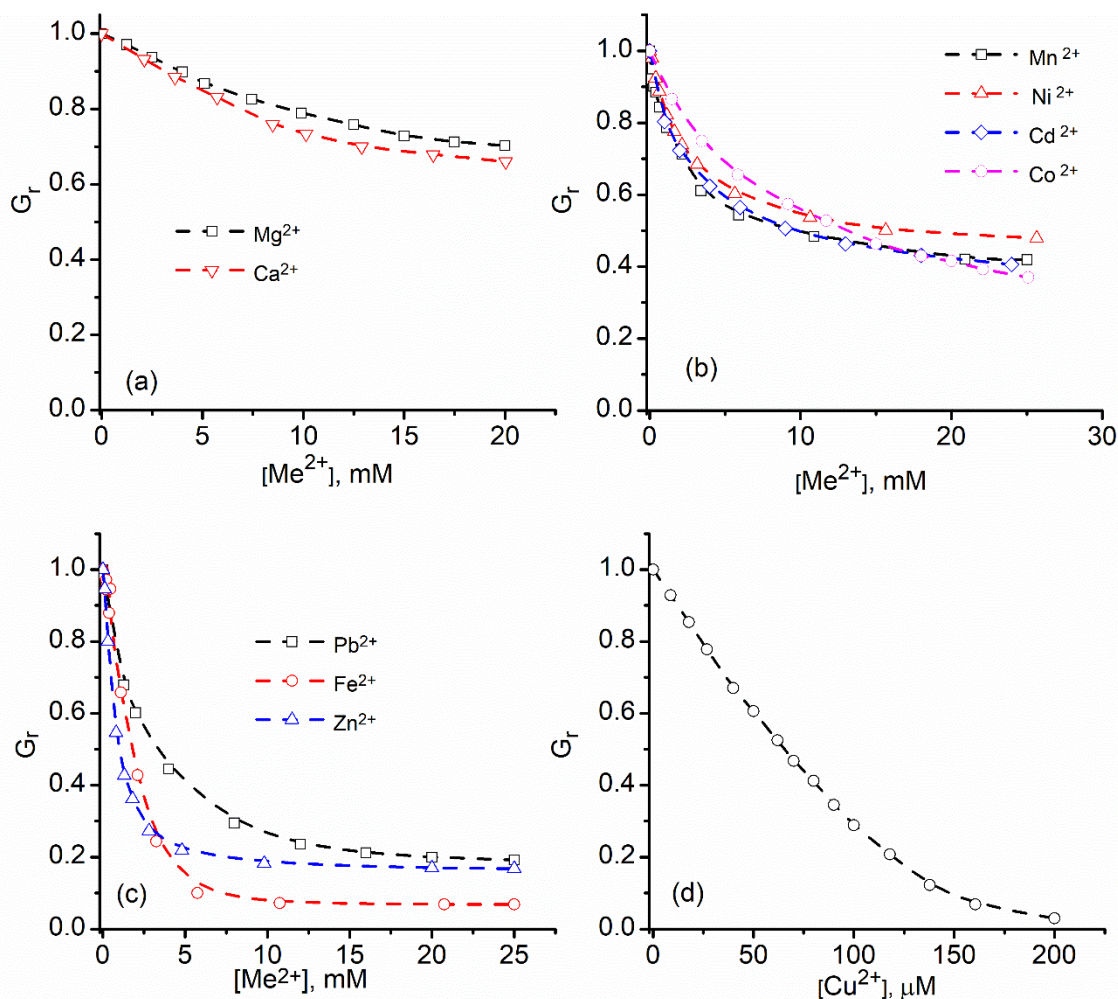
Figure 1-2. **Divalent metal cations inhibit the macroscopic conductance of lysenin channels in a concentration dependent manner. (a) Mg2+ and Ca2+ addition decreases the macroscopic conductance by ~30%; (b) Mn2+, Ni2+, Cd2+, and Co2+ inhibit the macroscopic conductance by 50-60%; (c) The third group of divalent cations (Pb2+, Fe2+, and Zn2+) shows greater inhibition efficiency; (d) Cu2+ is the most potent inhibitor among the tested divalent metal ions and practically suppresses the conducting properties at sub-mM concentrations. Adapted from ref. [62] (panels a, b, c) and ref. [61] (panel d), with permission.**

2.2 Trivalent metal cations strongly inhibit the macroscopic conductance of lysenin

channels

Addition of trivalent metal ions to the support electrolyte solutions also shows a

concentration-dependent decrease in the macroscopic conductance of lysenin channels

(Figure 1-3 [61, 62]. In contrast to the action of most divalent metal ions, the

macroscopic conductance is practically suppressed at trivalent metal ion concentrations in the sub-millimolar range; among all tested divalent metal ions, only Cu^{2+} shows such strong inhibitory capabilities. As with divalent ions, the extent of inhibition depends on concentration and chemical identity of trivalent ions. The tested lanthanides reduce the macroscopic conductance to negligible, near-zero values at concentrations ranging from 50 to 250 µM (Figure 1-3a), while Al^{3+} shows a much stronger inhibition and produces a similar effect in the µM range (Figure 1-3b). Nonetheless, the inhibition curves for these trivalent ions are qualitatively similar and resemble the effects recorded for divalent metal ions. A more intricate inhibition curve is presented by Cr^{3+} (Figure 1-3c), which significantly reduces the ionic transport through the channels at concentrations under 10 µM. However, the concentration dependency of the inhibition is qualitatively different from all the other ions; the pronounced sigmoidal shape suggests a strong positive cooperativity [61], with maximum effects in the range 2-4 µM.

18
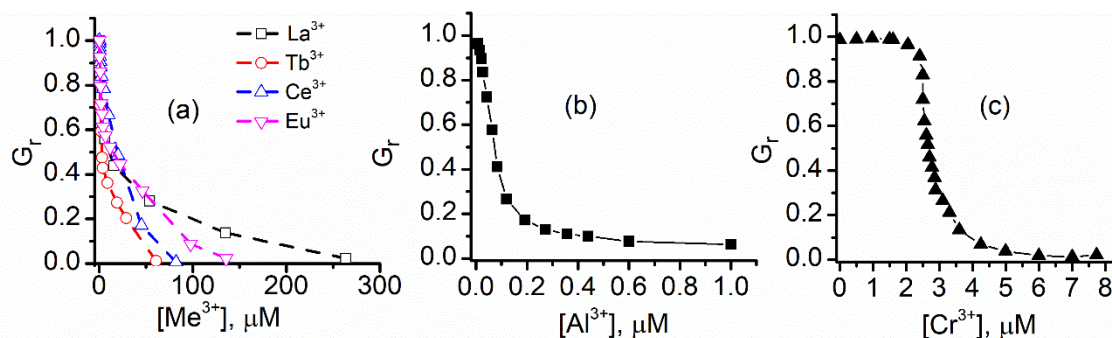
Figure 1-1. **Modulation of the macroscopic conductance of lysenin channels by trivalent metal ions. (a) Lanthanide addition completely suppresses the macroscopic conductance in a concentration-dependent manner; (b) Al^{3+} ions are strong inhibitors and reduce the conductance to negligible values in the µM range; (c) Cr^{3+}, a potent conductance inhibitor, presents an inhibition curve that suggests a cooperative process. Adapted from ref. [62] (panel a) and ref. [61] (panels b and c), with permission.**

2.3 The Changes in Macroscopic Conductance Elicited by Multivalent Cations Are

Reversible

The changes in macroscopic conductance of lysenin channels upon exposure to

multivalent metal ions may be further exploited for sensing applications. An important

feature of such sensors would be their reusability, which is conditioned by the

reversibility of interactions with multivalent ions. In this endeavor, a few studies focused

on investigating eventual changes in macroscopic conductance manifested upon removal

of multivalent ions from the support electrolyte [61, 62]. The decrease in macroscopic

conductance observed upon addition of small amounts of La^{3+} ions is completely

reversed by EDTA addition [62]. EDTA chelates the La^{3+} ions, which reinstates the

original macroscopic conductance; therefore, the channel-ion interactions are reversible.

This process is fast, which suggests that the multivalent ions likely interact with the

inserted channels and adjust their conducting properties rather than damaging or pulling

them from the support membrane [62]. Buffer exchange would be the most universal

method to remove the multivalent ions from solutions [59], but to avoid membrane

rupture during the procedure, chelators and precipitation agents may be used for this task [61, 62]. Al^{3+} ions are among the most potent inhibitors of lysenin channels' conductance but EDTA or EGTA do not chelate them (Figure 1-4a). However, addition of phosphate ions to the bulk solutions leads to precipitation and fast recovery of macroscopic conductance (Figure 1-4a) [61]. Cu^{2+} ions, the most powerful divalent inhibitors, may be easily chelated by EGTA (Figure 1-4b) or precipitated by phosphate (Figure 1-4c) in a matter of minutes [61], leading to a full restoration in conductance.

Although the interactions between many multivalent metal ions and lysenin channels proved reversible [61,62], Cr^{3+} is a notable exception. Any attempt to chelate or precipitate the Cr^{3+} failed (Figure 1-4d) [61], but this might be a consequence of the fact that the chemicals used were ineffective as chelators and precipitating agents. However, buffer exchange does not indicate any recovery of the macroscopic conductance even after 12 h [61]; this observation, together with the unique shape of the inhibition curve, indicates that the interactions between Cr^{3+} and lysenin channels are irreversible and realized by mechanisms different from the other multivalent ions.
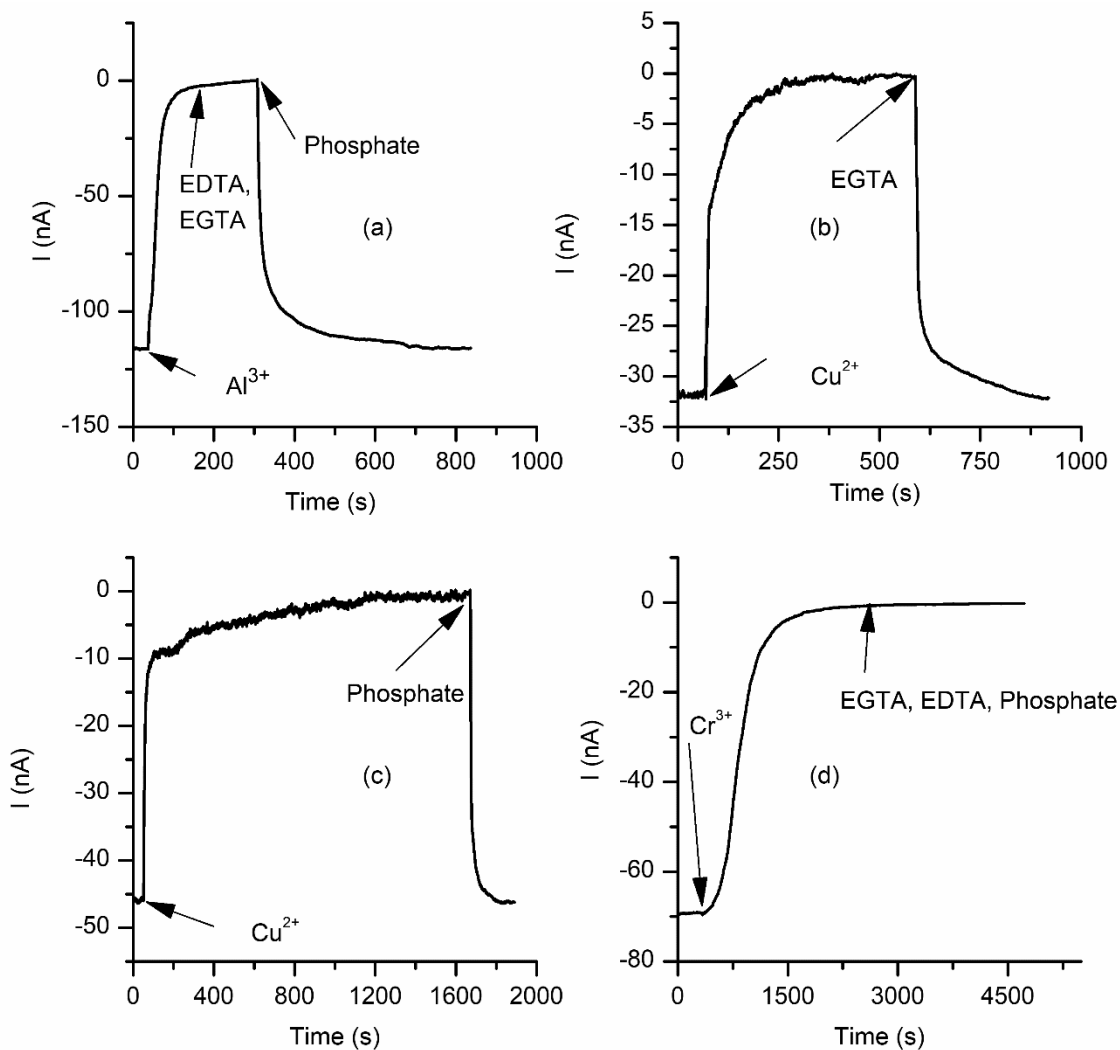
Figure 1-2. **Most, but not all, multivalent metals reversibly interact with lysenin channels. (a) Al^{3+} precipitation by phosphate addition reinstates the initial macroscopic conductance. Cu^{2+} removal by EGTA (b) or phosphate precipitation (c) quickly restores the ionic conductance; (d) EDTA, EGTA, or phosphate addition does not cancel the inhibitory effects of Cr^{3+}. Adapted from [61], with permission.**

2.4. Lysenin Channels Undergo Ligand-Induced Gating Upon Exposure to Multivalent Cations

An important question pertaining to sensing concerns how lysenin channels respond to multivalent ions and adjust their conductance accordingly. In answer to this question, a series of single-channel experiments that monitored the changes in macroscopic conductance upon addition of multivalent metal cations concluded that the

major mechanism of interaction is ligand-induced gating triggered by cation binding to a specific binding site present in the channel's structure [61,62]. After insertion of a few lysenin channels in the target membrane (Figure 1-5a), La^{3+} addition leads to a stepwise reduction of the single-channel currents (Figure 1-5b). In terms of ionic currents, the process is simply a reversal of the single channel insertion and the amplitude of the changes in ionic current for each step is identical for the two distinct processes. Addition of EDTA to the support electrolyte again reverses the process but shows an otherwise identical variation of the ionic currents in terms of change/step (Figure 1-5c). These experiments concluded that the trivalent metal ions induce conformational changes of the channels (gating) from open to fully closed states. Since the conductance of the fully closed channel is negligible, this partially explains the greater inhibition efficiency of trivalent metals by complete cancellation of the macroscopic conductance. Nonetheless, this explanation is not satisfactory for divalent metal ions, for which a flattening of the inhibition curve occurs (see Figure 1-2) while the macroscopic conductance still has large values. To identify the origin of this behavior, similar single-channel experiments were conducted by employing Ca^{2+} ions as inhibitors [61,62]. As Figure 1-5d shows, Ca^{2+} addition induces stepwise changes of the ionic currents, which also suggests a gating mechanism. However, the amplitude of each individual variation is roughly half the amplitude corresponding to a fully open channel. This discrepancy was explained by considering that, in contrast to trivalent metals, Ca^{2+} ions trigger conformational transitions from open to partially conducting states [62].
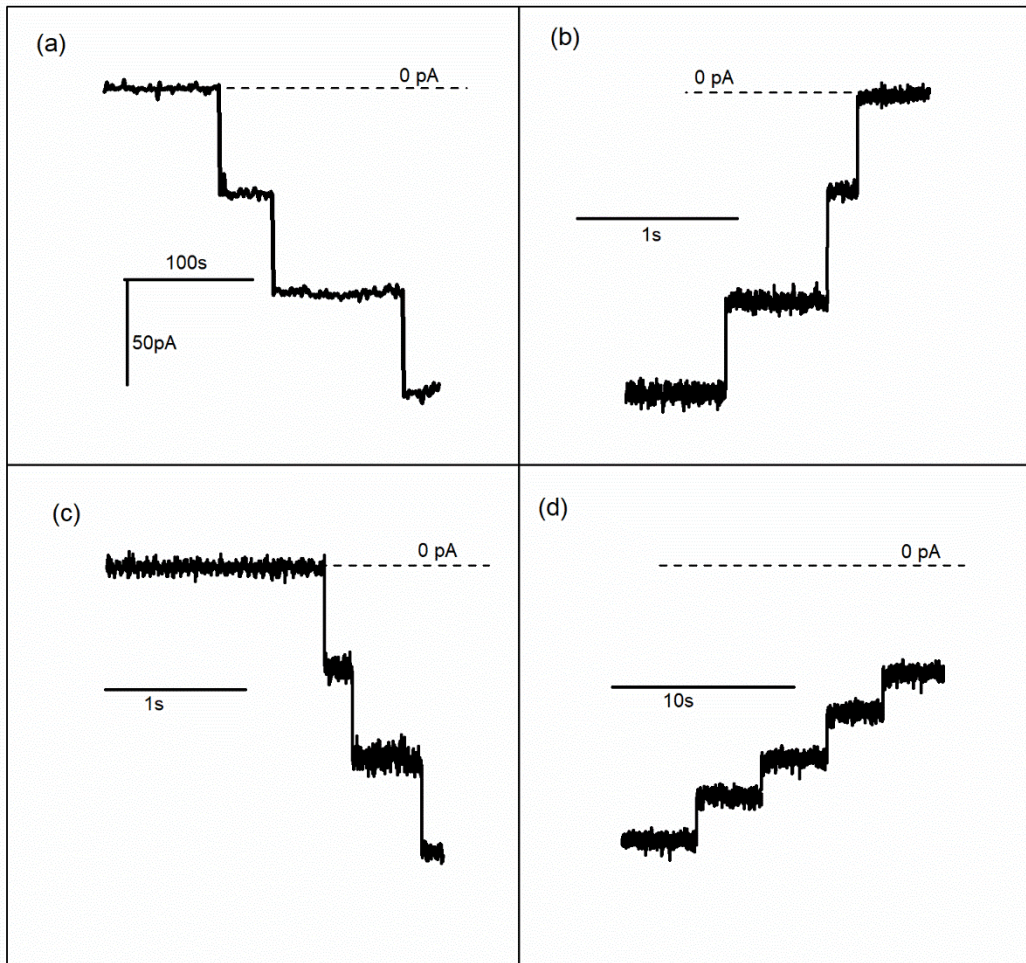
Figure 1-3. **The macroscopic conductance of lysenin channels is adjusted by channel transition to non-conducting or sub-conducting states. (a) Insertion of three lysenin channels in the bilayer membrane is indicated by the stepwise variation of the ionic currents; (b) La^{3+} addition (final concentration 0.1 mM) induces fast conformational transitions that lead to channel closing; (c) EDTA addition (1 mM final concentration) reopens lysenin channels previously closed by interactions with La^{3+} ions; (d) Ca^{2+} addition (20 mM final concentration) induces conformational transitions to sub-conducting states. Adapted from [62], with permission.**

The single channel recordings performed in the presence of Ca^{2+} ions do not provide sufficient information with regards to channels undergoing single transitions from open to sub-conducting states as opposed to full closing in two or more steps. To detail the mechanism, the interaction with divalent metals was described as a simple

Langmuir isothermal absorption process and a formula for the relative changes in macroscopic currents was derived [62]:

$$\frac{I}{I_t} = \left(\frac{(K_0 + b[Me^{2+}])}{K_0}\right)\left[1 - (1-f)\left(\frac{1}{1+\left(\frac{1}{\alpha[Me^{2+}]}\right)}\right)\right], \tag{1}$$

where I is the current through the fully open channels, I_t is the current after Me^{2+} addition (both currents are measured at the same voltage, therefore their ratio represents the relative change in macroscopic conductance G_r), K_0 is the specific conductivity of the bulk before Me^{2+} addition, b is a factor accounting for the linear changes in conductivity upon Me^{2+} addition, f is the ratio between the open/sub-conducting channel conductance in otherwise identical conditions, and α is the equilibrium constant of the channel–ion binding process [62]. The above equation predicts that for channels undergoing transitions to only sub-conducting states (no full closing, irrespective of the inhibitor's concentration), the currents should first decrease until all channels attain sub-conductance, after which the currents should increase upon ionic additions owing to the increased conductivity of the solution. In contrast, a full closing of the channel in two or more steps would lead to a continual decrease of the ionic currents in response to an increasing inhibitor concentration. This model was tested for investigating the macroscopic currents recorded in the presence of Ca^{2+} and Mg^{2+}, and the excellent fit of experimental data with Equation (1) (Figure 1-6a) demonstrate the existence of highly stable sub-conducting states upon influence exerted by the divalent cations. In the same line, stable sub-conducting states were also suggested for other divalent metal ions, as inferred from local minima in the inhibition curves (Figure 1-6b) [61]. The different

inhibitory effects may be explained by accounting for more than one sub-conducting state

or assuming that not all the ions lead to the same conductance ratio between the open and

sub-conducting states.
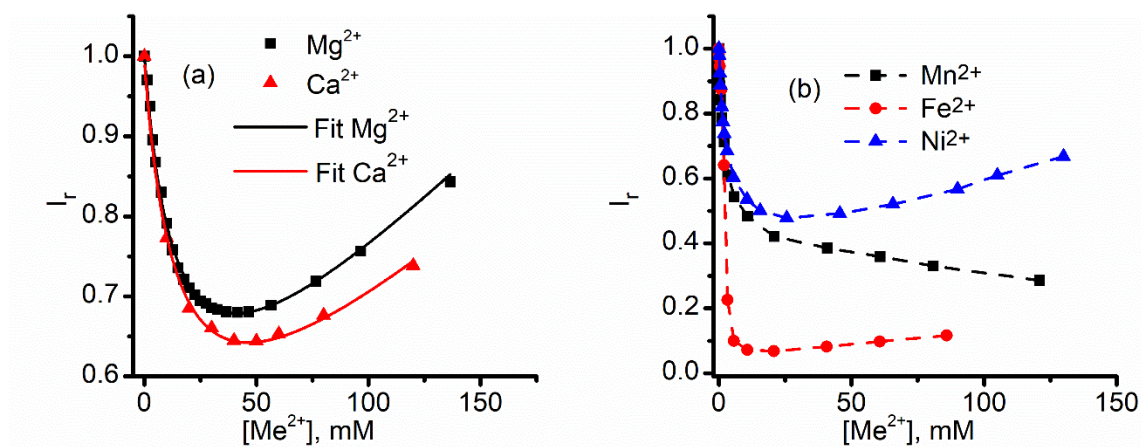
Figure 1-4.   Divalent metal cations induce conformational changes to sub-conducting states. (a) The inhibition curves recorded following successive Mg^{2+} and Ca^{2+} additions indicate that the channels are undergoing transitions to sub-conducting states without full closing. The continuous line represents the fit of experimental data with Equation (1); (b) The inflection point in the inhibition curves suggests that other divalent cations also induce transitions to stable sub-conducting states. Adapted from [62] (panel a) and [61] (panel b), with permission.

Cu^{2+} ions show a different behavior that does not match the typical description of

divalent ion effects in terms of inhibition efficiency and the shape of the inhibition curve

(does not present an inflection point), hence resembling trivalent-like effects. To identify

the origin of this behavior, single-channel experiments that employed Cu^{2+} ions as

inhibitors were conducted similarly to the other divalent and trivalent metal ions. After

insertion of only two lysenin channels in the bilayer membrane (Figure 1-7a), Cu^{2+}

addition (500 µM final concentration) completely cancels the individual conductance and

reduces the ionic currents to zero in a stepwise manner [61]. However, the transition from

open to close is not direct and comprises a short-lived intermediate sub-conducting state

(Figure 1-7b). EGTA addition fully restores the initial conductance of each channel, but

the close–open transition is also realized through short intermediate sub-conducting states [61] (Figure 1-7c). Therefore, Cu^{2+} induces transitions to sub-conducting states, as observed for other divalent metals, but the sub-conducting states are not stable and the channels may fully close by employing a second transition from the sub-conducting to fully closed states [61].
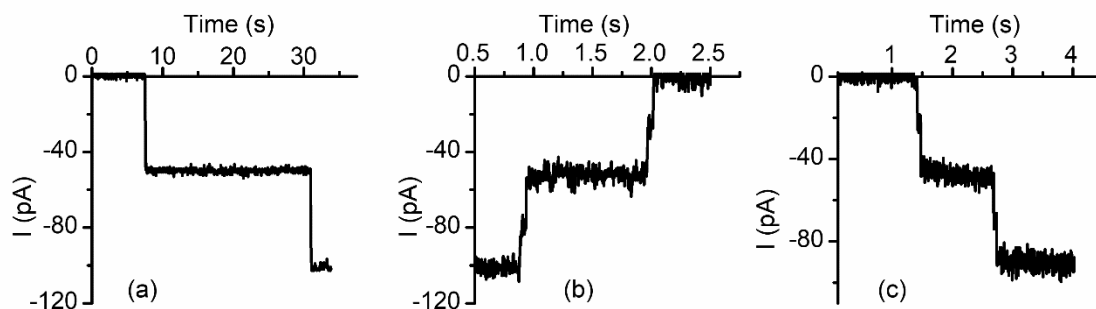
Figure 1-5. Cu^{2+} **induces full closing of lysenin channels through intermediate steps. (a) The insertion of two lysenin channels into a planar membrane is indicated by the stepwise variation of the ionic current; (b)** Cu^{2+} **addition (500 μM) induces full closure of the channels, but each closure comprises two steps; (c) Complete channel reopening upon** Cu^{2+} **removal by addition of EGTA (10 mM) is also realized through intermediate sub-conducting states. Adapted from [61], with permission.**

2.5. Which One Matters, Charge, or Size?

With a few exceptions, conductance inhibition is more potent for trivalent than divalent metal cations. The macroscopic currents decrease by a much larger extent for trivalent metal ions, and this may be partially explained by their ability to induce conformational changes that lead to complete channel closure. Nonetheless, the concentration required to achieve ligand-induced gating (full closing, or transitions to sub-conducting states) is much smaller for trivalent metals (in the μM range) than for divalent metals (mM range). This naturally leads to the hypothesis that the charge of the cations is central for the ligand-gating mechanism manifested in the presence of multivalent metal ions. This may be easily seen in Figure 1-8a, in which the inhibitory

effects of Fe ions are more prominent for Fe^{3+} than Fe^{2+} [62]. To better understand the

role played by the charge in the gating mechanism, the investigations employed the use

of larger organic multivalent ions, such as spermidine^{3+} and spermine^{4+} [61,62]. The

inhibition curves for the two voluminous ions (Figure 1-8b, and 1-8c) reveal that both

ions, despite bearing large charges, exhibit inhibition curves resembling the lysenin

channel behavior observed upon exposure to divalent ions. Apart from the necessity of

using relatively large cation concentrations to achieve conductance inhibition (in the mM

range), the inflection point in the inhibition plots suggests that the gating mechanism

implies transitions to sub-conducting states. Therefore, both charge and size (or in other

words charge density) play a major role in establishing the channel's sensitivity to ions

and modulating its transition to closed or sub-conducting states.
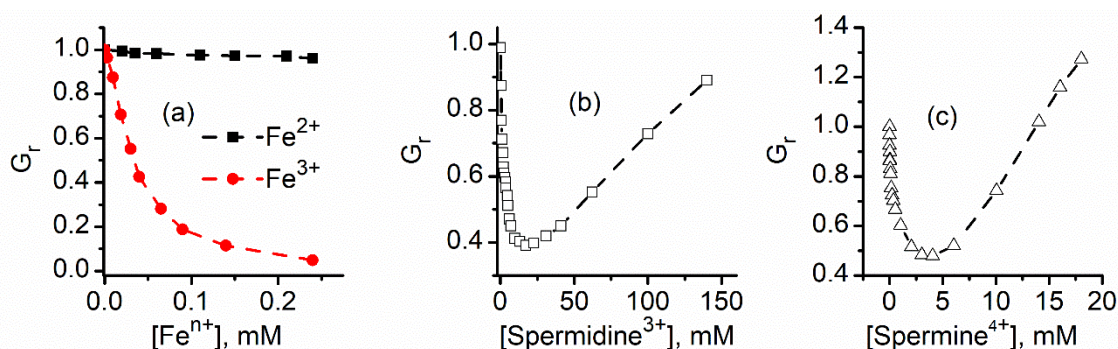
Figure 1-6.　Charge and size influence on the inhibitory effects of multivalent cations. (a) The inhibitory effects presented by Fe strongly depend on the ionic charge, and Fe^{3+} is a more efficient inhibitor than Fe^{2+}. Voluminous organic ions, such as spermidine^{3+} (b) or spermine^{4+} (c), present less inhibitory efficiency, in spite of their large charge. Additionally, the inflection point in the inhibition curves indicates that both cations modulate the channel's conductance by inducing transitions to sub-conducting states. Adapted from [62] (panels a and b) and [61] (panel c), with permission.

2.6. Cationic Polymers Irreversibly Block Lysenin Channels

Experimentations with multivalent inorganic and organic cations revealed conductance inhibitory effects dependent on both the charge and size of used ions. Conductance modulation is in most cases reversible, and inhibitor removal by chelation, precipitation, or buffer exchange restores the lysenin channel's conducting properties. However, the inorganic and organic ions used for these investigations were still small compared to the channel's opening and carried a relatively small charge. This led to questioning of the potential effects on the macroscopic conductance of lysenin channels presented by large and highly charged molecules, such as cationic polymers [63]. In this line of inquiries, the effects on macroscopic conductance of two polyions (i.e., polyethyleneimine (PEI) and chitosan) were evaluated [63]. Both polymers reduce the transport capabilities when added to the bulk electrolyte in the low concentration range (Figure 1-9), demonstrating strong inhibitory capabilities. However, a major difference was encountered with respect to reversibility: buffer exchange does not reveal any recovery of the conducting properties even after extended exposure to polymer-free electrolyte solutions [63].
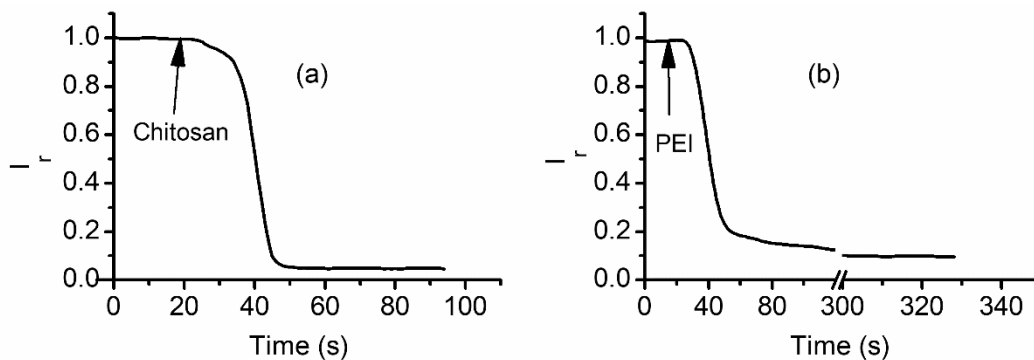
Figure 1-7. **Cationic polymers inhibit the ionic currents through lysenin channels. The evolution of the relative ionic currents measured through lysenin channels upon exposure to (a) 8 μM chitosan, and (b) 4 μM PEI. Published under Creative Common Attribution License in [63].**

This lack of reversibility is explained by considering a channel occlusion mechanism based on gating and trapping [63]. Once the long polymer enters the channel's lumen, the large positive charge induces transitions (gating) to either closed or sub-conducting states; this transition happens before the long polymer exits the pore, therefore the polymer is trapped inside the channel and the numerous positive charges present on the chain prevents reopening. This hypothesis is supported by experiments performed on single lysenin channels exposed to cationic polymers [63]. As Figure 1-10 shows, the two inserted channels undergo a stepwise variation of the open currents upon chitosan addition, which suggests a complete blockage of the conductance pathway. Such complete blockage may also be achieved even if the channels transition to a sub-conducting state but the polymer molecules are trapped within.
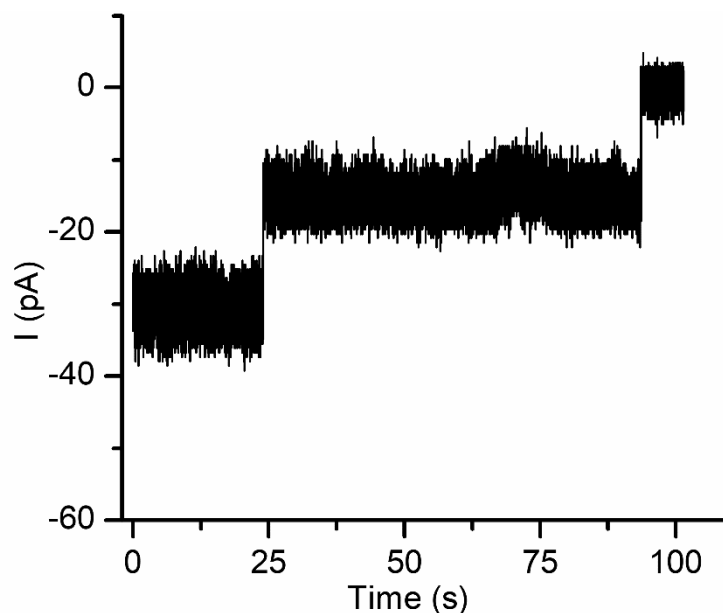
Figure 1-8. **Cationic polymers inhibit the ionic currents in a stepwise manner. PEI addition (10 μM final concentration) rapidly closes the two lysenin channels inserted into the bilayer lipid membrane. Published under Creative Commons Attribution License in [63].**

2.7. Ligand and Voltage Gating of Lysenin Channels are Not Coupled

A large body of evidence supports the hypothesis that lysenin channels exposed to multivalent cations transition to non-conducting or sub-conducting states by mechanisms characteristic to ligand-induced gating. However, lysenin channels also present a strong voltage-induced gating, which manifest as reversible complete channel closure at positive transmembrane voltages [40,41]. This regulatory mechanism raises the question whether the two gating mechanisms (i.e., voltage and ligand induced) are related. To address this fundamental question, the inhibitory effects of metal cations were evaluated in experiments that used neutral lipids to produce the lipid membrane, which suppressed the lysenin channel's voltage-induced gating [40,41]. Upon insertion into membranes containing anionic lipids, lysenin channels show a strong voltage-induced gating, while the use of electrically neutral lipids abrogates this remarkable regulatory feature and leads

to a linear I-V plot (Figure 1-11a). In spite of changes in voltage-gating regulation,

lysenin channels inserted into neutral membranes do not show changes in their sensitivity

to ions [61]: Ca^{2+} (Figure 1-11b) and Pb^{2+} (Figure 1-12c) additions inhibit the

macroscopic currents and the inhibition curve presents the inflection point characteristic

of stable sub-conducting states. In the same line, irreversible changes in the lysenin

channel's conductance induced by cationic polymers when neutral membranes are used

[63] support the hypothesis that voltage and ligand-induced gating are realized through

distinct mechanisms.
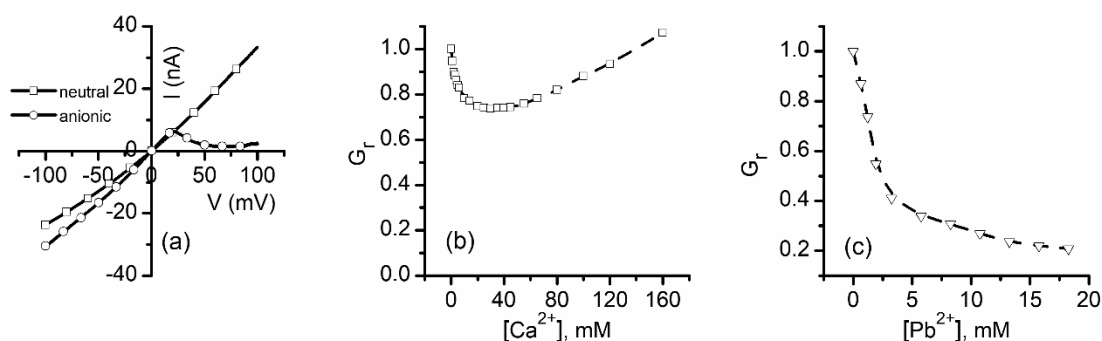
Figure 1-9.   Voltage and ligand-induced gating are realized through distinct mechanisms. (a) Lysenin channels inserted into a membrane containing anionic lipids shows the voltage induced gating; a membrane support composed of neutral lipids suppresses voltage regulation and leads to a straight I-V curve. A neutral membrane does not cancel the conductance inhibition presented by Ca^{2+} (b) or Pb^{2+} (c). Adapted from [61], with permission.

2.8. Cationic Ions and Polymers May Compete for the Binding Sites

The gating and gating/trapping mechanisms are different but may be triggered by

similar electrostatic interactions between charges and binding sites present in the

channel's structure. Are these binding sites the same? To answer this question, the

investigations focused on assessing a potential competition for occupancy between

divalent metal cations and cationic polymers [61]. The results presented in Figure 1-12

show that the inhibitory effects of PEI are canceled if the channels were previously

exposed to large amounts of Ca^{2+} ions. While this suggests that the two inhibitors may

compete for the same binding sites, it is also possible that the channel's transition to sub-

conducting states may prevent the polymer's access to the lumen and further trapping.
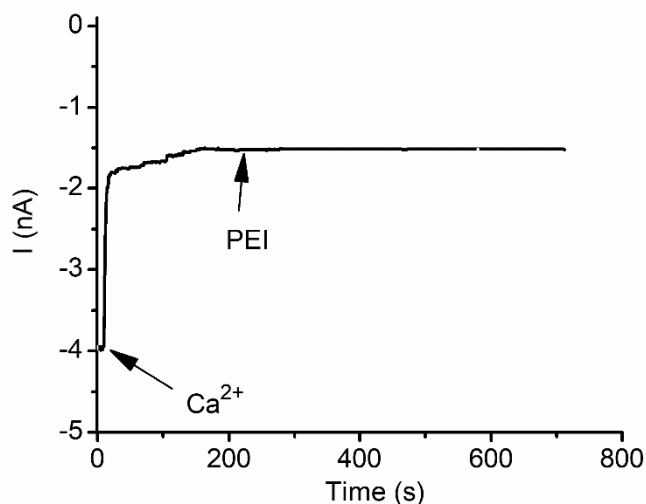
Figure 1-10.   Multivalent ions and cationic polymers compete for the binding sites present in the lysenin channel's structure. After channel blockage and transition to sub-conducting states by Ca^{2+} addition (40 mM final concentration), PEI (10 µM final concentration) does not show further inhibition of the ionic currents. Published under Creative Commons Attribution License in [63].

2.9. Lysenin Interactions with Purines

All the experiments conducted on inorganic and organic ions did not reveal any

influence on the channel's conductance presented by small inorganic anions, which

apparently do not interact with lysenin. However, a significant conductance modulation is

observed when purines (ATP, ADP, and AMP) are added to the support electrolyte [59].

Addition of ATP (20 mM final concentration) to the support electrolyte quickly reduces

the macroscopic ionic currents established through lysenin channels (Figure 1-13).

However, buffer exchange with ATP-free solutions fully reinstates the conducting

properties and proves reversibility. Single-channel experiments show that the interactions

between lysenin channels and ATP do not imply gating [59], and suggest binding and

partial occlusion as plausible explanations.
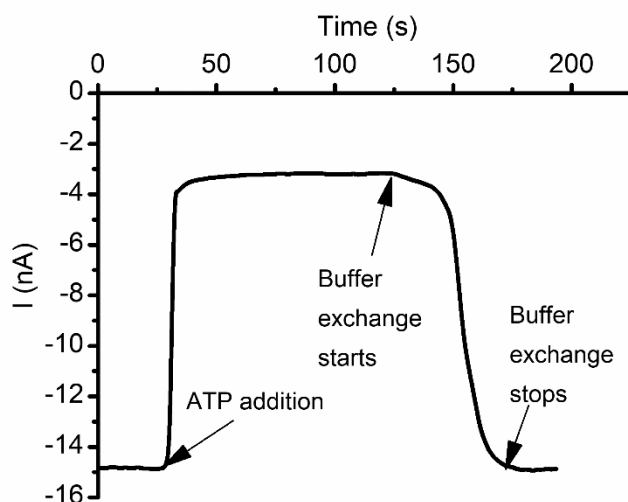
Figure 1-11.   ATP reversibly modulates the macroscopic ionic currents through lysenin channels. The open current through lysenin channels undergoes a major decrease after ATP addition (10 mM final concentration). Buffer exchange with ATP-free support electrolyte reinstates the original conductance, indicative of reversibility. Adapted from [59], with permission.

Figure 1-14 shows that the relative macroscopic conductance of lysenin channels

decreases upon ATP, ADP, or AMP addition in a concentration-dependent manner. The

inhibitory effects manifest in the mM range for all three purines, but their potency

decreases in the order ATP > ADP > AMP. The shape of the inhibition plots observed for

interactions with purines are slightly different than the typical parabola shape recorded

for most divalent and trivalent cations and suggest a cooperative process. To better

understand the effects of purine inhibitors in relation to cooperativity, a fit of the

experimental data was performed by employing the Hill equation [59]:

$$G_r = 1 - (1 - G_{min}) \frac{[x]^n}{[IC_{50}]^n + [x]^n},$$

(2)

where G_r is the relative macroscopic conductance, G_{min} is the minimum relative

conductance measured at saturation (all potential binding sites are occupied), IC_{50} is the

half-way inhibitory concentration, x is the purine concentration, and n is the Hill

coefficient.
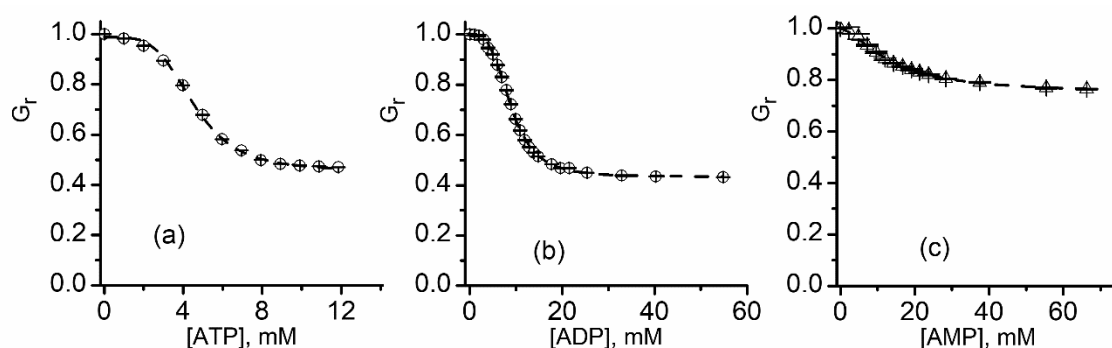
Figure 1-12. Changes in relative conductance induced by addition of ATP, ADP, or AMP. The relative changes in macroscopic conductance G_r show that ATP (a) and ADP (b) were more efficient inhibitors compared to AMP (c). The dashed lines in each panel represent the fit with the Hill equation, which is used to determine IC_{50} and n. Adapted from [59], with permission.

The results shown in Table 1 indicate that IC_{50} and n vary with the chemical

identity of the inhibitor; IC_{50} increases (lower binding affinity) and n decreases (less

cooperativity) as the net charge of the anion increases. This suggests that the inhibitory

mechanism relies on electrostatic binding of purines to specific sites present in the

channel's lumen [59], which are different from the binding sites implied in cation-

induced ligand gating.

Table 1-1. Fit values of IC_{50} and n for ATP, ADP, and AMP inhibition effects on lysenin channel conductance.

	IC_{50} (mM, ± SD)	n
ATP	4.53 ± 0.07	4.15 ± 0.2
ADP	8.92 ± 0.07	3.43 ± 0.16
AMP	13.43 ± 0.08	1.62 ± 0.17

The electrostatic nature of the interactions was confirmed in experiments that investigated the effects of ionic screening on ATP-induced inhibition; indeed, the inhibitory effects reported upon electrostatic screening (Figure 1-15) significantly depend on the ionic strength of the support electrolyte, and IC_{50} decreases as the ionic strength increases (Table 2). However, irrespective of the ionic strength, the Hill coefficient n does not significantly deviate between experiments (Table 2), hence providing a framework for including effects of molecular identity and structure to explain the differences in the binding affinity of purines [59].

Table 1-2. Fit values of IC_{50} and n for ionic screening effects on ATP inhibition of lysenin channel conductance.

KCl (mM)	IC_{50} (mM, ± SD)	n
50	3.83 ± 0.05	4.11 ± 0.16
135	4.36 ± 0.07	4.14 ± 0.2
500	6.94 ± 0.07	4.1 ± 0.14
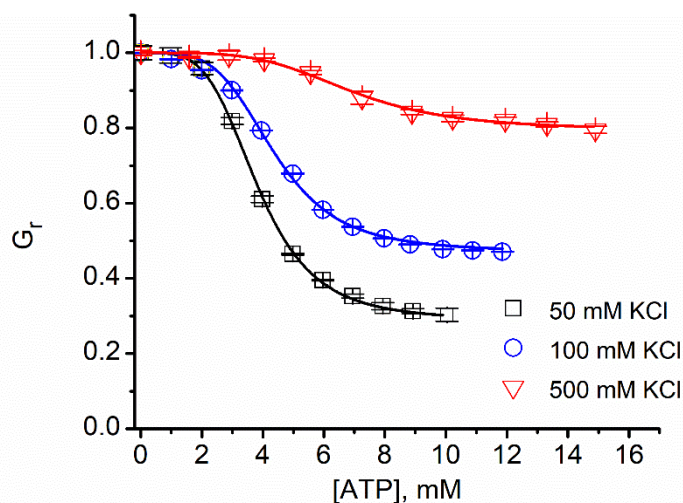
Figure 1-13.   Ionic screening reduces ATP inhibitory effects. The relative conductance indicates that increased ionic screening elicited by addition of KCl minimize the conductance changes induced by ATP addition. The continuous lines represent the fit with the Hill equation (Equation (2)). Adapted from [59], with permission.

3. Lysenin Channels as Stochastic Sensors: Translocation of Macromolecules

Since the pioneer work carried by Kasianowicz et al. showing that biological nanopores may be exploited as tools for single molecule detection and characterization [64], the field of nanopore-based technology has developed at an unprecedented pace. The principle of sensing, a direct expansion of the long-revered Coulter measuring method at the nano-scale [65], is deceptively simple: the resistive pulse technique relies on recording the changes of the ionic currents established through a nanopore when single molecules are electrophoretically driven through the conducting pathway. This research field was initiated by using α-hemolysin as a prototype pore; however, scientists developed and utilized a large variety of synthetic and biological nanopores for similar purposes [6,8,14,33,34,66–79]. The great interest in this topic is fueled by the promise of fast and reliable sequencing of nucleic acids and peptides [14,35,73,74,76,80], development of sensors for single molecule detection and characterization, fast and

reliable determination of biomolecules in complex biological samples, and many other analytical applications. The use of lysenin channels as resistive-pulse sensors may present some clear advantages over synthetic and natural nanopores: the channel's opening is relatively large and therefore able to accommodate large analytes, single and multiple channels may be easily reconstituted into membranes, and the inserted channels are very stable. The voltage-induced gating that manifests at positive bias potentials may be considered an impediment for some of the applications, but it may be easily suppressed by using neutral lipids to create the support lipid membrane.

3.1. DNA Translocation Experiments

In spite of its potential, reports on lysenin use as a stochastic sensor are scarce. Single-channel experiments developed by Aoki et al. [58] show that spikes in the open current occur when DNA is added to the bulk electrolyte solution. However, the focus of those investigations was different, and it is not clear if the recorded transients in the ionic current are indicative of DNA molecule translocation. Another report focused on investigating the lysenin channel's structure shows some preliminary investigations on DNA translocation [51]. The exploration indicates that wild-type lysenin channels are not able to support DNA translocation, most probably owing to the strong repulsion between charged polymers and charged domains in the channel's structure; in contrast, a mutant version constructed by replacing negatively charge amino acids with neutral and cationic ones shows transient changes in the ionic current, resembling translocation [51]. While the results indicate that the wild-type channel and the engineered one have different properties with regards to translocation, more experimental evidence should be provided in support of the claim that lysenin successfully captures and facilitates translocation of

DNA strands. The transient signal was obtained by using a mixture of aptamer DNA and its target molecule (thrombin), hence the source of the variation of the ionic currents is uncertain.

Therefore, it is worth mentioning and presenting investigations performed by our group on DNA translocation through lysenin channels [81]. To suppress the voltage-induced gating that manifests at positive voltages, single lysenin channels were reconstituted into a bilayer lipid membrane composed of neutral lipids [40,41]. No transient changes in the open ionic current were visible when 69 nt DNA (5 nM final concentration) was added to the reservoir wired to the headstage and biased by a negative potential (Figure 1-16a). Since the electric field for this configuration has the correct orientation to drive the DNA molecules through the channels into the opposite reservoir, the logical conclusion is that the DNA molecules do not thread the channels. However, polarity reversal (positive potential on the reservoir connected to the headstage) and ssDNA addition to the grounded reservoir elicits fast and deep changes in the open ionic current of a single lysenin channel, resembling translocation (Figure 1-16b). These observations confirm that wild-type lysenin may prevent DNA translocation (most probably due to electrostatic repulsions) when the molecules are added to the stem side of the channel. They also confirm the necessity to suppress the voltage-induced gating by using neutral lipids for ssDNA translocation experiments.

38
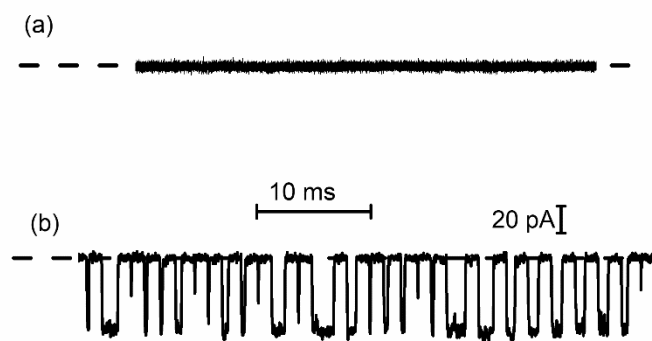
Figure 1-14. **DNA translocation through single lysenin channels. (a) ssDNA addition to the headstage wired reservoir biased by a negative potential does not elicit transient changes in the open current through a single lysenin channel, indicative of absence of translocation; (b) ssDNA addition to the opposite side (grounded reservoir) and application of a positive voltage to the headstage-wired reservoir leads to events resembling translocation.**

From Figure 1-15 and the distribution of the current blockage (I_D) and dwell time (T_D) (Figure 1-16), one may easily observe that the current drops are relatively uniform for the recorded events (~ 56 pA); however, some short and reduced-magnitude spikes are observed in both the current trace (Figure 1-16b) and I_D histogram (Figure 1-17a). This type of noise is common in translocation experiments, and it is considered a consequence of molecules colliding with the mouth of the pore without being captured by the electric field and translocated [70,80,82,83]. As opposed to the relatively uniform changes in the ionic current, the dwell time seems to be not only unusually long for some events but also extremely variable compared with other ssDNA translocation experiments (Figure 1-17b). This might be a consequence of DNA "stickiness" to the channel's lumen, which may be explained based on the investigations of lysenin channel interactions with purines (vide supra, and [59]). The resulting exponential decay shape of the dwell time distribution is common for macromolecule translocation through narrow "sticky" nanopores [34,80,82,84–86].
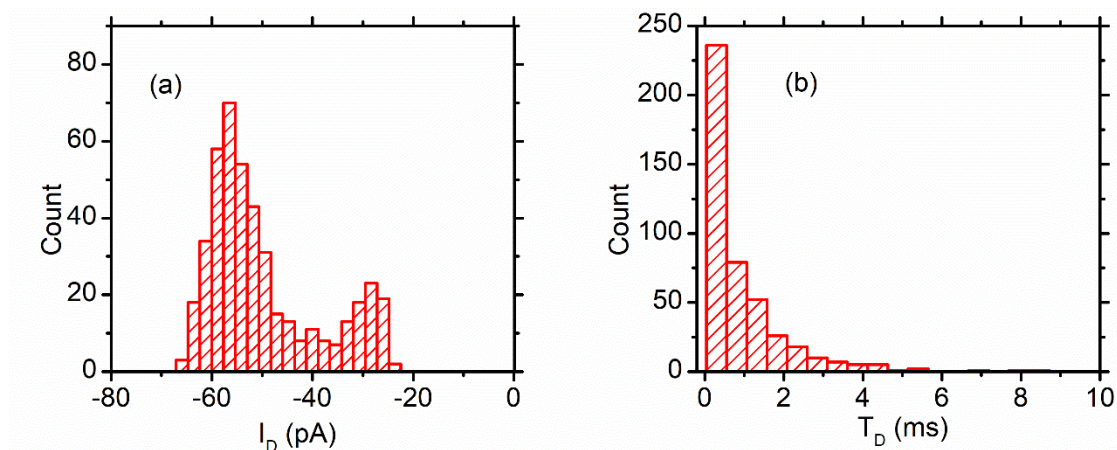
Figure 1-15. Analysis of translocation events. (a) The distribution of the current blockages indicates two peaks centered at ~55 and ~28 pA, respectively. The low amplitude peak may originate in ssDNA channel collisions, while the high amplitude peak represents putative translocations; (b) The dwell time of the events follows an exponential decay, characteristic to translocation through "sticky" pores.

Protein channel gating in the presence of DNA may lead to "events" that resemble translocation and additional evidence is needed to demonstrate DNA passage. Irrespective of the origin of the differences between events, PCR provides irrefutable evidence of DNA translocation [64]. In this case, DNA amplification by PCR after solution extraction from the reservoirs and further analysis shows that the DNA translocation process was successful. The gel electrophoresis analysis (Figure 1-18) of the PCR-amplified sequence in the presence of forward and reverse primers shows the presence of translocated DNA molecules, and the two markers aid identification by molecular weight. In addition, the sample collected from identical experiments but for which the voltage was reversed show no detectable amplicon in the reservoir, indicating that the current blockages represent DNA passage through lysenin channels.
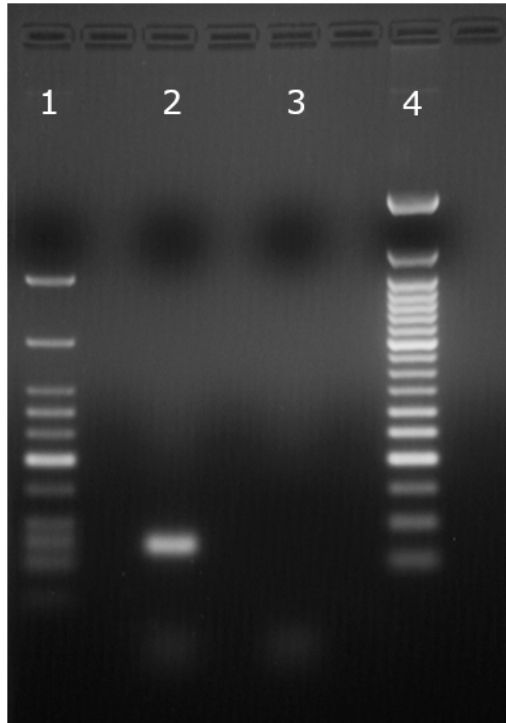
Figure 1-16.   The analysis of translocated ssDNA performed by gel electrophoresis (2% agarose) after PCR amplification. (1) Low Molecular Weight Marker (25-766 bp), New England Biolab; (2) Amplicon produced from ssDNA molecules translocated through lysenin channels; (3) The absence of DNA indicates that a reversed polarity prevents translocation. (4) 50 bp Ladder Marker, New England Biolabs.

3.2. Peptide Translocation

The large interest in DNA translocation was fueled by the promise of fast and reliable sequencing [64,66,87,88]. However, single molecule detection and characterization of peptides molecules is equally important; numerous synthetic and natural nanopore sensing platforms have been employed for such tasks [70,82,84,85,89,90], and lysenin is one of them [29]. Lysenin was investigated as a stochastic sensor for the short octameric peptide angiotensin II (Ang II) [29]. After single channel reconstitution in neutral lipid bilayers (Figure 1-19a), no transient changes in the ionic current established through two channels was observed at -80 mV bias potential (Figure 1-19b). A similarly quiet baseline was recorded after Ang II addition to the

reservoir hardwired to the headstage (Figure 1-19c); Ang II is a positively charged peptide, and the particular orientation of the electric field prevented its translocation. However, peptide addition to the ground reservoir in otherwise identical electrical and solution conditions shows frequent transient changes in the open ionic current, resembling translocation through other biological channels (Figure 1-19d).

Signal analysis in terms of the average current blockage $<I_B>$ and dwell time t_D performed with the Transalyzer software package [91] provides some important insights into the origin of recorded events. The density plot of the recorded events shows two relatively well separated clusters, E1 and E2, respectively (Figure 1-20a). Further analysis of the events in each cluster indicates a good separation in terms of current blockage $<I_B>$ (Figure 1-20b) and overlapping in terms of dwell time (Figure 1-20c). The existence of multiple clusters more or less overlapped is common for translocation experiments, especially when short peptides are used as analytes. In this case, based on previous explanations provided for similar experiments it was concluded that the events E1 are characteristic to Ang II molecules that translocated through the open channel, while E2 events represent collisions with the pore [29].
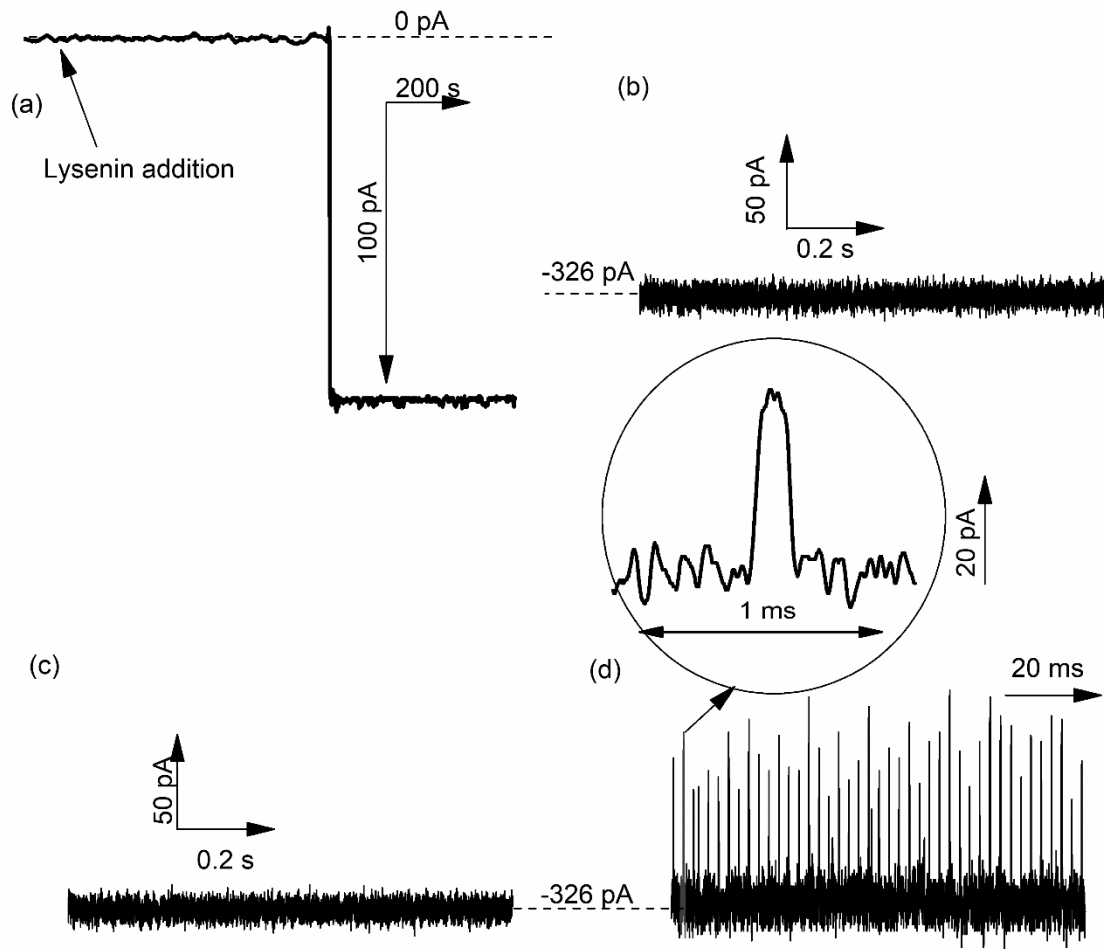
Figure 1-17.   Ang II peptide translocation through single lysenin channels. (a) The insertion of single channels was monitored at -60 mV transmembrane potential. No changes in the open current established through two lysenin channels at -80 mV is observed when: (b) no Ang II is added, and (c) Ang II is added to the reservoir held at negative potential; (d) Ang II addition to the positively-biased reservoir elicits transient changes that resemble translocation. The inset shows a single translocation event. Published under Creative Commons Attribution License in [29].
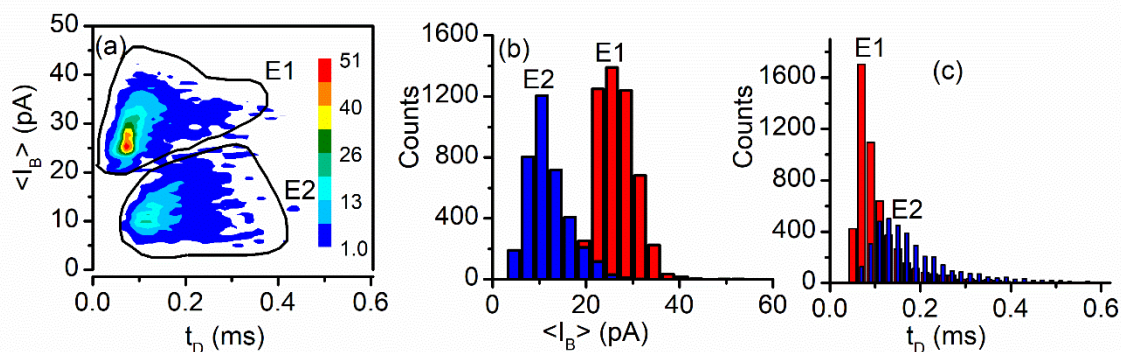
Figure 1-18. **Event analysis for Ang II translocation. (a) The density plot shows two well-defined clusters of recorded events; the color map indicates event density; (b) The current blockage distribution shows a good separation between the two types of events; (c) The distribution in terms of dwell type between the two types of events indicates overlapping and poor separation. Published under Creative Commons Attribution License in [29].**

An important exploration of the same work provides evidence of translocation [29]. Such strong evidence is quite rare for proteins and peptides since they cannot be amplified like DNA, therefore the number of translocated molecules is very small and their detection requires very sensitive techniques to be employed [75,92]. To bring evidence of translocation, the investigators took advantage of the long-term stability presented by large populations of lysenin channels reconstituted into planar lipid membranes. Extended translocation experiments (36 h), in conjunction with large amounts of analytes and numerous channels available for translocation (over 22,000) allowed liquid chromatography - mass spectrometry (LC-MS) identification of Ang II driven by electrophoretic forces on the other side of the membrane (Figure 1-21) through the channels [29].
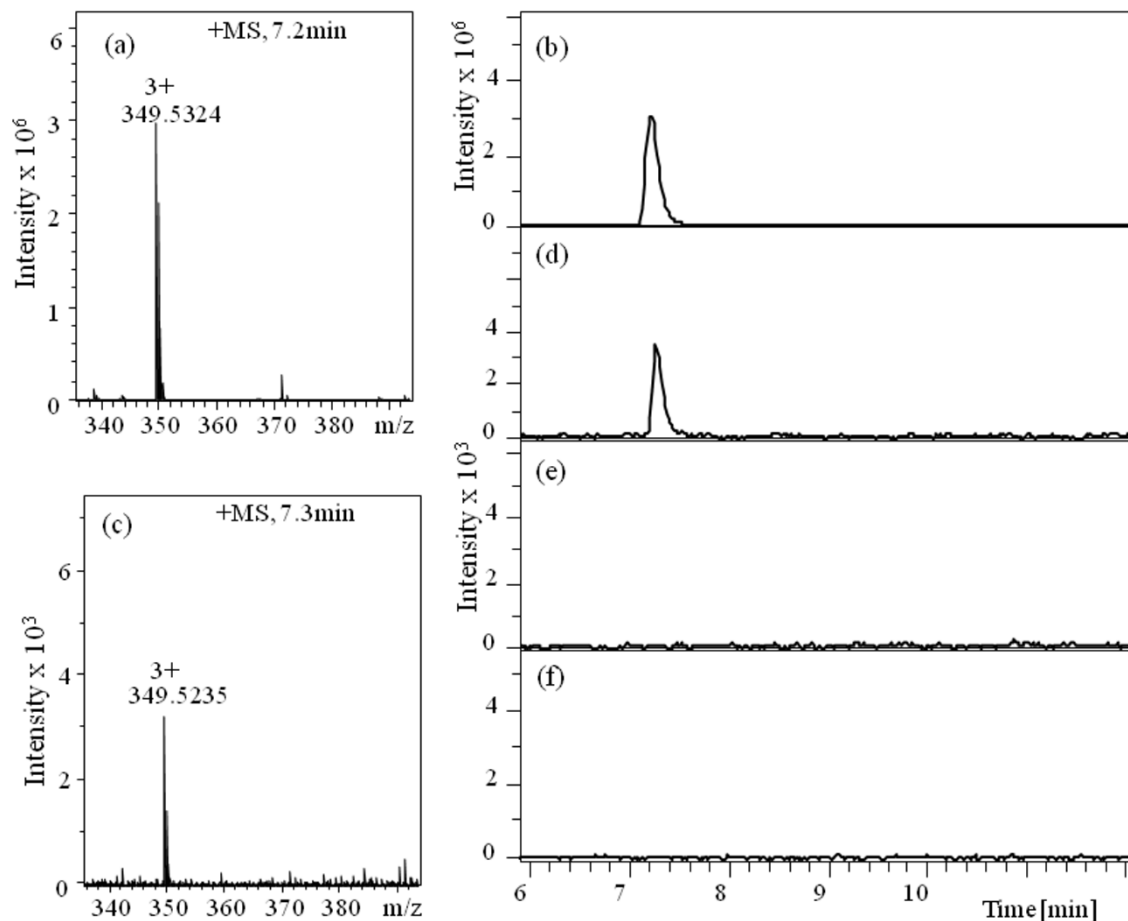
Figure 1-19. LC-MS identification of translocated Ang II peptide molecules. (a) MS reference indicates an m/z ratio of 349.5 (z = 3+) for a lysenin sample. (b) LC chromatogram of the reference Ang II. MS (c) and LC (d) detect and identify Ang II translocated into the negatively charged reservoir. No Ang II is detected upon application of positive transmembrane voltages (e) or following lysenin channel blockage by chitosan (f). Published under Creative Commons Attribution License in [29].

4. Conclusions and Perspective

Lysenin channels are molecular tools anticipated to significantly contribute to the development of high-performance sensing devices. Such devices may be realized based on the intrinsic properties of lysenin channels to adjust their conductance in response to interactions with multivalent ions. While the response is non-specific, such a simple device may find applicability for fast screening purposes. Irreversible channel blockage by cationic polymers can be realized at concentrations in the nM range [29]. Given the

bio-inertness of chitosan, this particular irreversible blockage was recently exploited for temporary permeabilization of live cells and access of non-permeant molecules to the cytosol while maintaining an excellent viability of the target cells [93]. Reversible permeabilization of artificial spherical cell membranes (liposomes) was achieved by employing lysenin channels, La^{3+} ions, and EDTA [93], which may open novel avenues for drug loading into liposomal carriers and controlled release at the desired sites.

Lysenin is a protein amenable to chemical and genetic modifications intended to adjust its sensitivity and specificity for analytes. A lysenin channel inserted into an artificial lipid membrane and endowed with a biorecognition element may lead to the development of single-molecule sensors for molecules and complexes too large to thread the pore; in this case, the binding event near the pore entrance may reduce the ionic flow and facilitate electrical detection from changes in ionic currents.

References

1. Panchal, R.G.; Smart, M.L.; Bowser, D.N.; Williams, D.A.; Petrou, S. Pore-Forming Proteins and their Application in Biotechnology. *Curr. Pharm. Biotechnol.* **2002**, *3*, 99–115.

2. Sugawara, M.; Hirano, A.; Buhlmann, P.; Umezawa, Y. Design and Application of Ion-Channel Sensors Based on Biological and Artificial Receptors. *Bull. Chem. Soc. Jpn.* **2002**, *75*, 187–201.

3. Krishnamurthy, V.; Monfared, S.M.; Cornell, B. Ion-Channel Biosensors—Part I: Construction, Operation, and Clinical Studies. *IEEE Trans. Nanotechnol.* **2010**, *9*, 303–312.

4. Steller, L.; Kreir, M.; Salzer, R. Natural and artificial ion channels for biosensing platforms. *Anal. Bioanal. Chem.* **2012**, *402*, 209–230.

5. Ayub, M.; Bayley, H. Engineered transmembrane pores. *Curr. Opin. Chem. Biol.* **2016**, *34*, 117–126.

6. Howorka, S. Building membrane nanopores. *Nat. Nanotechnol.* **2017**, *12*, 619–630.

7. Kisovec, M.; Rezelj, S.; Knap, P.; Cajnko, M.M.; Caserman, S.; Flasker, A.; Znidarsic, N.; Repic, M.; Mavri, J.; Ruan, Y.; et al. Engineering a pH responsive pore forming protein. *Sci. Rep.* **2017**, *7*, 42231.

8. Cressiot, B.; Ouldali, H.; Pastoriza-Gallego, M.; Bacri, L.; Van der Goot, F.G.; Pelta, J. Aerolysin, a Powerful Protein Sensor for Fundamental Studies and Development of Upcoming Applications. *ACS Sens.* **2019**, *4*, 530–548.

9. Majd, S.; Yusko, E.C.; Billeh, Y.N.; Macrae, M.X.; Yang, J.; Mayer, M. Applications of biological pores in nanomedicine, sensing, and nanoelectronics. *Curr. Opin. Biotechnol.* **2010**, *21*, 439–476.

10. Bayley, H.; Braha, O.; Gu, L.-Q. Stochastic Sensing with Protein Pores. *Adv. Mater.* **2000**, *12*, 139–142.

11. Bayley, H.; Cremer, P.S. Stochastic sensors inspired by biology. *Nature* **2001**, *413*, 226–230.

12. Block, B.M.; Stacey, W.C.; Jones, S.W. Surface Charge and Lanthanum Block of Calcium Current in Bullfrog Sympathetic Neurons. *Biophys. J.* **1998**, *74*, 2278–2284.

13. Braha, O.; Gu, L.-Q.; Zhou, L.; Xiaofeng, L.; Cheley, S.; Bayley, H. Simultaneous stochastic sensing of divalent metal ions. *Nat. Biotechnol.* **2000**, *18*, 1005–1007.

14. Deamer, D.; Akeson, M.; Branton, D. Three decades of nanopore sequencing. *Nat. Biotechnol.* **2016**, *34*, 518–524.

15. Armstrong, C.M.; Cota, G. Calcium block of Na^+ channels and its effect on closing rate. *Proc. Natl. Acad. Sci. USA* **1999**, *96*, 4154–4157.

16. Kasianowicz, J.J.; Burden, D.L.; Han, L.C.; Cheley, S.; Bayley, H. Genetically Engineered Metal Ion Binding Sites on the Outside of a Channel's Transmembrane β-Barrel. *Biophys. J.* **1999**, *76*, 837–845.

17. Zhang, Y.; Niu, X.; Brelidze, T.I.; Magleby, K.L. Ring of Negative Charge in BK Channels Facilitates Block by Intracellular Mg^{2+} and Polyamines through Electrostatics. *J. Gen. Physiol.* **2006**, *128*, 185–202.

18. Elinder, F.; Arhem, P. Metal effects on ion channel gating. *Q. Rev. Biophys.* **2004**, *36*, 373–427.

19. Rotem, D.; Jayasinghe, L.; Salichou, M.; Bayley, H. Protein detection by nanopores equipped with aptamers. *J. Am. Chem. Soc.* **2012**, *134*, 2781–2787.

20. Stefureac, R.I.; Madampage, C.A.; Andrievskaia, O.; Lee, J.S. Nanopore analysis of the interaction of metal ions with prion proteins and peptides. *Biochem. Cell Biol.* **2010**, *88*, 347–358.

21. Andersen, O.S.; Ingolfsson, H.I.; Lundbaek, J.A. *Ion Channels*; In: Wiley Encyclopedia of Chemical Biology, *Hoboken, NJ, USA,* 2008; pp. 1–14.

22.   Bezanilla, F. Ion Channels: From Conductance to Structure. *Neuron* **2008**, *60*, 456–468.

23.   Phung, T.; Zhang, Y.; Dunlop, J.; Dalziel, J. Bilayer lipid membranes supported on Teflon Filters: A functional environment for ion channels. *Biosens. Bioelectron.* **2011**, *26*, 3127–3135.

24.   Studer, A.; Demarche, S.; Langenegger, D.; Tiefenauer, L. Integration and recording of a reconstituted voltage-gated sodium channel in planar lipid bilayers. *Biosens. Bioelectron.* **2011**, *26*, 1924–1928.

25.   Subrahmanyam, S.; Piletsky, S.A.; Turner, A.P.F. Application of Natural Receptors in Sensors and Assays. *Anal. Chem.* **2002**, *74*, 3942–3951.

26.   Bashford, C.L. Pore-Forming Toxins: Attack and Defence at the Cell Surface. *Cell. Mol. Biol. Lett.* **2001**, *6*, 328–333.

27.   Delcour, A.H. Structure and Function of Pore-Forming—Barrels from Bacteria. *J. Mol. Microbiol. Biotechnol.* **2002**, *4*, 1–10.

28.   Gilbert, R.J. Pore-forming toxins. *Cell. Mol. Life Sci.* **2002**, *59*, 832–844.

29.   Shrestha, N.; Bryant, S.L.; Thomas, C.; Richtsmeier, D.; Pu, X.; Tinker, J.; Fologea, D. Stochastic sensing of Angiotensin II with lysenin channels. *Sci. Rep.* **2017**, *7*, 2448.

30.   Butler, T.Z.; Gundlach, J.H.; Troll, M. Ionic Current Blockades from DNA and RNA Molecules in the α-Hemolysin Nanopore. *Biophys. J.* **2007**, *93*, 3229–3240.

31.   Derrington, I.M.; Craig, J.M.; Stava, E.; Laszlo, A.H.; Ross, B.C.; Brinkerhoff, H.; Nova, I.C.; Doering, K.; Tickman, B.I.; Ronaghi, M.; et al. Subangstrom single-molecule measurements of motor proteins using a nanopore. *Nat. Biotechnol.* **2015**, *33*, 1073–1075.

32.   Haque, F.; Li, J.; Wu, H.C.; Liang, X.J.; Guo, P. Solid-State and Biological Nanopore for Real-Time Sensing of Single Chemical and Sequencing of DNA. *Nano Today* **2013**, *8*, 56–74.

33. Cao, C.; Ying, Y.-L.; Hu, Z.-L.; Liao, D.-F.; Tian, H.; Long, Y.-T. Discrimination of oligonucleotides of different lengths with a wild-type aerolysin nanopore. *Nat. Nanotechnol.* **2016**, *11*, 713–718.

34. Cao, C.; Yu, J.; Wang, Y.-Q.; Ying, Y.-L.; Long, Y.-T. Driven Translocation of Polynucleotides through an Aerolysin Nanopore. *Anal. Chem.* **2016**, *88*, 5046–5049.

35. Bayley, H. Nanopore sequencing: From imagination to reality. *Clin. Chem.* **2015**, *61*, 25–31.

36. Gurnev, P.A.; Nestorovich, E.M. Channel-Forming Bacterial Toxins in Biosensing and Macromolecule Delivery. *Toxins* **2014**, *6*, 2483–2540.

37. Shakor, A.-B.A.; Czurylo, E.A.; Sobota, A. Lysenin, a unique sphingomyelin-binding protein. *FEBS Lett.* **2003**, *542*, 1–6.

38. Yamaji-Hasegawa, A.; Makino, A.; Baba, T.; Senoh, Y.; Kimura-Suda, H.; Sato, S.B.; Terada, N.; Ohno, S.; Kiyokawa, E.; Umeda, M.; et al. Oligomerization and pore formation of a sphingomyelin-specific toxin, lysenin. *J. Biol. Chem.* **2003**, *278*, 22762–22770.

39. Bruhn, H.; Winkelmann, J.; Andersen, C.; Andra, J.; Leippe, M. Dissection of the mechanisms of cytolytic and antibacterial activity of lysenin, a defense protein of the annelid *Eisenia fetida*. *Dev. Comp. Immunol.* **2006**, *30*, 597–606.

40. Ide, T.; Aoki, T.; Takeuchi, Y.; Yanagida, T. Lysenin forms a voltage-dependent channel in artificial lipid bilayer membranes. *Biochem. Biophys. Res. Commun.* **2006**, *346*, 288–292.

41. Kwiatkowska, K.; Hordejuk, R.; Szymczyk, P.; Kulma, M.; Abdel-Shakor, A.-B.; Plucienniczak, A.; Dolowy, K.; Szewczyk, A.; Sobota, A. Lysenin-His, a sphingomyelin-recognizing toxin, requires tryptophan 20 for cation-selective channel assembly but not for membrane binding. *Mol. Membr. Biol.* **2007**, *24*, 121–134.

42. Shogomori, H.; Kobayashi, T. Lysenin: A sphingomyelin specific pore-forming toxin. *Biochim. Biophys. Acta* **2008**, *1780*, 612–618.

43. Yamaji, A.; Sekizawa, Y.; Emoto, K.; Sakuraba, H.; Inoue, K. Lysenin, A novel sphingomyelin-specific binding protein. *J. Biol. Chem.* **1998**, *273*, 5300–5306.

44. De Colibus, L.; Sonnen, A.F.; Morris, K.J.; Siebert, C.A.; Abrusci, P.; Plitzko, J.; Hodnik, V.; Leippe, M.; Volpi, E.; Anderluh, G.; et al. Structures of lysenin reveal a shared evolutionary origin for pore-forming proteins and its mode of sphingomyelin recognition. *Structure* **2012**, *20*, 1498–1507.

45. Kulma, M.; Dadlez, M.; Kwiatkowska, K. Insight into the Structural Dynamics of the Lysenin During Prepore-to-Pore Transition Using Hydrogen—Deuterium Exchange Mass Spectrometry. *Toxins* **2019**, *11*, 462.

46. Munguira, I.L.B.; Takahashi, H.; Casuso, I.; Scheuring, S. Lysenin Toxin Membrane Insertion is pH-Dependent but Independent of Neighboring Lysenins. *Biophys. J.* **2017**, *113*, 2029–2036.

47. Bokori-Brown, M.; Martin, T.G.; Naylor, C.E.; Basak, A.K.; Titball, R.W.; Savva, C.G. Cryo-EM structure of lysenin pore elucidates membrane insertion by an aerolysin family protein. *Nat. Commun.* **2016**, *7*, 11293.

48. Yilmaz, N.; Kobayashi, T. Visualization of Lipid Membrane Reorganization Induced by a Pore-Forming Toxin Using High-Speed Atomic Force Microscopy. *ACS Nano* **2015**, *9*, 7960–7967.

49. Yilmaz, N.; Yamada, T.; Greimel, P.; Uchihashi, T.; Ando, T.; Kobayashi, T. Real-Time Visualization of Assembling of a Sphingomyelin-Specific Toxin on Planar Lipid Membranes. *Biophys. J.* **2013**, *105*, 1397–1405.

50. Yilmaz, N.; Yamaji-Hasegawa, A.; Hullin-Matsuda, F.; Kobayashi, T. Molecular mechanisms of action of sphingomyelin-specific pore-forming toxin, lysenin. *Semin. Cell Dev. Biol.* **2018**, *73*, 188–198.

51. Podobnik, M.; Savory, P.; Rojko, N.; Kisovec, M.; Wood, N.; Hambley, R.; Pugh, J.; Wallace, E.J.; McNeill, L.; Bruce, M.; et al. Crystal structure of an invertebrate cytolysin pore reveals unique properties and mechanism of assembly. *Nat. Commun.* **2016**, *7*, 11598.

52. Kulma, M.; Herec, M.; Grudzinski, W.; Anderluh, G.; Gruszecki, W.I.; Kwiatkowska, K.; Sobota, A. Sphingomyelin-rich domains are sites of lysenin oligomerization: Implications for raft studies. *Biochim. Biophys. Acta. Biomembr.* **2010**, *1798*, 471–481.

53. Fologea, D.; Krueger, E.; Lee, R.; Naglak, M.; Mazur, Y.; Henry, R.; Salamo, G. Controlled gating of lysenin pores. *Biophys. Chem.* **2010**, *146*, 25–29.

54. Fologea, D.; Krueger, E.; Mazur, Y.I.; Stith, C.; Okuyama, Y.; Henry, R.; Salamo, G.J. Bi-stability, hysteresis, and memory of voltage-gated lysenin channels. *Biochim. Biophys. Acta. Biomembr.* **2011**, *1808*, 2933–2939.

55. Ishitsuka, R.; Sato, S.B.; Kobayashi, T. Imaging Lipid Rafts. *J. Biochem.* **2005**, *137*, 249–254.

56. Krueger, E.; Bryant, S.; Shrestha, N.; Clark, T.; Hanna, C.; Pink, D.; Fologea, D. Intramembrane congestion effects on lysenin channel voltage-induced gating. *Eur. Biophys. J.* **2016**, *45*, 187–194.

57. Ishitsuka, R.; Kobayashi, T. Lysenin: A new tool for investigating membrane lipid organization. *Anat. Sci. Int.* **2004**, *79*, 184–190.

58. Aoki, T.; Hirano, M.; Takeuchi, Y.; Kobayashi, T.; Yanagida, T.; Ide, T. Single channel properties of lysenin measured in artificial lipid bilayers and their application to biomolecule detection. *Proc. Jpn. Acad. Ser. B Phys. Biol. Sci.* **2010**, *86*, 920–925.

59. Bryant, S.; Shrestha, N.; Carnig, P.; Kosydar, S.; Belzeski, P.; Hanna, C.; Fologea, D. Purinergic control of lysenin's transport and voltage-gating properties. *Purinergic Signal.* **2016**, *12*, 549–559.

60. Bryant, S.L.; Eixenberger, J.E.; Rossland, S.; Apsley, H.; Hoffmann, C.; Shrestha, N.; McHugh, M.; Punnoose, A.; Fologea, D. ZnO nanoparticles modulate the ionic transport and voltage regulation of lysenin nanochannels. *J. Nanobiotechnol.* **2017**, *15*, 90.

61. Fologea, D.; Al Faori, R.; Krueger, E.; Mazur, Y.I.; Kern, M.; Williams, M.; Mortazavi, A.; Henry, R.; Salamo, G.J. Potential analytical applications of lysenin channels for detection of multivalent ions. *Anal. Bioanal. Chem.* **2011**, *401*, 1871–1879.

62. Fologea, D.; Krueger, E.; Al Faori, R.; Lee, R.; Mazur, Y.I.; Henry, R.; Arnold, M.; Salamo, G.J. Multivalent ions control the transport through lysenin channels. *Biophys. Chem.* **2010**, *152*, 40–45.

63. Fologea, D.; Krueger, E.; Rossland, S.; Bryant, S.; Foss, W.; Clark, T. Cationic Polymers Inhibit the Conductance of Lysenin Channels. *Sci. World J.* **2013**, 316758, doi: 10.1155/2013/316758.

64. Kasianowicz, J.J.; Brandin, E.; Branton, D.; Deamer, D.W. Characterization of individual polynucleotide molecules using a membrane channel. *Proc. Natl. Acad. Sci. USA* **1996**, *93*, 13770–13773.

65. Bezrukov, S.M. Ion Channels as Molecular Coulter Counters to Probe Metabolite Transport. *J. Membr. Biol.* **2000**, *174*, 1–13.

66. Deamer, D.W.; Akeson, M. Nanopores and nucleic acids: Prospects for ultrarapid sequencing. *TIBTECH* **2000**, *18*, 147–151.

67. Li, J.; Gershow, M.; Stein, D.; Brandin, E.; Golovchenko, J.A. DNA Molecules and Configurations in a Solid-state Nanopore Microscope. *Nat. Mater.* **2003**, *2*, 611–615.

68. Storm, A.J.; Chen, J.H.; Ling, X.S.; Zandbergen, H.W.; Dekker, C. Fabrication of solid-state nanopores with single-nanometre precision. *Nat. Mater.* **2003**, *2*, 537–540.

69. Dekker, C. Solid-state nanopores. *Nat. Nanotechnol.* **2007**, *2*, 209–215.

70. Stefureac, R.; Waldner, L.; Howard, P.; Lee, J.S. Nanopore Analysis of a Small 86-Residue Protein. *Small* **2008**, *4*, 59–63.

71. Stoloff, D.H.; Wanunu, M. Recent trends in nanopores for biotechnology. *Curr. Opin. Biotechnol.* **2013**, *24*, 699–704.

72. Traversi, F.; Raillon, C.; Benameur, S.M.; Liu, K.; Khlybov, S.; Tosun, M.; Krasnozhon, D.; Kis, A.; Radenovic, A. Detecting the translocation of DNA through a nanopore using graphene nanoribbons. *Nat. Biotechnol.* **2013**, *8*, 939–945.

73. Ashton, P.M.; Nair, S.; Dallman, T.; Rubino, S.; Rabsch, W.; Mwaigwisya, S.; Wain, J.; O'Grady, J. MinION nanopore sequencing identifies the position and structure of a bacterial antibiotic resistance island. *Nat. Biotechnol.* **2014**, *33*, 296–300.

74. Laszlo, A.H.; Derrington, I.M.; Ross, B.C.; Brinkerhoff, H.; Adey, A.; Nova, I.C.; Craig, J.M.; Langford, K.W.; Samson, J.M.; Daza, R. Decoding long nanopore sequencing reads of natural DNA. *Nat. Biotechnol.* **2014**, *32*, 829–833.

75. Pastoriza-Gallego, M.; Breton, M.-F.; Discala, F.; Auvray, L.; Betton, J.-M.; Pelta, J. Evidence of Unfolded Protein Translocation through a Protein Nanopore. *ACS Nano* **2014**, *8*, 11350–11360.

76. Feng, Y.; Zhang, Y.; Ying, C.; Wang, D.; Du, C. Nanopore-based Fourth-generation DNA Sequencing Technology. *Genom. Proteom. Bioinform.* **2015**, *13*, 4–16.

77. Deng, Y.; Huang, Q.; Zhao, Y.; Zhou, D.; Ying, C.; Wang, D. Precise fabrication of a 5 nm graphene nanopore with a helium ion microscope for biomolecule detection. *Nanotechnology* **2017**, *28*, 045302.

78. Butler, T.Z.; Pavlenok, M.; Derrington, I.M.; Niederweis, M.; Gundlach, J.H. Single-molecule DNA detection with an engineered MspA protein nanopore. *Proc. Natl. Acad. Sci. USA* **2008**, *105*, 20647–20652.

79. Wang, S.; Haque, F.; Rychahou, P.G.; Evers, B.M.; Guo, P. Engineered Nanopore of Phi29 DNA-Packaging Motor for Real-Time Detection of Single Colon Cancer Specific Antibody in Serum. *ACS Nano* **2013**, *7*, 9814–9822.

80. Wanunu, M. Nanopores: A journey towards DNA sequencing. *Phys. Life Rev.* **2012**, *9*, 125–158.

81. Belzeski, P.; Shrestha, N.; Bryant, S.; Tinker, J.; Thomas, C.A.; Richtsmeier, D.; Fologea, D. Sensing ssDNA Molecules with Single Lysenin Channels. *Biophys. J.* **2017**, *112*, 153a–154a.

82. Stefureac, R.; Long, Y.-t.; Kraatz, H.-B.; Howard, P.; Lee, J.S. Transport of—Helical Peptides through—Hemolysin and Aerolysin Pores. *Biochemistry* **2006**, *45*, 9172–9179.

83. Diederichs, T.; Pugh, G.; Dorey, A.; Xing, Y.; Burns, J.R.; Hung Nguyen, Q.; Tornow, M.; Tampe, R.; Howorka, S. Synthetic protein-conductive membrane nanopores built with DNA. *Nat. Commun.* **2019**, *10*, 5018.

84. Ji, Z.; Wang, S.; Zhao, Z.; Zhou, Z.; Haque, F.; Guo, P. Fingerprinting of Peptides with a Large Channel of Bacteriophage Phi29 DNA Packaging Motor. *Small* **2016**, *12*, 4572–4578.

85. Singh, P.R.; Barcena-Uribarri, I.; Modi, N.; Kleinekathofer, U.; Benz, R.; Winterhalter, M.; Mahendran, K.R. Pulling Peptides across Nanochannels: Resolving Peptide Binding and Translocation through the Hetero-oligomeric Channel from Nocardia farcinica. *ACS Nano* **2012**, *6*, 10699–10707.

86. Zhao, Q.; Jayawardhana, D.A.; Wang, D.; Guan, X. Study of Peptide Transport through Engineered Protein Channels. *J. Phys. Chem. B* **2009**, *113*, 3572–3578.

87. Elliott, I.; Batty, E.M.; Ming, D.; Robinson, M.T.; Nawtaisong, P.; de Cesare, M.; Newton, P.N.; Bowden, R. Oxford Nanopore MinION Sequencing Enables Rapid Whole Genome Assembly of Rickettsia typhi in a Resource-Limited Setting. *Am. J. Trop. Med. Hyg.* **2020**, *102*, 408–414.

88. Patel, A.; Belykh, E.; Miller, E.J.; George, L.L.; Martirosyan, N.L.; Byvaltsev, V.A.; Preul, M.C. MinION rapid sequencing: Review of potential applications in neurosurgery. *Surg. Neurol. Int.* **2018**, *9*, 157–157.

89. Lamichhane, U.; Islam, T.; Prasad, S.; Weingart, H.; Mahendran, K.R.; Winterhalter, M. Peptide translocation through the mesoscopic channel: Binding kinetics at the single molecule level. *Eur. Biophys. J.* **2013**, *42*, 363–369.

90. Mereuta, L.; Roy, M.; Asandei, A.; Lee, J.K.; Park, Y.; Andricioaei, I.; Luchian, T. Slowing down single-molecule trafficking through a protein nanopore reveals intermediates for peptide translocation. *Sci. Rep.* **2014**, *4*, 3885.

91. Plesa, C.; Dekker, C. Data analysis methods for solid-state nanopores. *Nanotechnology* **2015**, *26*, 084003.

92. Fologea, D.; Ledden, B.; McNabb, D.S.; Li, J. Electrical characterization of protein molecules by a solid-state nanopore. *Appl. Phys. Lett.* **2007**, *91*, 0539011.

93. Shrestha, N.; Thomas, C.A.; Richtsmeier, D.; Bogard, A.; Hermann, R.; Walker, M.; Abatchev, G.; Brown, R.J.; Fologea, D. Temporary Membrane Permeabilization via the Pore-Forming Toxin Lysenin. *Toxins* **2020**, *12*, 343.

CHAPTER THREE: THE IONIC SELECTIVITY OF LYSENIN CHANNELS IN OPEN

AND SUB-CONDUCTING STATES

Andrew Bogard [1,2], Pangaea W. Finn [1], Fulton McKinney [1], Ilinca M. Flacau [1], Aviana R. Smith [1], Rosey Whiting [1,2] and Daniel Fologea [1,2,]*

[1] Department of Physics, Boise State University, Boise, ID 83725, USA

[2] Biomolecular Sciences Graduate Program, Boise State University, Boise, ID 83725, USA

*Correspondence: danielfologea@boisestate.edu

Abstract

The electrochemical gradients established across cell membranes are paramount for execution of biological functions. Besides ion channels, other transporters, such as exogenous pore-forming toxins, may present ionic selectivity upon reconstitution in natural and artificial lipid membranes and contribute to the electrochemical gradients. In this context, we utilized electrophysiology approaches to assess the ionic selectivity of the pore-forming toxin lysenin reconstituted in planar bilayer lipid membranes. The membrane voltages were determined from the reversal potentials recorded upon channel exposure to asymmetrical ionic conditions, and the permeability ratios calculated from the fit with the Goldman-Hodgkin-Katz equation. Our work shows that lysenin channels are ion-selective and the determined permeability coefficients are cation and anion-species dependent. We also exploited the unique property of lysenin channels to transition to a stable sub-conducting state upon exposure to calcium ions and assessed their subsequent change in ionic selectivity. The observed loss of selectivity was implemented in an electrical model describing the dependency of reversal potentials on calcium concentration. In conclusion, our work demonstrates that this pore-forming toxin presents ionic selectivity but this is adjusted by the particular conduction state of the channels.

Introduction

The biological activity of ion channels is a direct consequence of three common characteristics: high transport rate, regulation, and selectivity [1]. Ionic selectivity is a salient feature of ion channels leading to creating and maintaining electrochemical gradients needed for the correct functionality of cells [2-6], and the modulation of these

gradients by physical and chemical stimuli is essential for excitability [1,7,8]. In addition, dynamic resting membrane potentials originating in ionic selectivity are now considered critical for a larger variety of processes such as cell cycle, volume control, cell migration, wound healing, and cell proliferation [9]. Another category of membrane transporters that shares similarities with ion channels is represented by pore-forming toxins (PFTs), which introduce conducting pathways in the host membrane, capable of sustaining high transport rates [10]. Some PFTs may also present regulation by physical and chemical stimuli [11-14], and selectivity [15-19]. Although the ionic selectivity of PFTs is generally far under that of ion channels, prior investigations provided valuable information on the nature of the selectivity filters, and even allowed intentional selectivity modulation by chemical modifications [16]. Such achievements are anticipated not only to improve our understanding of the selectivity mechanisms and physiological relevance but also for developing new drugs, therapeutic strategies, and applications in synthetic biology. In this respect, we focused our work on investigating the ionic selectivity of lysenin channels. Lysenin is an intriguing PFT extracted from the red earthworm *E. fetida*, which inserts very stable channels in membranes containing sphingomyelin [13,17,20-24]. The pore-forming mechanism comprises binding to sphingomyelin and deployment of beta-sheets through the host membrane [25,26]. Lysenin exhibits high transport rate, and is also regulated by voltage and ligands [12-14]. Interestingly, the voltage-gating feature requires anionic lipids in the host membrane, and is suppressed when neutral lipids are used [13]. However, the gating induced by multivalent ions acting as ligands is preserved in both neutral and charged lipid membranes [14]. Previous investigations on lysenin suggest a weak cation selectivity

[15,17], as inferred from measuring the membrane voltage achieved upon creating asymmetrical ionic conditions. However, these are single point measurements, and no extensive study of the selectivity in various ionic conditions is available. To fill this gap in our knowledge, we employed electrophysiology measurements and expanded the investigations on the selectivity of lysenin channels inserted into planar lipid membranes by considering multiple ions and concentration conditions. These investigations allowed us to provide quantitative analyses of the cation selectivity and show differences between cationic ion species (i.e., Na^+, K^+, Cs^+, and Li^+). In addition, we also demonstrated that lysenin channels present different permeabilities for anionic species (i.e., Cl^-, and I^-). These features, identified for fully-open lysenin channels, resemble the selectivity of ion channels. However, ion channels such as VDAC [27-30], mechano-sensitive, [31-33], sodium [34], and potassium [35,36] may undergo conformational transitions that lead to intermediate, sub-conducting states. Although the physiological relevance of sub-conductance is poorly understood, adjustments of the ionic permeabilities in such sub-conducting states have been reported [27-29]. For a better understanding of how intermediate conductance states adjust the transport properties of protein pores, we exploited a unique feature of lysenin channels, which is the attainment of stable sub-conducting states in the presence of divalent ions (i.e., Ca^{2+}) [12,14]. In this line, our experimental work demonstrates that the selectivity of lysenin channels to monovalent ions is significantly diminished when they are in the sub-conducting state, which leads to vanishing membrane voltages. The diminished selectivity was assessed by employing a simple electrical model, which in conjunction with the Langmuir isothermal adsorption

model describing the divalent ion – channel interaction [12] provided a good match of the experimental data.

Materials and Methods

Materials

The bilayer lipid membranes (BLMs) utilized for all the experiments described in this work were composed of asolectin (Sigma-Aldrich, St. Louis, MO, USA), cholesterol (Sigma-Aldrich), and sphingomyelin (Avanti Polar Lipids, Alabaster, AL, USA). The lipids in powder form were solubilized in n-decane (TCI America, Portland, OR, USA) and mixed at a 10:4:4 molar ratio for a final concentration of 50 mg asolectin/mL mixture. NaCl, KCl, CsCl, LiCl, KI, and $CaCl_2$ (ThermoFisher Scientific, Waltham, MA, USA) were dissolved in deionized water and buffered with 20 mM Hepes (ThermoFisher Scientific) for a final pH of 7.2. The utilized solutions were either starting support electrolyte (50 mM salt concentration) or high-concentration stock solutions for ionic additions (2-3 M final concentration).

Lysenin was produced and purified in our Biomolecular Research Center core facility [37] through established protocols [37-40]. Briefly, lysenin cDNA for the full-length protein (accession number D85846) was synthesized and subcloned in pMAL-c5x (GenScript, Piscataway, NJ, USA). This construct generates a maltose binding protein-linked lysenin with a Factor Xa cleavage site between them. Following transformation of the plasmid into *Escherichia coli* BL21 competent cells and purification [37-40], the full-length protein was thoroughly tested for activity and transport properties: channel insertion and voltage regulation [13,17], ligand-induced gating [12,14], and attainment of sub-conducting states in the presence of Ca^{2+} ions [12,14]. A stock solution of lysenin

dissolved in Phosphate Buffered Saline (PBS1x, pH = 7.2, Sigma-Aldrich) at 1μg/mL

concentration was utilized for channel reconstitution in artificial membranes. All other

common chemicals were purchased from various producers and distributors.

Methods

BLM production, characterization, and channel insertion

To investigate the selectivity of lysenin channels we utilized a typical planar BLM

setup detailed in prior work [12]. The membrane was formed by the painting method in a

small hole (~100 μM diameter) produced in a thin PTFE film (125 μm thickness) by an

electric spark. The two ~1mL reservoirs were filled with support electrolyte (50 mM salt,

if not otherwise indicated). The electrical connections with the Axopatch 200B amplifier

(Molecular Devices, San Jose, CA, USA) were made via Ag/AgCl electrodes connected

to the electrolyte solutions through salt bridges made with 2% TopVision Low Melting

Point Agarose (ThermoFisher Scientific) and 1M NaCl to minimize the junction

potential. The electrodes were wired to the headstage of the electrophysiology amplifier.

The signal was digitized with the Digitizer 1440A (Molecular Devices) and recorded on a

computer for further analyses. All the experiments were performed at room temperature

(22.5 ± 0.5 °C).

The bilayer formation and its integrity were monitored by employing membrane

capacitance and conductance measurements. After a stable and intact, non-conducting

membrane was formed, channel insertion was initiated by addition of small amounts of

lysenin (~0.3 nM final concentration) to the grounded reservoir. Channel insertion was

observed as a step-wise variation of the ionic currents recorded at -80 mV bias potential

(to avoid the voltage-induced gating) and under solution stirring with a low noise magnetic stirrer (Warner Instruments, Hamden, CT, USA).

Voltage measurements

Insertion completion was indicated by stable ionic currents, achieved in approximately one hour after lysenin addition. The amplitude of the macroscopic ionic currents and the unitary conductance of single channels were used to estimate the number of inserted channels, which varied from several hundred to a few thousand for each membrane we used. After stabilization, we determined the membrane voltages originating from the chemical gradients produced by addition of small and known amounts of concentrated ionic solutions to the grounded reservoir. The experimental data were recorded with pClamp 10.6.2.2 (Molecular Devices), plotted with Clampfit 10.6.2.2 (Molecular Devices), and the membrane voltages V_m determined as the x-intercept of the IV plots (the reversal potentials) recorded for each of the asymmetrical ionic conditions (including symmetrical ionic conditions controls) [7,15,17,18,30]. For each IV plot we set a voltage range of 20 mV and lower and upper limits such that the plots crossed the x axis. A single voltage sweep was set for 20 s, and the sampling rate was set to 10 samples/s (hence a 0.1 mV resolution). As detailed in Figure 2-1 as an example for NaCl, for each of the concentration ratio (c_r) conditions (c_r = 1, 2.35, and 5.12, respectively) we recorded three sweeps within the same experiment; the excellent overlapping of the sweeps for identical ionic conditions indicates attaining a steady state. The linear fit of the experimental data in Clampfit provided the y-intercepts and slopes, which were next used to determine the x-intercepts (membrane voltages).
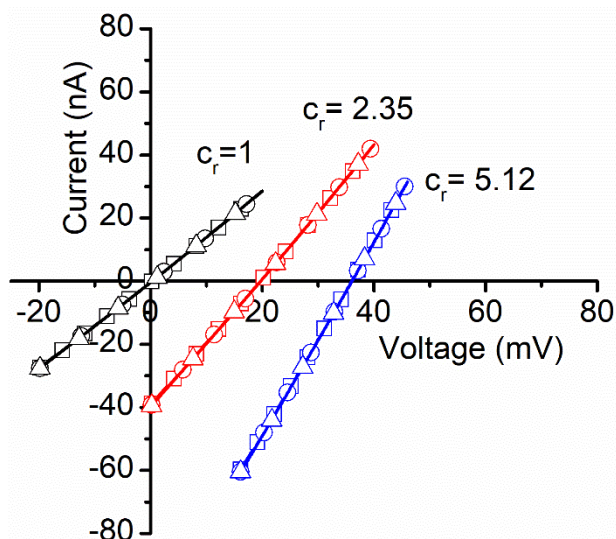
Figure 20. **Experimental determination of membrane voltages for lysenin channels reconstituted into planar BLMs. Addition of NaCl to the grounded reservoirs leads to a right shift of the IV plots, indicative of membrane voltage occurrence. An individual experiment employed three IV sweeps for each NaCl concentration ratio c_r, and their average was used to calculate the membrane voltage as the x-intercept. All the points in the plots are experimental; the symbols have been added as visual aids to discriminate between sweeps recorded in identical experimental conditions.**

The averaged values of the membrane voltage were determined by using a custom-made analysis program in R, which also calculated the concentration ratios for each of the experimental conditions by accounting for added ions. The averaged membrane voltages and concentration ratios were plotted and fitted (Origin 8.5.1, OriginLab Corporation, Northampton, MA) with the Goldman-Hodgkin-Katz (GHK) equation [7,15-18,30], adjusted for one cation (C^+) and one anion (A^-) monovalent ion species:

$$Vm = -\frac{RT}{F}\ln\left(\frac{P_{C^+}[C^+]_h + P_{A^-}[A^-]_g}{P_{C^+}[C^+]_g + P_{A^-}[A^-]_h}\right)$$

Eq. 1

where R is the universal gas constant (R=8.31 J mol^{-1} K^{-1}), T is the absolute temperature, F is the Faraday number (F = 96,485.35 C mol^{-1}), P denotes the permeabilities of the ionic species, and the square brackets indicates their concentrations in the ground (g) and headstage (h) reservoirs, respectively.

The GHK fit provided the permeability ratio of cations to anions (i.e., P_{C+}/P_{A-}) under the assumption that ionic diffusion does not change the ionic concentrations achieved by salt addition, i.e. the concentrations of cations and anions in the same reservoir are equal after electrochemical equilibrium is achieved. This assumption is fully justified by the very small number of ions (relative to the bulk number) needed to diffuse for establishing the membrane voltages. The experiments for determining the membrane voltages and estimating the permeability ratios were independently replicated three times, and the statistical analyses performed in Origin 8.5.1 provided the average values and standard deviations of the permeability ratios. No significant differences in membrane voltages were determined from experiments comprising identical solution conditions but different numbers of inserted channels.

Investigations on sub-conducting channels

To investigate the selectivity of lysenin channels in sub-conducting conditions we utilized buffered KCl (50 mM) solutions as starting support electrolyte. The first set of experiments comprised sub-conductance achievement by addition of $CaCl_2$ to both reservoirs (36 mM final concentration), followed by measurements of the membrane voltage upon successive KCl additions to the grounded reservoir. The next set of experiments comprised achieving a membrane voltage by establishing chemical gradients with KCl addition to the grounded reservoir, followed by monitoring the changes in the

membrane voltage upon additions of $CaCl_2$ to both reservoirs. The membrane voltage was determined from the IV plots by following the same procedure described above for monovalent ions. The influence of the Ca^{2+} ions on permeability was assessed by employing an electrical model of the membrane and equations detailed in the corresponding results and discussion section.

Results

Lysenin channels in open state are cation-selective

The selectivity of lysenin channels for monovalent ions was first investigated for chlorides by additions of small volumes (ranging from 10 to 50 µL) of buffered 3M stock solutions to the grounded reservoir. The starting solutions in both reservoirs were buffered 50 mM electrolyte solutions of the same chemical species as stocks, with the exception of experiments that comprised mixtures of chlorides and iodides (detailed in the results section). The control IV plots were run to ensure the absence of any offset transmembrane voltage in symmetrical ionic conditions, after which the membrane voltages were determined for each particular chemical gradient. The results depicted in Figure 2-2 show typical recordings (i.e., average values obtained from three sweeps within the same experimental setup) and the fit with the GHK equations for NaCl, KCl, CsCl, and KCl. Subsequent addition of chlorides to the grounded reservoir led to the development of transmembrane voltages with amplitude that increased monotonically with the concentration ratios (Figure 2-2) for each of the ionic species, which is a direct consequence of ionic selectivity. The P_{C+}/P_{A-} values determined from three independent experiments for the different ionic compositions are 22.4 ± 1.3 for NaCl, 7.5 ± 0.5 for KCl, 12.3 ± 0.5 for CsCl, and 12.9 ± 0.9 for LiCl. All these values clearly indicate that

lysenin channels are slightly selective for cations, as suggested in prior work from single-point measurements [15,17]. Since we have no reason to assume that the permeability of Cl^- is different when the ions originated in the dissociation of different salts, the different permeability ratio values also indicate that the selectivity of lysenin channels also manifests between cationic species. For example, our experimental results suggest that the permeability for Na^+ is ~3 times larger than the one for K^+, while Cs^+ and Li^+ have similar permeabilities. Such features are essential for many ion channels; however, their capabilities with regard to discriminating between similar ionic species may attain significantly larger values compared to lysenin channels.
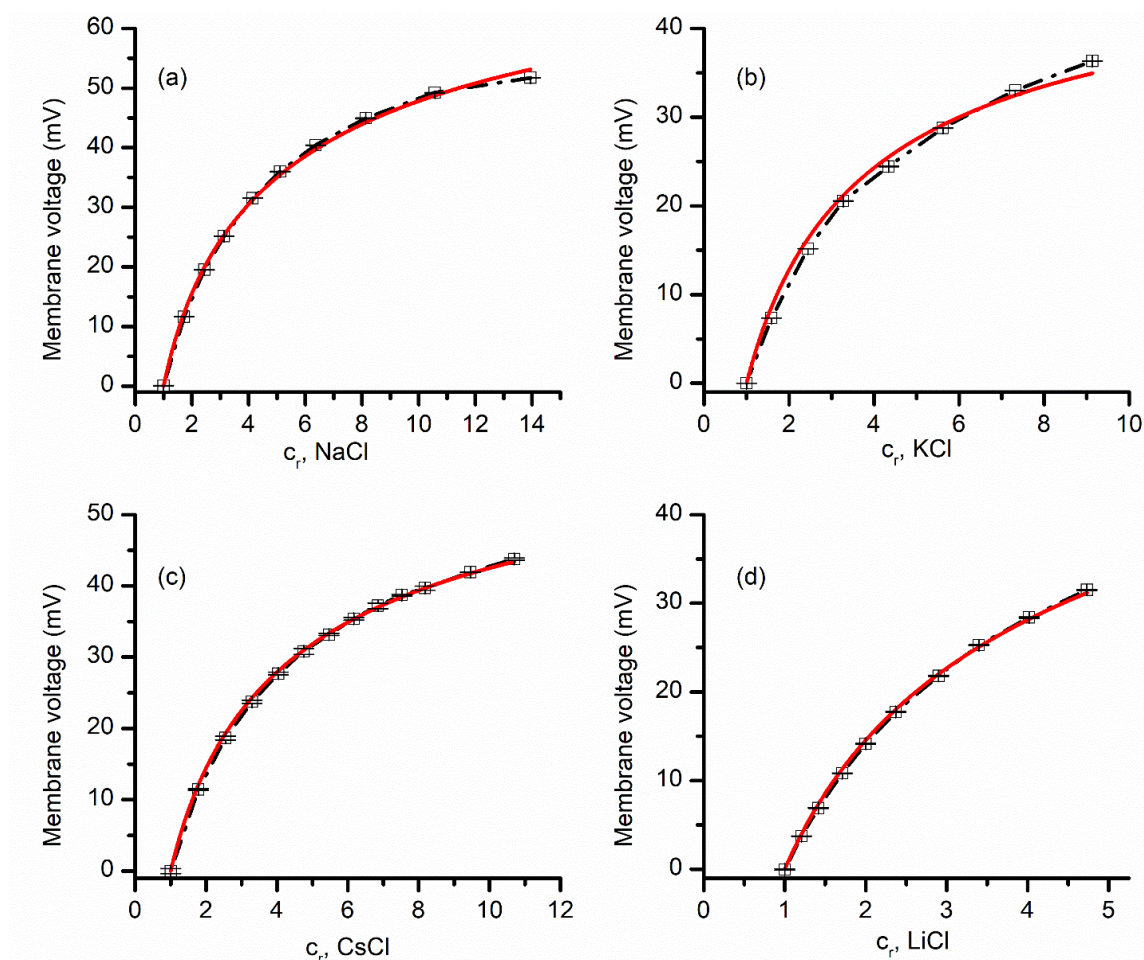
Figure 23-2. Lysenin has selectivity for monovalent cations. The membrane voltage as a function of concentration ratio cr, measured for NaCl (a), KCl (b), CsCl (c), and LiCl (d). Each experimental point in the plot (symbols) shows the average value ±SD (n=3) from three sweeps recorded in single experiments. The full lines are the fit with the GHK equation (single experiments), which was used to determine the permeability ratio of cations over anions from the membrane voltage and concentration ratio cr values for each of the indicated ionic species.

Lysenin channels in open state present different permeability for anions

The above experiments provided information with regards to lysenin channels' selectivity for cations versus anions, together with an indication that lysenin also discriminates between similar cation species. Next, we asked whether lysenin channels present different selectivity for similar anion species. To answer this question, we ran experiments employing KI for the 50 mM support electrolyte and a 3 M KI stock solution

for creating chemical gradients. The plot of the transmembrane voltage versus concentration ratio depicted in Figure 2-3 shows that a concentration ratio of ~5 led to a transmembrane voltage of ~32 mV. This value is slightly larger than what was obtained for a similar KCl ratio (see Figure 2-2), indicative of different permeabilities of I^- and Cl^- ions. The permeability ratio P_{C+}/P_{A-} determined from the GHK equation for KI (i.e., 27.3 ± 0.7) was larger than what we obtained for the KCl case (~7.5); this result suggests that the lysenin's permeability for I^- is a few times smaller than for Cl^-. Since the two permeabilities are different, we predicted that the membrane voltages established across a membrane containing lysenin channels would be different from addition of KI over KCl support solutions, or KCl over KI. This prediction was confirmed experimentally (Figure 2-3). Addition of KCl over KI support electrolyte produced a membrane voltage significantly smaller than what was measured for the same concentration ratios when KI was added over KCl. Moreover, addition of KCl over KI resembled the KCl-only behavior (shown in Figure 2-2), while KI addition over KCl was rather similar to the KI-only measurements (Figure 2-3a).
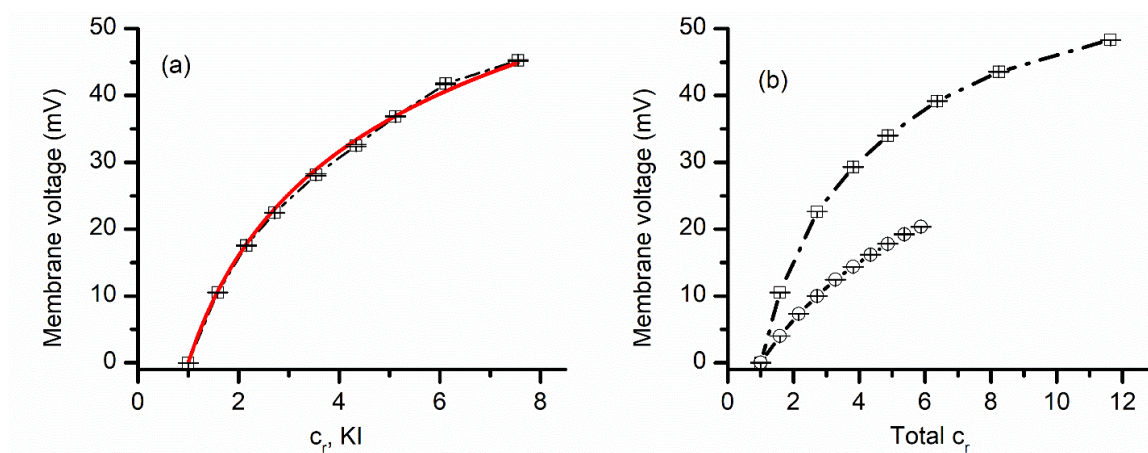
Figure 24. **Lysenin channels present different permeability for anions. The membrane voltage as a function of concentration ratio measured for KI addition to a KI support electrolyte solution (a). The full line is the fit with the GHK equation, which was used to determine the permeability ratio of K+ over I-. Panel (b) shows the measured membrane voltage as a function of total salt concentration ratio when KI was added over 50 mM KCl (open circles), or KCl was added over 50 mM KI (open squares) to the grounded reservoir. The dashed line is used as a visual aid. For each panel, the experimental points in the plot (symbols) show the average value ±SD (n=3) from three sweeps recorded in individual experiments.**

Investigations on the selectivity of lysenin channels in sub-conducting states

Our next investigations focused on less explored aspects of gated channels, which are potential hidden changes of their biophysical properties that occur when the conformational changes lead to transitions to sub-conducting states. Several channels are known to undergo sub-conducting states [29,31], i.e. an intermediate state between open and closed, characterized by a non-zero, intermediate conductance. The physiological relevance of such sub-conducting states is still unclear [28], and deep investigations of such aspects are hindered not only by the limited channel species that present such states, but also by a certain inability to control these generally unstable states. Lysenin is a notable exception, and prior experiments demonstrate that lysenin channels may be forced to adopt a stable sub-conducting state upon exposure to divalent organic and

inorganic divalent cations [12]. For example, Ca^{2+} or Mg^{2+} at concentrations over 20 mM

force the lysenin channels to adopt a stable half-closed state, for which the conductance is

~20% of the conductance of a fully open channel [12]. Therefore, we exploited this

remarkable property of lysenin channels to investigate their selectivity in sub-conducting

states and compare it with the open state. To achieve this objective, we first tested the

development of a transmembrane voltage by imposing non-symmetrical ionic

concentrations of KCl upon a membrane containing sub-conducting lysenin channels. In

this respect, we used a typical experimental approach for inserting fully open lysenin

channels in a membrane bathed by 50 mM KCl. After stabilization, we added 36 mM

$CaCl_2$ to both reservoirs to force the channels to transition to a sub-conducting state.

Although prior work suggests that Ca^{2+} ions permeate the lysenin channels in both open

and sub-conducting states [12], we added $CaCl_2$ to both sides to avoid asymmetrical

divalent ion concentrations potentially leading to supplementary membrane voltages; the

absence of such a voltage was verified by running an IV plot from -10 mV to 10 mV,

which showed the absence of any ionic current at 0 mV (Figure 2-4). Next, we exposed

the grounded side of the membrane to increased concentrations of KCl by adding to it

small amounts of the 3M KCl solution. To our surprise, none of the additions revealed a

transmembrane voltage larger than a few mV (Figure 2-4) even for concentrations for

which we otherwise measured tens of mV in the absence of Ca^{2+} (as shown in Figure 2-

2).
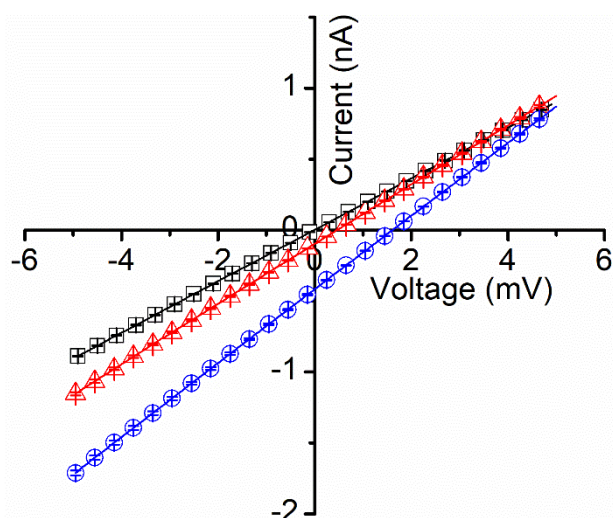
Figure 25. **Lysenin's selectivity is diminished in sub-conducting states. After exposure of lysenin channels to 36 mM Ca2+ ions (for inducing stable sub-conducting states), symmetrical KCl concentration conditions indicated the absence of any membrane voltage (open squares). KCl addition to the ground side (concentration ratio of 3 (open triangles), and 13 (open circles), respectively) led to the development of negligible membrane voltages, in the mV range. All the data in the plots are experimental; the symbols have been added as a visual aid, and they represent average values ± SD from three IV sweeps recorded in the same experiments.**

A reasonable assumption for this unexpected behavior would be the loss of selectivity for channels in the sub-conducting state. We excluded the hypothesis that no ions may move through sub-conducting channels since the ionic conductance in the sub-conducting state is still very large. To reasonably explain the diminished membrane voltage observed experimentally, we modeled the membrane containing lysenin channels in either state by a combination of a voltage source (fully open channels), a serial resistance (R_1, the resistance of the fully open channels), and another resistance (R_2) parallel to the entire assembly and representing all the sub-conducting channels (Figure 2-5). For slow-varying voltage measurements the capacitance of the membrane may be neglected. Also, although the channels may present a very weak selectivity in the sub-conducting state, we opted to exclude a second voltage source for these channels since

the results presented in Figure 2-4 show only a negligible voltage for sub-conducting

channels exposed to asymmetrical KCl conditions. This low resting voltage also suggests

that CaCl$_2$ addition, although changes the Cl$^-$ concentrations on both sides of the

membrane, has at most a small contribution to the membrane voltage. Therefore, the

monovalent ions may be considered the major contributors to the membrane voltage for

these experimental conditions, which simplifies the electrical model of the membrane.
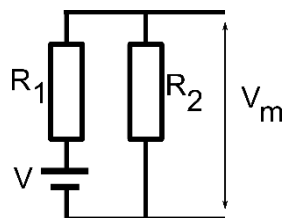
Figure 21.   The electrical model for a membrane containing lysenin channels in both open and sub-conducting states. The model includes a voltage source V, open channels of total resistance R$_1$, and sub-conducting channels of total resistance R$_2$. The resulting membrane voltage V$_m$ may be estimated from the electrical parameters of the equivalent circuit.

The membrane voltage for the model shown in Figure 2-5 may be calculated from

Ohm's law:

$$V_m = V \frac{R_2}{R_1 + R_2} \quad \text{Eq. 2}$$

The other premises of the proposed model are as follows: i) the membrane

contains N channels, from which n$_1$ are in the open state and n$_2$ in the sub-conducting

state (N = n$_1$+n$_2$); ii) for given ionic conditions the resistance of an individual open

channel is r$_1$, and the resistance of an individual sub-conducting channel is r$_2$; and iii) the

ratio between the individual resistances of sub-conducting and conducting channels in

otherwise identical solution conditions is $r_1/r_2 = f = 0.2$ [12]. With these assumptions, the

membrane voltage becomes:

$$V_m = \frac{V}{\left(\dfrac{fn_2}{N-n_2}\right)+1}$$

Eq. 3

Assessing the evolution of the membrane voltage when variable populations of

fully conducting and sub-conducting channels coexist in the membrane requires

estimating n_2. This was previously performed by considering the interactions between

Ca^{2+} ions and lysenin channels a Langmuir isothermal adsorption process [12], for which:

$$n_2 = \frac{K[Ca^{2+}]N}{1+K[Ca^{2+}]}$$

Eq. 4

where K is the Langmuir constant, $[Ca^{2+}]$ is Ca^{2+} concentration in the bulk

solution, and N is the total number of lysenin channels inserted into the membrane.

The combination of the last two equations leads to a simplified formula for the

membrane voltage:

$$V_m = \frac{V}{fK[Ca^{2+}]+1}$$

Eq. 5

The last equation predicts that the membrane voltage established from chemical

gradients must monotonically decrease with increasing Ca^{2+} concentration. To verify this

hypothesis, we measured the variation of the membrane voltage created by KCl gradients

upon successive Ca^{2+} addition. We utilized buffered KCl (50 mM) support electrolyte

and created a membrane voltage of ~22.4 mV by adding KCl to the grounded reservoir

(for a concentration ratio of 4.1). Addition of Ca^{2+} up to 25 mM to both reservoirs

decreased the membrane voltage in a concentration-dependent manner, as predicted by

Eq. 5 (Figure 2-6). The plot was fit with Eq. 5, in which we utilized an f value of 0.2, as

previously determined from conductance measurements [12]. The fit provided a K value

of 0.32 ± 0.07 mM (n = 2). This Langmuir constant is several times larger than what was

determined from macroscopic conductance measurements (i.e., K = 0.05 mM [12]).

However, those experiments were performed by utilizing 150 mM salt for the support

electrolyte, and our experiments employed 50 mM. Since the primary interaction between

divalent metal cations and lysenin channels is presumably electrostatic [12], one may

easily anticipate that a lower ionic strength of the solution environment augments the

electrostatic interactions by reducing ionic screening; as our experimental determinations

indicate, this clearly leads to an increased adsorption constant.
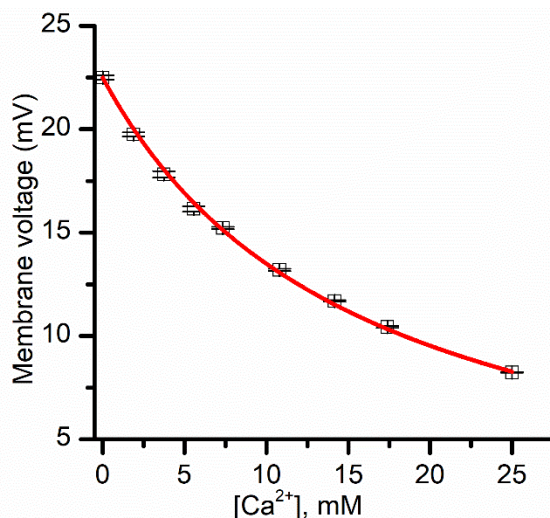
Figure 27.   Influence of Ca2+ ions on the transmembrane voltage resulting from asymmetrical KCl salt conditions. The membrane voltage (averaged from three sweeps) is diminished upon Ca2+ addition to both sides of the membrane, suggesting that lysenin channels in sub-conducting states have reduced selectivity. The continuous line is the fit with Eq. 5.

Ionic selectivity is a salient feature of ion channels, largely utilized for establishing fundamental physiological processes in all living systems. Our work demonstrates that lysenin channels also present ionic selectivity, and that the permeability is different for monovalent anions and cations. Although the permeability ratios are much smaller than what is typically encountered for many ion channels, the selectivity function may lead to the development of large resting potentials, comparable to the ones measured for cells. Consequently, this may be further exploited to modulate the membrane voltage of natural membrane systems. Lysenin reconstitution into artificial membrane systems (i.e., liposomes) may provide the means to create electrochemical gradients to be utilized for energy production and control of metabolic processes in synthetic cell-like systems. The ability of lysenin to attain stable sub-conducting states allowed us to investigate its selectivity to monovalent ions, which was significantly diminished. To explain the loss of this function, one may consider it an effect originating in the binding of Ca^{2+} ions to the channel, which will change the electrostatic properties and the energy landscape. However, this may require a direct binding to the selectivity filter in order to annihilate its function. Another hypothesis, which we consider more attractive, is that the channel's conformational changes during the transition from the open to sub-conducting state [12] leads to a displacement of the selectivity filter, hence hindering its function.

The selectivity function presented by lysenin, together with the high transport rate and exquisite regulation by voltage and ligands, closely resembles the salient features of ion channels. It is not clear why a pore-forming toxin meant to kill the target cells is endowed with such remarkable functionalities, which are rather descriptive of ion channels. In this respect, the hypothesis that lysenin is part of a defense system is not

fully supported by its unusual characteristics. Future extended work is needed to better understand the ionic permeability of lysenin channels in open and sub-conducting states, identify conformational changes induced by divalent ions, elucidate their physiological role, and develop applications emerging from its unique biophysical properties.

References

1. Hille, B. *Ion channels of excitable membranes,* 3rd ed.; Sinauer Associates, Inc., Sunderland, MA, USA, 2001.

2. Bezanilla, F.; Ion Channels: From Conductance to Structure. *Neuron* **2008**, *60*, 456-468, DOI:10.1016/j.neuron.2008.10.035.

3. Carvalho-de-Souza, J.L.; Saponaro, A.; Bassetto, C.A.Z.; Rauh, O.; Schroeder, I.; Franciolini, F.; Catacuzzeno, L.; Bezanilla, F.; Thiel, G.; Moroni, A. Experimental challenges in ion channel research: uncovering basic principles of permeation and gating in potassium channels. *Adv. Phys.- X* **2022**, *7*, 1978317, DOI:10.1080/23746149.2021.1978317.

4. de Lera Ruiz, M.; Kraus, R.L. Voltage-Gated Sodium Channels: Structure, Function, Pharmacology, and Clinical Indications. *J. Med. Chem.* **2015**, *58*, 7093-7118, DOI:10.1021/jm501981g.

5. Dudev, T.; Lim, C. Ion Selectivity Strategies of Sodium Channel Selectivity Filters. *Acc. Chem. Res.* **2014**, *47*, 3580-3587, DOI:10.1021/ar5002878.

6. Roux, B. Ion channels and ion selectivity. *Essays Biochem.* **2017**, *61*, 201-209, DOI:10.1042/EBC20160074.

7. Cymes, G.D.; Grosman, C. Identifying the elusive link between amino acid sequence and charge selectivity in pentameric ligand-gated ion channels. *Proc. Nat. Acad. Sci. U.S.A.* **2016**, *113*, E7106, DOI:10.1073/pnas.1608519113.

8. Westhoff, M.; Eldstrom, J.; Murray, C.I.; Thompson, E.; Fedida, D. I_{Ks} ion-channel pore conductance can result from individual voltage sensor movements. *Proc. Nat. Acad. Sci. U.S.A.* **2019**, *116*, 7879-7888, DOI:10.1073/pnas.1811623116.

9. Abdul Kadir, L.; Stacey, M.; Barrett-Jolley, R. Emerging Roles of the Membrane Potential: Action Beyond the Action Potential. *Front. Physiol.* **2018**, *9*, DOI:10.3389/fphys.2018.01661.

10. Peraro, M.D.; van der Goot, F.G. Pore-forming toxins: ancient, but never really out of fashion. *Nat. Rev. Microbiol.* **2016**, *14*, 77-92, DOI:10.1038/nrmicro.2015.3.

78

11. Bainbridge, G.; Gokce, I.; Lakey, J.H. Voltage gating is a fundamental feature of porin and toxin β–barrel membrane channels. *FEBS Lett.* **1998**, *431*, 305-308, DOI:10.1016/S0014-5793(98)00761-3.

12. Fologea, D.; Krueger, E.; Al Faori, R.; Lee, R.; Mazur, Y.I.; Henry, R.; Arnold, M.; Salamo, G.J. Multivalent ions control the transport through lysenin channels. *Biophys. Chem.* **2010**, *152*, 40-45, DOI:10.1016/j.bpc.2010.07.004.

13. Ide, T.; Aoki, T.; Takeuchi, Y.; Yanagida, T. Lysenin forms a voltage-dependent channel in artificial lipid bilayer membranes. *Biochem. Biophys. Res. Commun.* **2006**, *346*, 288-292, DOI:10.1016/j.bbrc.2006.05.115.

14. Bogard, A.; Abatchev, G.; Hutchinson, Z.; Ward, J.; Finn, P.W.; McKinney, F.; Fologea, D. Lysenin Channels as Sensors for Ions and Molecules. *Sensors* **2020**, *20*, 6099, DOI:10.3390/s20216099.

15. Aoki, T.; Hirano, M.; Takeuchi, Y.; Kobayashi, T.; Yanagida, T.; Ide, T. Single channel properties of lysenin measured in artificial lipid bilayers and their applications to biomolecule detection. *Proc. Jpn. Acad., Ser. B* **2010**, *86*, 920-925, DOI:10.2183/pjab.86.920.

16. Gu, L.-Q.; Dalla Serra, M.; Vincent, J.B.; Vigh, G.; Cheley, S.; Braha, O.; Bayley, H. Reversal of charge selectivity in transmembrane protein pores by using noncovalent molecular adapters. *Proc. Nat. Acad. Sci. U.S.A.* **2000**, *97*, 3959-3964, DOI:10.1073/pnas.97.8.3959.

17. Kwiatkowska, K.; Hordejuk, R.; Szymczyk, P.; Kulma, M.; Abdel-Shakor, A.-B.; Plucienniczak, A.; Dolowy, K.; Szewczyk, A.; Sobota, A. Lysenin-His, a sphingomyelin-recognizing toxin, requires tryptophan 20 for cation-selective channel assembly but not for membrane binding. *Mol. Membr. Biol.* **2007**, *24*, 121-134, DOI:10.1080/09687860600995540.

18. Nestorovich, E.M.; Karginov, V.A.; Bezrukov, S.M. Polymer partitioning and ion selectivity suggest asymmetrical shape for the membrane pore formed by epsilon toxin. *Biophys. J.* **2010**, *99*, 782-789, DOI:10.1016/j.bpj.2010.05.014.

19. Ostolaza, H.; Gonzalez-Bullon, D.; Uribe, K.B.; Martin, C.; Amuategi, J.; Fernandez-Martinez, X. Membrane Permeabilization by Pore-Forming RTX Toxins: What Kind of Lesions Do These Toxins Form? *Toxins* **2019**, *11*, 354, DOI:10.3390/toxins11060354.

20. Shogomori, H.; Kobayashi, T. Lysenin: A sphingomyelin specific pore-forming toxin. *Biochim. Biophys. Acta Gen. Subj.* **2008**, *1780*, 612-618, DOI:10.1016/j.bbagen.2007.09.001.

21. Yamaji-Hasegawa, A.; Makino, A.; Baba, T.; Senoh, Y.; Kimura-Suda, H.; Sato, S.B.; Terada, N.; Ohno, S.; Kiyokawa, E.; Umeda, M., Kobayashi, T. Oligomerization and pore formation of a sphingomyelin-specific toxin, lysenin. *J. Biol. Chem.* **2003**, *278*, 22762-22770, DOI:10.1074/jbc.M213209200.

22. Yilmaz, N.; Yamada, T.; Greimel, P.; Uchihashi, T.; Ando, T.; Kobayashi, T. Real-Time Visualization of Assembling of a Sphingomyelin-Specific Toxin on Planar Lipid Membranes. *Biophys. J.* **2013**, *105*, 1397-1405, DOI:10.1016/j.bpj.2013.07.052.

23. Shakor, A.-B.A.; Czurylo, E.A.; Sobota, A. Lysenin, a unique sphingomyelin-binding protein. *FEBS Lett.* **2003**, *542*, 1-6, DOI:10.1016/S0014-5793(03)00330-2.

24. Bruhn, H.; Winkelmann, J.; Andersen, C.; Andra, J.; Leippe, M. Dissection of the mechanisms of cytolytic and antibacterial activity of lysenin, a defense protein of the annelid *Eisenia fetida*. *Dev. Comp. Immunol.* **2006**, *30*, 597-606, DOI:10.1016/j.dci.2005.09.002.

25. Yilmaz, N.; Kobayashi, T.; Assemblies of pore-forming toxins visualized by atomic force microscopy. *Biochim. Biophys. Acta - Biomembr.* **2016,** 1858, 500-511, DOI:10.1016/j.bbamem.2015.11.005.

26. Yilmaz, N.; Yamaji-Hasegawa, A.; Hullin-Matsuda, F.; Kobayashi, T.; Molecular mechanisms of action of sphingomyelin-specific pore-forming toxin, lysenin. *Semin. Cell Dev. Biol.* **2018,** 73, 188-198, DOI:10.1016/j.semcdb.2017.07.036.

27. Najbauer, E.E.; Becker, S.; Giller, K.; Zweckstetter, M.; Lange, A.; Steinem, C.; de Groot, B.L.; Griesinger, C.; Andreas, L.B. Structure, gating and interactions of the voltage-dependent anion channel. *Eur. Biophys. J.* **2021,** *50*, 159-172, DOI:10.1007/s00249-021-01515-7.

28. Sander, P.; Gudermann, T.; Schredelseker, J. A Calcium Guard in the Outer Membrane: Is VDAC a Regulated Gatekeeper of Mitochondrial Calcium Uptake? *Int. J. Mol. Sci* **2021**, *22*, 946, DOI:10.3390/ijms22020946.

29. Briones, R.; Weichbrodt, C.; Paltrinieri, L.; Mey, I.; Villinger, S.; Giller, K.; Lange, A.; Zweckstetter, M.; Griesinger, C.; Becker, S.; Steinem, C.; de Groot, B.L. Voltage Dependence of Conformational Dynamics and Subconducting States of VDAC-1. *Biophys. J.* **2016**, *111*, 1223-1234, DOI:10.1016/j.bpj.2016.08.007.

30. Gincel, D.; Silberberg, S.D.; Shoshan-Barmatz, V. Modulation of the Voltage-Dependent Anion Channel (VDAC) by Glutamate. *J. Bioenerg. Biomembr.* **2000**, *32*, 571-583, DOI:10.1023/a:1005670527340.

31. Cox, C.D.; Nomura, T.; Ziegler, C.S.; Campbell, A.K.; Wann, K.T.; Martinac, B. Selectivity mechanism of the mechanosensitive channel MscS revealed by probing channel subconducting states. *Nat. Commun.* **2013**, *4*, 2137, DOI:10.1038/ncomms3137.

32. Flegler, V.J.; Rasmussen, T.; Böttcher, B. More Than Just Closed and Open: Unraveling a Mechanosensor. *Trends Bioche. Sci* **2021**, *46*, 623-625, DOI:10.1016/j.tibs.2021.04.002.

33. Shapovalov, G.; Lester, H.A. Gating transitions in bacterial ion channels measured at 3 microns resolution. *J. Gen. Physiol.* **2004**, *124*, 151-161, DOI:10.1085/jgp.200409087.

34. Jo, A.; Hoi, H.; Zhou, H.; Gupta, M.; Montemagno, C.D.; Single-molecule study of full-length NaChBac by planar lipid bilayer recording. *PLOS ONE* **2017**, 12, e0188861. DOI:10.1371/journal.pone.0188861.

35. Chapman, M.L.; VanDongen, A.M.J.; K Channel Subconductance Levels Result from Heteromeric Pore Conformations. *J. Gen. Physiol.* **2005,** 126, 87-103, DOI:10.1085/jgp.200509253.

36. Cheng, W.W.L.; Enkvetchakul, D.; Nichols, C.G.; KirBac1.1: It's an Inward Rectifying Potassium Channel. *J. Gen. Physiol.* **2009,** 133, 295-305, DOI:10.1085/jgp.200810125.

37. Warner, L.R.; Mass, O.; Donnelly, L. N.; Grantham, B.R.; Oxford, J.T. Growing and Handling of Bacterial Cultures within a Shared Core Facility for Integrated Structural Biology Program. In *Growing and Handling of Bacterial Cultures*, Mishra, M., Ed.; IntechOpen Limited, London, UK, 2018, DOI:10.5772/intechopen.81932.

38. Duong-Ly, K.C.; Gabelli, S.B.; Lorsch, J.R. Affinity Purification of a Recombinant Protein Expressed as a Fusion with the Maltose-Binding Protein (MBP) Tag. In *Methods in Enzymology*, Lorsch, J.R., Ed.; Academic Press, 2015; Vol. 559, pp. 17-26. DOI:10.1016/bs.mie.2014.11.004.

39. Jenny, R.J.; Mann, K.G.; Lundblad, R.L. A critical review of the methods for cleavage of fusion proteins with thrombin and factor Xa. *Protein Expr. Purif.* **2003**, *31*, 1-11, DOI:10.1016/S1046-5928(03)00168-2.

40. Lebendiker, M.; Danieli, T. Purification of Proteins Fused to Maltose-Binding Protein. In *Protein Chromatography: Methods and Protocols*, Walls. D., Loughran, S.T., Eds.; Humana Press, New York, NY, 2017; pp. 257-273. DOI:10.1007/978-1-4939-6412-3_13.

CHAPTER FOUR: CU^{2+} IONS ADJUST LYSENIN CHANNEL REGULATION IN

ANIONIC AND NEUTRAL LIPID MEMBRANES

Abstract

In this work we employed electrophysiology approaches and investigated the

influence of Cu^{2+} ions on the voltage-induced gating, hysteretic conductance, and

memory of lysenin channels reconstituted in artificial lipid membranes made of two

different lipid compositions. When reconstituted in membranes comprising anionic lipids,

lysenin channels present voltage-gating and hysteretic conductance in response to slow-

varied oscillatory voltage stimuli, yet they re-open at low positive voltages. Cu^{2+} addition

within a few µM concentration range strongly modulates the voltage-gating by inducing a

leftward shift of the open probability during increasing depolarizing voltages. However,

our experiments show that the presence of Cu^{2+} arrests the channels in the voltage-

induced closed state and prevents complete re-opening upon removing the voltage

stimulus. In addition, the macroscopic conductance may be re-instated by re-application

of negative voltages, indicative of molecular memory and memristive functionality. Our

next investigations employed reconstitution of lysenin channels in membranes composed

of neutral lipids, which are known for suppressing the voltage-gated feature and leading

to a linear, ohmic behavior of the macroscopic currents during membrane depolarization.

Nevertheless, in the presence of µM concentrations of Cu^{2+} ions in the support

electrolyte, the voltage, hysteresis, and memory functions are fully reinstated, suggesting

a strong interaction between Cu^{2+} and proteins—as opposed to an interaction with lipids—as modulator of the voltage regulation mechanism.

Introduction

Lysenin, a pore-forming toxin (PFT) extracted from the red earthworm *E. fetida* interacts with natural and artificial lipid membranes containing sphingomyelin and self-assemble into a large pore of ~ 3nm diameter [1-8]. The reconstituted channels presents outstanding biophysical properties commonly shared by ion channels [9-11] such as large transport rate, regulation, and selectivity [3, 4, 12-16] . Besides the large transport rate, lysenin channels present intrinsic regulatory mechanisms which adjust the channel conformation and implicitly its conductance in response to physical and chemical stimuli [15-17]. When reconstituted in artificial lipid membranes composed of anionic lipids, lysenin channels manifest voltage-gating and close at transmembrane potentials larger than a few tens of mV [3, 18, 19]. Interestingly, this feature vanishes when the anionic lipids in the supporting bilayer membrane are replaced by neutral ones, in which situation the channels will remain in the open state for a large range of positive bias potentials [3, 13]. Another salient feature of lysenin channels, commonly shared by ion channels is ligand-induced gating. Lysenin channels interact with multivalent cations and adjust their conducting state by gating. However, the response to multivalent cations seems to be size- and charge dependent [13, 15, 17]. Small trivalent metal cations interact with lysenin channels and induce reversible transitions to the closed state; as opposed to this, interactions with divalent cations or voluminous multivalent ions generally lead to sub-conducting states, a state in which the channels lose their ionic selectivity. The ligand- and voltage-gating are not coupled since neutral lipids do not abrogate the conformational

changes induced by multivalent ions although the voltage-gating feature is lost in such experimental conditions. However, lysenin channels present a remarkable feature not shared by many ion channels, which is the hysteresis in conductance [18-21]. Prior work shows that the opening and closing of lysenin channels in response to external voltage stimuli is dependent not only on the applied voltage but also the previous state of the channels (i.e., open, or closed, respectively). This non-Markovian behavior leads to a strong, persistent hysteresis in conductance, which is indicative of molecular memory [20]. Simply put, the macroscopic ionic currents measured at given voltages depend on the channels' history, and this hysteretic behavior manifests for both large channel populations as well as at the single-channel level. Investigations of this interesting phenomenon concluded that the hysteresis originates in an invariant reopening pathway of the channels which were previously in a closed state [18, 20]. Several factors significantly affecting the voltage-gating of channels transitioning from open to closed states, such as temperature, or monovalent and multivalent metal ions do not adjust the reopening pathway (i.e., the close-open transition of channels which have been previously closed by bias voltages), which remains invariant [18, 20]. The major differences between the open probabilities for open-close and close-open transitions lead to the observed hysteresis in conductance and molecular memory. Technically speaking, the lysenin channels behave like memristors (memory-resistors) [22, 23]; such features are not completely uncommon among ion channels, but the time scale of its manifestation for lysenin channels greatly exceeds what is usually observed for ion channels [24-28].

Although the hysteretic behavior of biomolecules presents the potential to revolutionize our understanding of molecular memory and lead to unprecedented

developments in bioelectronics, such investigations in this direction are scarce. This scarcity may simply originate in the fact that such behavior is not often observed in experiments, but this may be a result of overlooking. To contribute to filling this gap, we proposed investigations aiming at adjusting the hysteresis in conductance of lysenin channels by manipulating their interactions with metal cations. Earlier investigations indicate that many metal cations significantly enhance the hysteretic behavior of lysenin channels [18]. However, these investigations comprised either large amounts of monovalent or small amounts of trivalent ions. Therefore, we decided to investigate the influence of divalent metals on lysenin channel hysteresis, which induce sub-conducting states [13, 15]. While Ca^{2+} and Mg^{2+} ions force the channels into a stable sub-conducting state [13, 15], Cu^{2+} has a very different behavior and completely closes lysenin channels in two steps [13, 15]. Consequently, we assessed the memory of lysenin in response to Cu^{2+} ions by employing traditional electrophysiology measurements. Our investigations revealed that the presence of Cu^{2+} ions not only significantly improves the memory function of lysenin but also enables its manifestation in the absence of any transmembrane voltage. The enhanced hysteresis observed upon Cu^{2+} addition also prompted us to investigate the voltage gating and hysteresis of lysenin channels reconstituted in neutral bilayer lipid membranes, which are well-known for suppressing the voltage-induced gating [3]. To our surprise, Cu^{2+} not only restored the gating at positive transmembrane voltages but also enabled the manifestation of a strong hysteresis in conductance.

Materials and Methods

Our experiments comprised a typical experimental setup largely utilized for electrophysiology experiments [3, 4, 13, 14, 29]. Briefly, the setup consisted of two PTFE reservoirs (1 mL each) separated by a thin PTFE film in which we produced a small circular hole (~100 um diameter) by an electric spark. The lipid membrane produced in the hole was made from mixtures containing asolectin (Aso, Sigma-Aldrich), sphingomyelin (SM, Avanti Polar Lipids), and cholesterol (Chol, Sigma Aldrich) dissolved in n-decane (Fisher Scientific) at a weight ratio of 10:5:4. The same ratios were used for producing neutral membranes but Aso was replaced by Diphytanoyl-PC (DiPhyt-PC, Avanti Polar Lipids). The reservoirs were filled with buffered electrolyte solutions (135 mM KCl, 20 mM HEPES, pH 7.2 – if not otherwise indicated). The electrical connections with the Axopatch 200B amplifier (Molecular Devices) were ensured through salt bridges (2% low melting point agarose-Sigma Aldrich, dissolved in 1 M NaCl – Fisher Scientific) and Ag/AgCl electrodes wired to the input of the electrophysiology amplifier. The analog signal digitized with the DigiData 1440A digitizer (Molecular Devices) was fed into a PC for recording and further analysis with the pClamp 10.1 software package (Molecular Devices). The recorded data were also analyzed and plotted with the Origin 8.5.1 (OriginLab) software package.

Membrane formation and stabilization was monitored by monitoring the membrane capacitance C and resistance R. Membrane capacitance was estimated from the capacitive current measured in response to a triangle-wave signal (provided from a Keithley 3390 function generator), and the seal was checked by applying a DC voltage to the membrane. When a stable membrane was formed (C > 65 pF, R > 100 GOhm), we

proceeded with channel insertion. 10 nM of recombinant lysenin custom-made in our lab [14] was added to the grounded reservoir under continuous stirring (with a Warner Instruments low noise magnetic stirrer) and upon application of -80 mV bias potential (manual command). Channel insertion was monitored from the step-wise variation of the ionic currents [3, 4, 12, 15, 16]; after achieving a steady state of the macroscopic current in ~ 2 hours, we proceeded with electrophysiology measurements without and with Cu^{2+} ions addition. For this purpose, we used a 1M CuSO4 stock solution (Fisher Scientific) after proper serial dilution in buffered electrolyte solutions. After each Cu^{2+} addition to both sides of the membrane, we maintained stirring for several minutes to allow mixing and enable interactions between channels and ions.

DC measurements employing variable DC signals (i.e., ramps) were performed by creating the stimulus voltages with the digitizer and using episodic stimulation [16, 20]. The automated protocols have been adjusted for each measurement performed for our experiments. For ramp stimulations (ascending, and descending voltages, respectively) we used a sampling rate of 1 sample/second, a hardware low-pass filter of 1 kHz, a software low-pass filter of 10 Hz, and a voltage rate of no more than 0.2 mV/s to allow channel equilibration [20, 30]. For the manual step voltages applied to the channel-containing membrane, we adjusted the sampling times (0.002 – 1 second) and the low-pass filters (cut off frequencies at least 10 times higher than the sampling frequency) to mitigate signal suppression by filtering.

The combined AC/DC experiments implied connecting the AC and DC signals at independent inputs of the instrument. The DC signals were applied with the manual command, while the AC signals were applied from the function generator via the external

input of the amplifier (see Scheme 1 in Appendix B). The AC stimulation was a 10 Hz

AC sine wave with peak-to-peak amplitude of no more than 2 mV. These settings were

chosen to prevent channel closing by voltage (which may not occur at very low positive

voltages, or fast sweeps [20]) and eliminate artifacts coming from measuring large values

for the capacitive currents (proportional with dV/dt). To be able to record only AC

signals devoid of any DC component as indicative of channel conductance at any DC

voltage, we imposed a high-pass software filter of 2 Hz. In the same line, to avoid

chopping or filtering the AC stimulus, we utilized a sampling time of 2 msec, a 10 kHz

low-pass hardware filter, and no other low-pass software filter. Preliminary visualization

of the signal demonstrated that these recording conditions did not distort or attenuate the

AC stimulus in any way.

All experiments were performed at room temperature (22 C), which did not vary

by more than 1 C between independent experiments, even those performed on different

days.

Results and Discussion

Our first investigation focused on assessing the effect of small Cu^{2+} ion

concentrations on the voltage-induced gating of lysenin channels in response to slow

ascending and descending voltage ramps. In the absence of Cu^{2+} ions, the I-V plot

recorded in response to an ascending ramp voltage showed the typical response of lysenin

channels to external voltages [16, 18, 20, 21, 29]. From -20 mV and up to ~15 mV, the

ohmic relationship between macroscopic currents and voltages indicated that the channels

remained in the open state (Figure 3-1a). Channel closure occurred at ~20 mV, and the

voltage-dependent gating was inferred from the significant decrease of the current

recorded as the voltage increased over 20 mV. Channel closing continued up to the

maximum applied bias voltage of 60 mV. Application of a descending voltage led to the

observation of hysteresis in conductance (Figure 3-1a): the channel reopening followed a

different pathway, and full reopening occurred at a smaller positive voltage compared to

the ascending voltage ramp. However, at descending voltages under ~10 mV, the linear I-

V plot indicated full reopening and ohmic behavior identical to the one recorded for

ascending voltages.
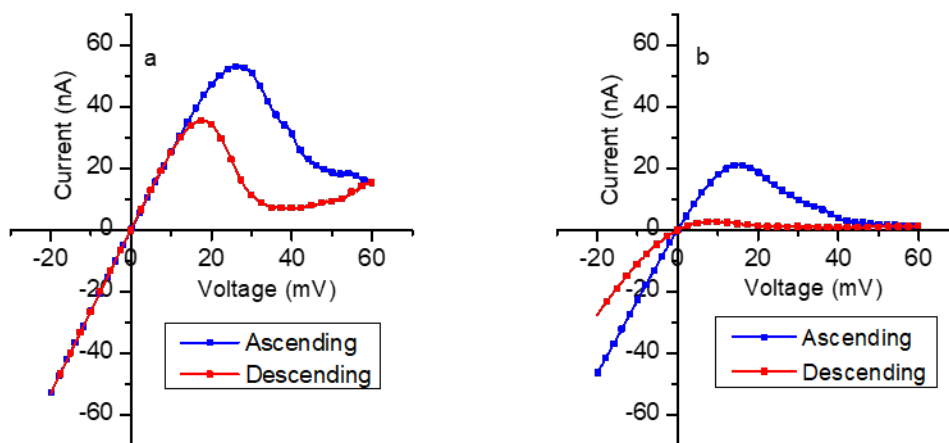
Figure 22. **Comparative analysis of the effect of Cu^{2+} on the macroscopic currents established through lysenin channels in response to stimulation with ascending and descending voltage ramps. a) The I-V plots recorded in absence of Cu^{2+} ions. b) Addition of 4 μM Cu^{2+} elicits major changes in the I-V plots for both ascending and descending voltages. Both I-V plots are indicative of hysteresis in conductance.**

The I-V plot also indicated that not all the channels closed at +60 mV, (the

macroscopic current was still significant) but this is a typical behavior encountered when

the number of inserted lysenin channels is very large [21]. Since Cu^{2+} ions may also close

the lysenin channels by a two-step ligand-induced gating mechanism [13, 17], we opted

for a large number of channels to start with so we would record sufficiently large

macroscopic currents after closing many channels in the population by addition of Cu^{2+}.

This is also the reason for limiting the negative voltages to -20 mV: larger voltages would

rapidly lead to macroscopic currents beyond the measuring capabilities of the

electrophysiology amplifier (which is ~ 180 nA).

Significant differences between the response to ascending and descending voltage

ramps were recorded after addition of Cu^{2+} ions to both reservoirs (4 µM final

concentration in each reservoir). The response to ascending voltage ramps was

qualitatively similar to what was recorded before Cu^{2+} addition (Figure 3-1). The

macroscopic currents obeyed a linear relationship at negative voltages, but the closing

occurred at much smaller positive voltages. The slightly smaller slope of this linear

portion is indicative of a smaller number of open channels in the membrane, which is a

direct consequence of ligand-gating elicited by Cu^{2+} [13, 17]. The channels started to

close at smaller positive voltages and an almost complete closure was recorded at bias

potentials exceeding 40 mV (for which the macroscopic currents were negligible). What

was unexpected is the behavior of the channels during ascending voltages: little, almost

negligible reopening of the channels manifested at any positive voltage during the

descending ramps. In addition, the smaller slope of the I-V plot at negative voltages

suggests that the channels did not fully reopen (in which case the I-V plot will overlap

with the one recorded for the ascending voltages within the same voltage range). In the

same line of observations, the non-linear shape recorded at negative voltages suggests

that the re-opening process is also voltage dependent in the negative voltage range.

The plots of the open probability before and after Cu^{2+} addition (Figure 3-2) were constructed from the ratio between measured currents and hypothetical currents estimated for the same population of open channels in the open state at each voltage (these currents are estimated from the linear portion of the response to ascending voltages [16, 18-20, 31]) and by considering a leakage current [16, 19].
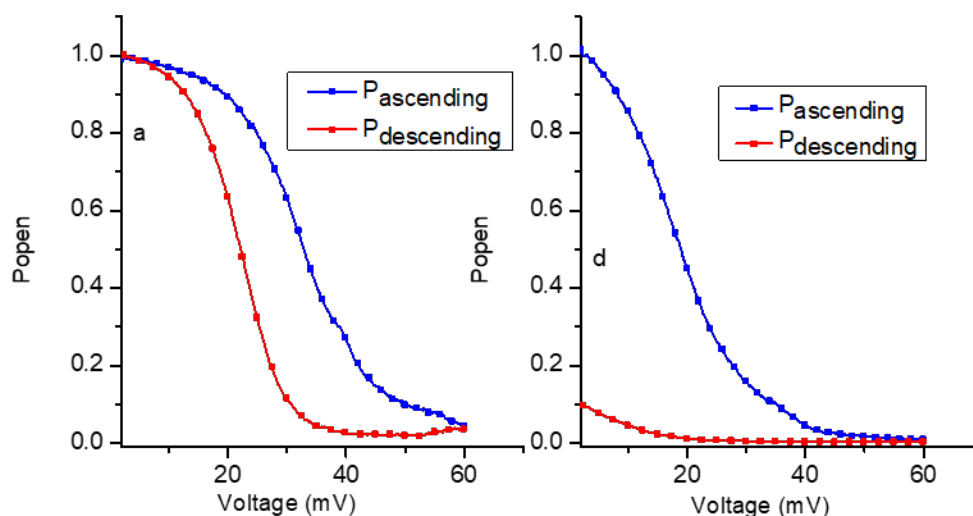
Figure 23. **The influence of Cu^{2+} on the open probability (Popen) of lysenin channels measured for ascending and descending voltage ramps. a) A typical open probability plot of lysenin channels in the absence of Cu^{2+} ions indicates the status of the channels as a function of voltage and hysteresis. b) Cu^{2+} addition elicits a leftward shift of the open probability during ascending voltage ramps and prevents full reopening at 0 mV during descending voltage ramps.**

Substantial differences, both qualitative and quantitative, have been observed regarding the influence of Cu^{2+} on Popen (Figure 3-2b). In the absence of Cu^{2+} ions, ascending voltage ramps led to channel closing and a midway voltage of activation (the voltage for which Popen = 0.5 [16, 21]) of ~32 mV, which is a typical value for lysenin channels in similar solution and electrical conditions. However, the returning pathway recorded for descending voltage ramps is different and indicative of hysteresis in

conductance. The midway voltage of activation shifted to ~20 mV, indicating that the closed channels preferred to remain in the closed state for longer. Nonetheless, lower voltages led to complete reopening, hence leading to an open probability equal to one. Cu^{2+} addition presented multiple effects on the open probability. The midway voltage of activation during ascending voltage ramps decreased to ~20 mV, the channels' closing was nearly completed at higher positive voltages (no leakage was included for these calculations), and the full reopening did not manifest at all during the descending voltage ramps. The midway voltage of activation vanished, and the open probability was ~0.1 at very low positive voltages (only a few mV). One may notice that we intentionally omitted from all the Popen plots points very close to the origin (up to a few mV); these may not be correctly plotted for either experiment since numerous divisions by zero are encountered. Nonetheless, there is no doubt that a small value characterizes the open probability during descending voltage ramps recorded in the presence of Cu^{2+} ions.

To better understand the behavior of lysenin channels and the influence of Cu^{2+} ions on their voltage-induced closing and reopening we investigated the response to step voltages (Figure 3-3).
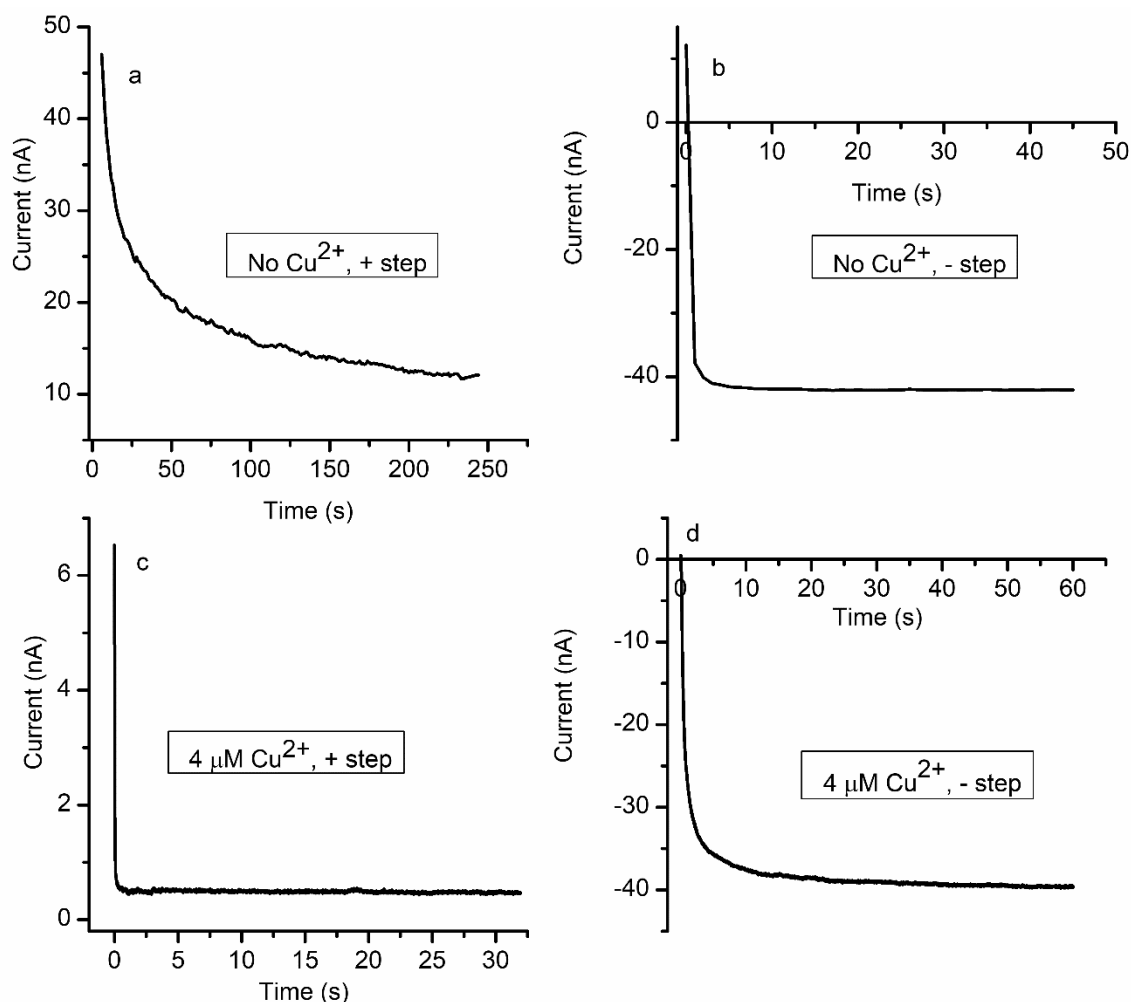
Figure 24. **Cu²⁺ ions adjust the closing and reopening rates of lysenin channels upon application of step voltages. Macroscopic current measurements of lysenin channels stimulated with a +60 mV DC step voltage indicate their gradual closing (a); further stimulation with -60mV leads to a quick reopening (b). The presence of Cu²⁺ (4 µM) greatly enhances channel closure at +60 mV (c) and reduces channel reopening upon further application of -60 mV(d).**

In the absence of Cu²⁺ ions, lysenin channels responded to a +60 mV step voltage by voltage-induced gating, which manifested as an exponential decay of the macroscopic currents (Figure 3-3a). However, after achieving a steady state, the application of a -60 mV step voltage quickly restored the macroscopic conductance in a matter of seconds (Figure 3-3b). In the presence of 4 µM Cu²⁺, the channels presented a similarly qualitative behavior, but the rate of the changes was very different. The +60 mV step

voltage still closed the channels, but this happened at a much faster rate (Figure 3-3c); as a matter of fact, we are convinced that signal filtering and sampling time were not appropriate for visualization of such rapid transients. Nonetheless, the channel reopening at -60 mV in the presence of Cu^{2+} ions was much slower than what we observed before Cu^{2+} addition, indicative of a significantly lower recovery rate (Figure 3-3c).

The above data shows major changes in the hysteretic behavior of lysenin channels in the presence of Cu^{2+} ions, indicative of significant influence on their memory capabilities. However, major questions still unanswered at this point relate to the behavior of channels at 0 mV (no bias transmembrane potential applied to the membrane containing channels). The I-V plots showed that in the absence or presence of Cu^{2+} ions the channels are still open at 0 mV during ascending voltage ramps. However, when we constructed the I-V plots for ascending ramps the voltage was first set at negative voltages, which forces open the channels (as inferred from the steps experiments). The first question to answer is whether the channels are open at 0 mV if no prior negative voltages are applied. Another important issue regarding potential memory is the status of the channel at 0 mV in the presence of Cu^{2+} ions but after applying the positive voltage to adjust their conformation and close the conducting pathway. To answer these important questions, we adapted the experimental setup and designed the experiment to enable estimating the status of the channels at any voltage, including 0 mV. The combination of DC/AC, together with custom filtering of the signal by the procedure described in the Materials and Methods section allowed us to perform assessments of channel conductance at all the voltages of interest. The recording performed on channels in the absence of Cu^{2+} ions is depicted in Figure 3-4, for each voltage condition. At 0 mV, the

amplitude of the current recorded upon application of the 10 Hz AC signal (~785 pA) was uniform and less influenced by noise. Application of a step voltage (+60 mV) gradually reduced the amplitude of the AC signal down to ~400 pA, indicative of a macroscopic conductance reduced by ~50% and originating in channel closing induced by the applied voltage. However, re-application of 0 mV (end of the positive step voltage) adjusted the amplitude of the AC signal to practically the initial value (~770 pA), indicative of a quick recovery of the original conductance. This experiment suggests that in the absence of Cu^{2+} ions the channels were open at 0 mV, closed at positive voltages, and rapidly re-instated their initial conductance after removal of the voltage stimulus (i.e., application of 0 mV bias potential).
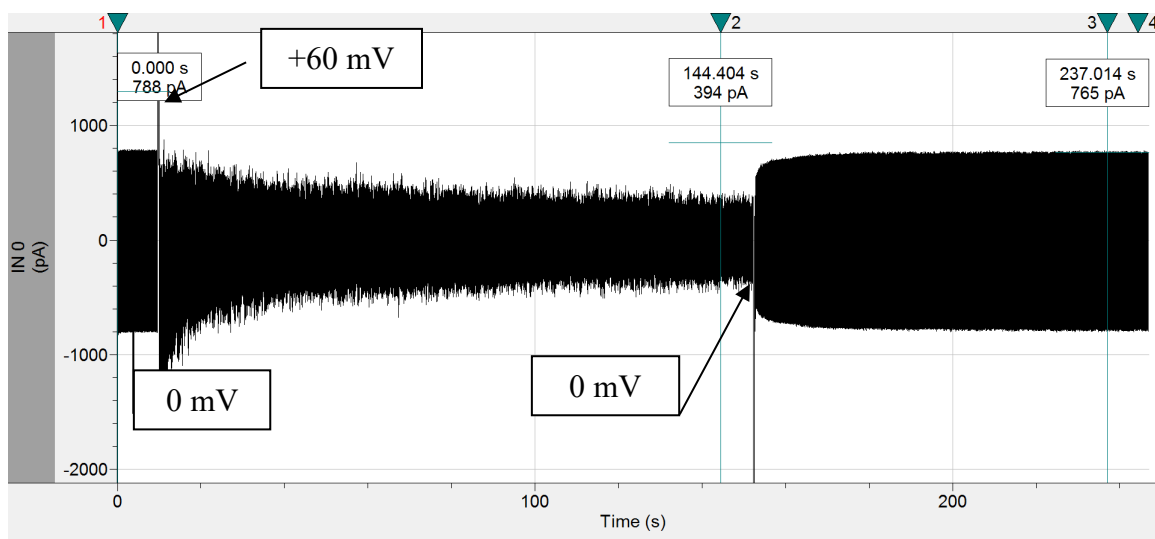
Figure 25.   **Determination of lysenin channels' status and conductance from combined AC/DC stimulation. Initial AC application with no (0 mV) DC bias voltage results in a large AC current amplitude with low noise, indicative of open channels. Upon a positive step voltage stimulation (+60 mV) lysenin channels undergo closing, leading to the gradually decreasing AC signal. Subsequent reopening of the lysenin channels after stimulus removal (0 mV) results in a fast restoration of the initial current amplitude. The DC component was removed by the high-pass filtering.**

A very different behavior of the channels in response to step voltages was recorded after addition of Cu^{2+} ions to both sides of the membrane (4 μM final concentration in each reservoir). The large amplitude of the AC signal recorded at 0 mV (~655 pA) indicated channels in the open state (Figure 3-5). However, upon application of a +60 mV step voltage, the channels transitioned very quickly to the closed state, as indicated by the significantly reduced amplitude of the AC signal (~25 pA, mostly electric noise). Nonetheless, removal of the voltage stimuli (i.e., 0 mV bias potential) led to a slow increase of the AC amplitude, indicative of conductance recovery. However, after ~ 5 minutes, the amplitude gradually and asymptotically approached a steady state characterized by a much lower current (~230 pA) compared to the one recorded before the closing of the channels by the applied voltage (~ 655 pA). This experiment brings evidence that in the presence of Cu^{2+} ions lysenin channels closed by voltages were not capable of full conductance recovery within the indicated time frame. This strong hysteresis in conductance manifested in the presence of Cu^{2+} ions indicates that lysenin channels have at least short memory capabilities, which do not vanish upon eliminating the external voltage stimuli.
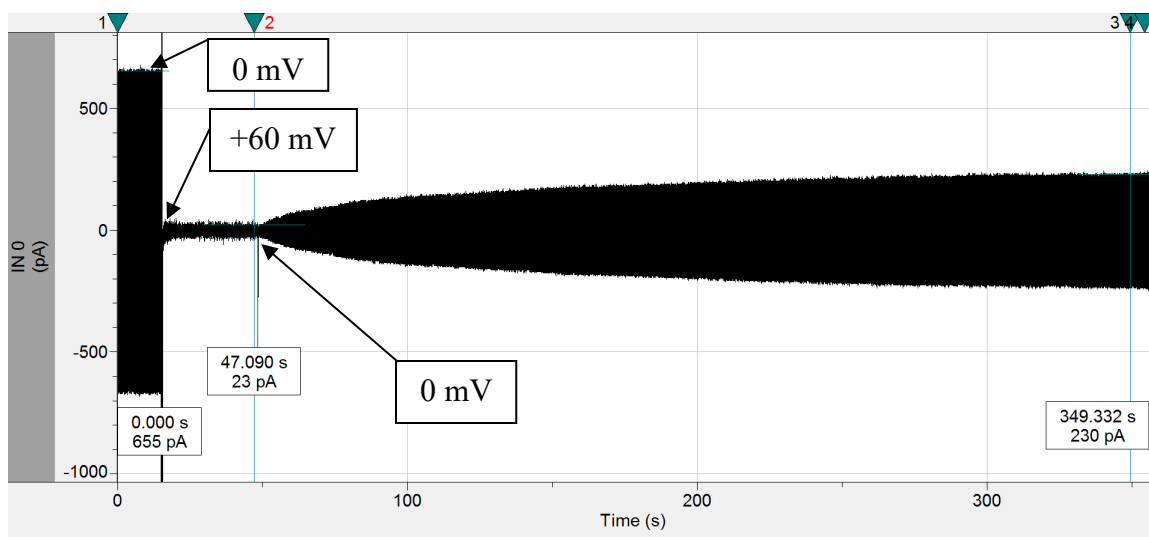
Figure 26.   **Estimation of lysenin channels' status and conductance upon exposure to Cu²⁺ ions from the response to a combination of AC and DC stimulations indicates a hysteretic behavior at 0 mV. Initially open channels display large AC currents upon AC stimulation and no bias voltage (0 mV). Application of a +60 mV step voltage induces rapid channel closure. Removing the positive bias (0 mV applied after channel closure) allows a slow recovery of current but only partial reopening is observed, indicative of hysteresis. The DC component was removed by the high-pass filtering.**

Next, we asked whether fast recovery and bistability may be achieved by exploiting the forced opening of lysenin channels upon application of negative voltages. The previous experiment was repeated in otherwise similar electrical and solution conditions, but we introduced an additional step of forced reopening by switching the voltage to -60 mV, followed by application of 0 mV. The necessity to utilize a fast sampling rate (together with appropriate filtering) implies recording very large files for further analysis. To mitigate this problem, we opted for temporary pause of the recording during the experiment, hence preventing the overloading of the system and enabling further analysis of the recordings. The recorded trace depicted in Figure 3-6 provides further evidence of short term memory and the appropriateness of the experimental conditions for such explorations. The ~710 pA amplitude of the 10 Hz AC signal measured at 0 mV indicated the expected large macroscopic conductance of the open

channels. Application of a +60 mV step voltage led to a rapid decrease of the amplitude to ~34 pA, indicative of channel closing. After a short time (~10 seconds), the bias voltage has been removed so the membrane was biased again by 0 mV after the voltage-induced closing. The amplitude of the AC signal started to slowly increase but reached a steady state value in ~10 minutes. The value of the AC amplitude stabilized at ~70 pA, which is about 90% smaller than the value recorded for the open channels. This experiment suggests that Cu^{2+} addition stabilized the voltage-closed state of the lysenin channels such that they did not reopen after removing the transmembrane potential even after extended time periods. Next, we applied a negative voltage step (-60 mV), which forced the channels to open. Channel re-opening was observed as a quick restoration of the AC amplitude; when the AC signal reached a relatively steady state, we removed again the transmembrane potential while still applying the AC. The amplitude of the AC signal at 0 mV was practically identical to the amplitude recorded at 0 mV before the voltage-induced closing (~710 pA), which was certainly larger than the amplitude of the AC signal recorded for closed channels.
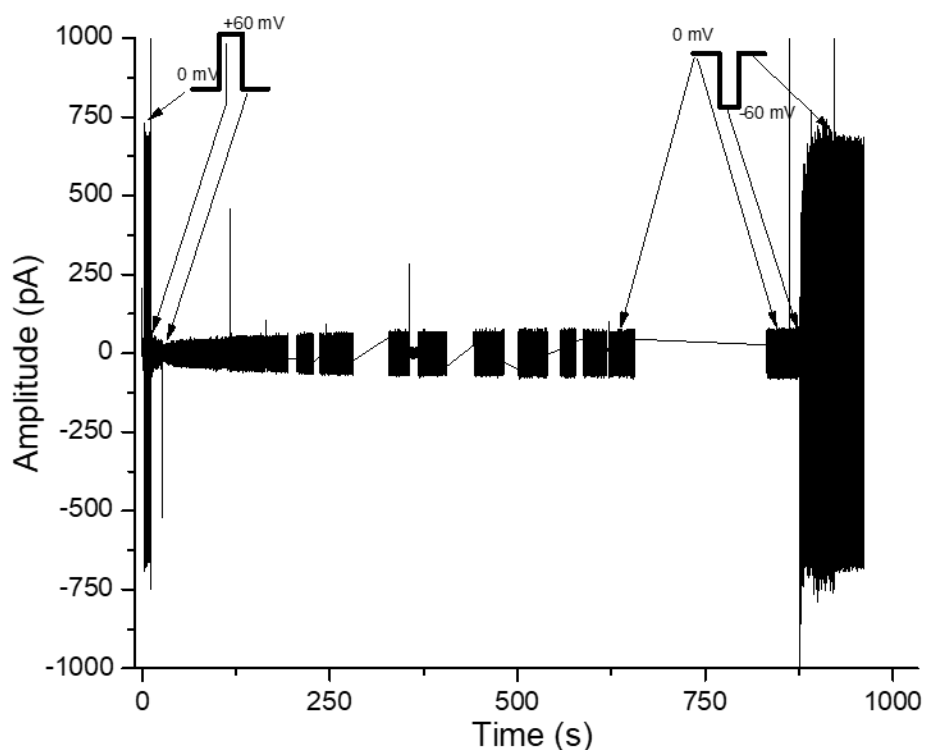
Figure 27.   **Lysenin channels display history-dependent states in the presence of Cu^{2+} ions. A fully open channel population (0 mV) displays high AC current amplitude (open state) before forced closure at positive DC bias voltage (+60 mV). Removal of bias voltage (0 mV) results in a gradual reopening of a small portion of channels leading to a smaller and steady AC amplitude for an extended duration (more than 10 minutes). Forcing the channels to reopen with a negative bias voltage step (-60 mV), followed by subsequent removal of the DC stimulus (i.e., reapplication of 0 mV) reinstates the current prior to channel closure, demonstrating a bistable system.**

This experiment provided additional evidence of bistability and memory function

of lysenin channels. At 0 mV and upon exposure to small Cu^{2+} concentrations, the

macroscopic conductance achieved either large or small values, depending on the

previous state of the channels. The channels presented a large conductance in the absence

of transmembrane potentials if they were biased by 0 mV after being in the open state.

Application of a positive voltage led to a significantly decreased macroscopic

conductance (channels are closed). However, when re-biased by 0 mV from the closed state, the lysenin channels do not recover their initial conductance and the stable state is characterized by a significantly diminished conductance. To restore the initial conductance (reset function), channels may be forced to re-open by a short application of negative bias potentials.

In addition, a few more details demonstrate the appropriateness of our experimental conditions for these experiments. One may have concerns about the influence of the AC signal on the channel status. The AC signal had a very low amplitude (1 mV$_{pp}$) and frequency (10 Hz). This signal is too fast and its amplitude too low to induce conformational changes of the channel in the absence of Cu^{2+} ions since the equilibration is very low [20]. At applied voltages of 0 mV/open state and -60 mV/open state the peak amplitude of the AC is the same (some noise occurs at -60 mV, vide infra). Therefore, we concluded that the AC does not influence the state of the channels.

The inset of the currents recorded in various electrical conditions (traced in Figure 3-6) and the corresponding power spectra are shown in Figure 3-7. The 0 mV/open state (Figure 3-7a) indicates a smooth sine-wave, which was expected since we used a sine-shaped voltage for stimulation. The power spectrum at the same 0 mV/open state shows a reduced noise in the low-frequency range (we used a high pass filter), the excitation signal centered exactly at 10 Hz, and an increasing noise at higher frequencies (Figure 3-7f). At +60 mV bias potential the channels closed, and the amplitude of the AC signal is barely visible (Figure 3-7b). The noise is predominant in such experimental conditions since the sine-shaped current may also originate in capacitive currents. These observations were confirmed by the power spectrum (Figure 3-7f), in which the

excitation signal at 10 Hz is barely visible. At the 0 mV/closed state, the sine-wave

shaped currents were also visible (Figure 3-7c) yet the amplitude was much smaller than

the one recorded for the 0 mV/open state. The wave was not distorted but the

signal/noise ratio was clearly diminished. This is also observed in the power spectrum,

which clearly shows the 10 Hz stimulus wave together with noise of amplitude increasing

with frequency. Application of -60 mV (Figure 3-7d) reopened the channels and restored

the 10 Hz peak (Figure 3-7f), but also led to an increased noise (which is expected at

larger currents). After this hard reset, the reapplication of 0 mV indicates a smooth sine

wave of large amplitude (Figure 3-7e), also characterized by a reduced noise (Figure 3-

7f).
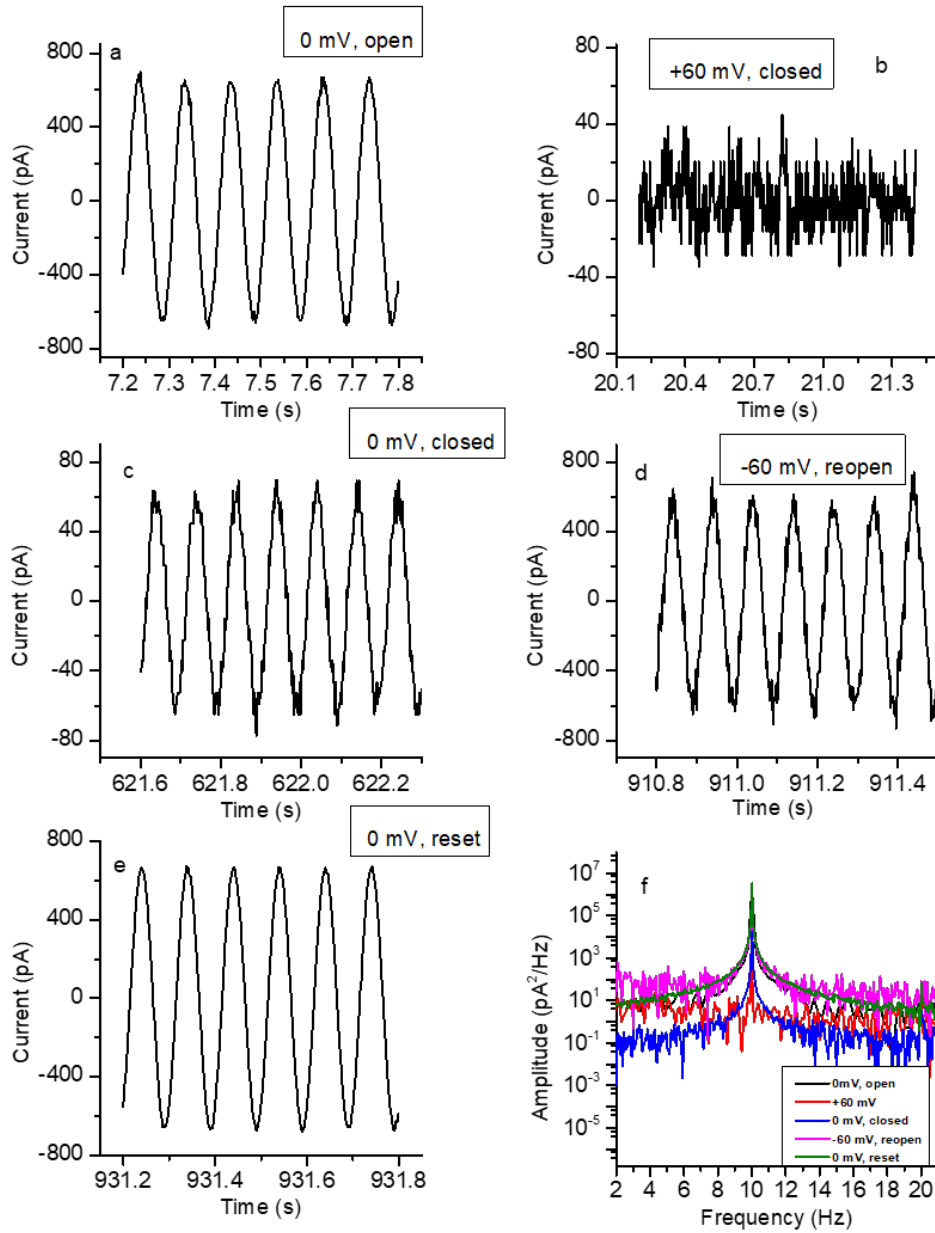
Figure 28. Comparison and analysis of AC signals from electrical and channel conditions showcased in Figure 3-6. (a) A larger, smooth sinusoidal signal is observed with open channels and no DC application; (b) The fully closed channel population results in an AC signal with greatly diminished amplitude chiefly consisting of noise; (c) Reapplication of 0 mV to previously closed channels restores the sinusoidal signal but with a significantly diminished amplitude and signal-to-noise ratio; (d) The channels subsequently reopened under negative bias potential produce a full amplitude signal with some additional noise from the larger macroscopic currents originating in the DC application; (e) Removal of the negative bias potential (i.e., reapplication of 0 mV) restores original signal from (a). The power spectrum (f) reveals low amounts of noise in all cases for low frequencies (<10 Hz), clear peaks at the frequency of AC stimulation (10 Hz) for all states but +60 mV-closed channels, and greater noise for open channels stimulated by DC.

The I-V plots recorded in the presence of Cu^{2+} indicated not only major changes in hysteresis but also adjustments of the voltage-elicited response: faster gating, together with left-shifted midway voltages of activation were observed in our experiments. This is contrary to the influence presented by monovalent and other multivalent cations, which usually shift the midway voltage of activation at larger values and slow down the response to positive voltage stimuli in response to steps or ascending voltage ramps [18]. These observations prompted us to hypothesize that Cu^{2+} ions promote voltage-induced gating of channels for which this important feature was weakened or even suppressed by particular experimental conditions. In this line, lysenin channels are well known for losing their voltage-induced gating upon reconstitution in neutral bilayer lipid membranes [3, 13, 17]. To investigate the influence of Cu^{2+} on lysenin channels in neutral bilayers, we reconstituted them in a support lipid membrane in which we replaced the anionic Asolectin mixture with the neutral DiPhyt-PC. In the absence of Cu^{2+} ions, the quasi-linear shape of the I-V plot (Figure 3-8a) indicated that no voltage-induced gating manifested for the entire voltage range under consideration, as previously reported [13, 17]. However, after addition of Cu^{2+} ions to both sides (4 μM final concentration in each reservoir), a completely unexpected behavior was encountered: the lysenin channels started to gate at low positive voltages (~10 mV), and practically closed completely at applied voltages exceeding 20 mV (Figure 3-8a).
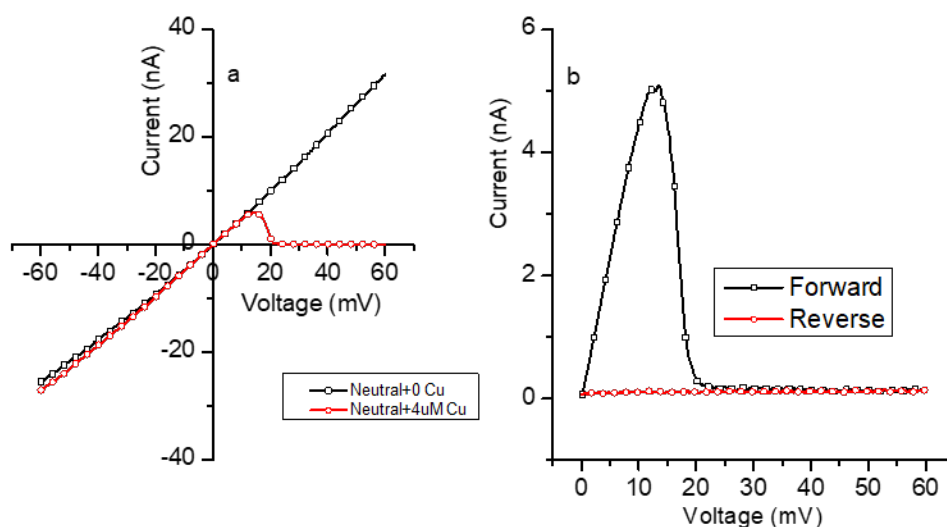
Figure 29. **Lysenin channels reconstituted in membranes made with neutral lipids regain voltage-regulation and hysteresis in the presence of Cu^{2+} ions. (a) Lysenin channels in a neutral lipid membrane subjected to a -60 to +60 mV voltage ramp present ohmic conductivity (black line), indicative of lack of gating. The voltage-gating function is fully re-instated after Cu^{2+} addition (red line, 4 μM). (b) The same channels reconstituted in the neutral membrane also display a strong hysteresis upon exposure to Cu^{2+} ions (4 μM).**

This result clearly demonstrates that lysenin channels may recover this important regulatory feature through a particular, unknown interaction with Cu^{2+}. Moreover, the hysteretic behavior, including the arresting in the closed state at positive voltages and the absence of reopening at 0 mV was also reinstated (Figure 3-8b). Therefore, one may question the hypothesis that voltage-gating is only a consequence of interactions between lysenin and charged lipids [3]. If that would be the case, a potential electrostatic interaction between Cu^{2+} and lipids would predominantly manifest when using anionic lipids, while neutral lipids would present at most much weaker interactions. Our results suggest that the recovery of gating is most likely a consequence of interactions between Cu^{2+} and channels. The Cu^{2+} concentration required to achieve full closure of all the lysenin channels in a population is ~200 μM, which is significantly greater than we used

in our experiments (several μM). Although we observed smaller changes in the macroscopic conductance of the channels upon closing induced by Cu^{2+} additions, these were minimal. Consequently, we may conclude that besides the ligand-induced gating Cu^{2+} presents additional interactions with lysenin channels which significantly influences the voltage regulation, hysteresis, and memory.

References

1.   Shakor, A.-B.A., Czurylo, E.A., and Sobota, A., *Lysenin, a unique sphingomyelin-binding protein.* FEBS Letters, 2003. **542**(1-3): p. 1-6 DOI: 10.1016/S0014-5793(03)00330-2

2.   Bokori-Brown, M., Martin, T.G., Naylor, C.E., Basak, A.K., Titball, R.W., and Savva, C.G., *Cryo-EM structure of lysenin pore elucidates membrane insertion by an aerolysin family protein.* Nature Communications, 2016. **7**: p. 11293 DOI: 10.1038/ncomms11293

3.   Ide, T., Aoki, T., Takeuchi, Y., and Yanagida, T., *Lysenin forms a voltage-dependent channel in artificial lipid bilayer membranes.* Biochemical and Biophysical Research Communications, 2006. **346**(1): p. 288-292 DOI: 10.1016/j.bbrc.2006.05.115

4.   Kwiatkowska, K., Hordejuk, R., Szymczyk, P., Kulma, M., Abdel-Shakor, A.-B., Plucienniczak, A., Dolowy, K., Szewczyk, A., and Sobota, A., *Lysenin-His, a sphingomyelin-recognizing toxin, requires tryptophan 20 for cation-selective channel assembly but not for membrane binding.* Molecular Membrane Biology, 2007. **24**(2): p. 121-134 DOI: 10.1080/09687860600995540

5.   Podobnik, M., Savory, P., Rojko, N., Kisovec, M., Wood, N., Hambley, R., Pugh, J., Wallace, E.J., McNeill, L., Bruce, M., Liko, I., Allison, T.M., Mehmood, S., Yilmaz, N., Kobayashi, T., Gilbert, R.J.C., Robinson, C.V., Jayasinghe, L., and Anderluh, G., *Crystal structure of an invertebrate cytolysin pore reveals unique properties and mechanism of assembly.* Nature Communications, 2016. **7**: p. 11598

6.   Shogomori, H. and Kobayashi, T., *Lysenin: A sphingomyelin specific pore-forming toxin.* Biochimica et Biophysica Acta, 2008. **1780**: p. 612-618 DOI: 10.1016/j.bbagen.2007.09.001

7. Yamaji-Hasegawa, A., Makino, A., Baba, T., Senoh, Y., Kimura-Suda, H., Sato, S.B., Terada, N., Ohno, S., Kiyokawa, E., Umeda, M., and Kobayashi, T., *Oligomerization and pore formation of a sphingomyelin-specific toxin, lysenin.* Journal of Biological Chemistry, 2003. **278**(25): p. 22762-22770 DOI: 10.1074/jbc.M213209200

8. Yilmaz, N., Yamaji-Hasegawa, A., Hullin-Matsuda, F., and Kobayashi, T., *Molecular mechanisms of action of sphingomyelin-specific pore-forming toxin, lysenin.* Seminars in Cell & Developmental Biology, 2018. **73**: p. 188-198 DOI: 10.1016/j.semcdb.2017.07.036

9. Andersen, O.S., Ingolfsson, H.I., and Lundbaek, J.A., *Ion Channels.* Wiley Encyclopedia of Chemical Biology, 2008: p. 1-14 DOI: 10.1002/9780470048672.wecb259

10. Bezanilla, F., *Ion Channels: From Conductance to Structure.* Neuron, 2008. **60**: p. 456-468 DOI: 10.1016/j.neuron.2008.10.035

11. Hille, B., *Ion channels of excitable membranes, Third edition.* 3rd ed. 2001, Sunderland, MA, USA: Sinauer Associates, Inc.

12. Aoki, T., Hirano, M., Takeuchi, Y., Kobayashi, T., Yanagida, T., and Ide, T., *Single channel properties of lysenin measured in artificial lipid bilayers and their applications to biomolecule detection.* Proceedings of the Japan Academy, Series B, 2010. **86**(9): p. 920-925 DOI: 10.2183/pjab.86.920

13. Bogard, A., Abatchev, G., Hutchinson, Z., Ward, J., Finn, P.W., McKinney, F., and Fologea, D., *Lysenin Channels as Sensors for Ions and Molecules.* Sensors, 2020. **20**(21): p. 6099 DOI: 10.3390/s20216099

14. Bogard, A., Finn, P.W., McKinney, F., Flacau, I.M., Smith, A.R., Whiting, R., and Fologea, D., *The Ionic Selectivity of Lysenin Channels in Open and Sub-Conducting States.* Membranes, 2021. **11**(11): p. 897

15. Fologea, D., Krueger, E., Al Faori, R., Lee, R., Mazur, Y.I., Henry, R., Arnold, M., and Salamo, G.J., *Multivalent ions control the transport through lysenin channels.* Biophysical Chemistry, 2010. **152**(1-3): p. 40-45

16. Fologea, D., Krueger, E., Lee, R., Naglak, M., Mazur, Y., Henry, R., and Salamo, G., *Controlled gating of lysenin pores.* Biophysical Chemistry, 2010. **146**(1): p. 25-9 DOI: 10.1016/j.bpc.2009.09.014

17. Fologea, D., Al Faori, R., Krueger, E., Mazur, Y.I., Kern, M., Williams, M., Mortazavi, A., Henry, R., and Salamo, G.J., *Potential analytical applications of lysenin channels for detection of multivalent ions.* Analytical and Bioanalytical Chemistry, 2011. **401**: p. 1871-1879

18. Bryant, S.L., Clark, T., Thomas, C.A., Ware, K.S., Bogard, A., Calzacorta, C., Prather, D., and Fologea, D., *Insights into the Voltage Regulation Mechanism of the Pore-Forming Toxin Lysenin.* Toxins, 2018. **10**(8): p. 334

19. Krueger, E., Al Faouri, R., Fologea, D., Henry, R., Straub, D., and Salamo, G., *A model for the hysteresis observed in gatuing of lysenin channels.* Biophysical Chemistry, 2013. **184**: p. 126-130

20. Fologea, D., Krueger, E., Mazur, Y.I., Stith, C., Okuyama, Y., Henry, R., and Salamo, G.J., *Bi-stability, hysteresis, and memory of voltage-gated lysenin channels.* Biochimica et Biophysica Acta, Biomembranes, 2011. **1808**: p. 2933-2939

21. Krueger, E., Bryant, S., Shrestha, N., Clark, T., Hanna, C., Pink, D., and Fologea, D., *Intramembrane congestion effects on lysenin channel voltage-induced gating.* European Biophysics Journal : EBJ, 2016. **45**(2): p. 187-194 DOI: 10.1007/s00249-015-1104-z

22. Chua, L.O. and Kang, S.M., *Memristive Devices and Systems.* Proceedings of the IEEE, 1976. **64**(2): p. 209-223

23. Strukov, D.B., Snider, G.S., Stewart, D.R., and Williams, R.S., *The missing memristor found.* Nature, 2008. **453**: p. 80-83

24. Andersson, T., *Exploring voltage-dependent ion channels in silico by hysteretic conductance.* Math. Biosci., 2010. **226**: p. 16-27

25. Bennekou, P., Barksmann, T.L., Jensen, L.R., Kristensen, B.I., and Christopersen, P., *Voltage activation and hysteresis of the non-selective voltage-dependent channel in the intact human red cell.* Bioelectrochemistry, 2004. **62**: p. 181-185

26. Kaestner, L., Christophersen, P., Bernhardt, I., and Bennekou, P., *The non-selective voltage-activated cation channel in the human red blood cell membrane: reconciliation between two conflicting reports and further characterization.* Bioelectrochemistry, 2000. **52**: p. 117-125

27. Mannikko, R., Pandey, S., Larsson, H.P., and Elinder, F., *Hysteresis in the Voltage Dependence of HCN Channels: Conversion between Two Modes Affects Pacemaker Properties.* Journal of General Physiology, 2005. **125**: p. 305-326

28. Nowak-Gudowska, E., Flyvbjerg, H., Bennekou, P., and Christopersen, P., *Hysteresis in Channel Gating*, in *Unsolved Problems of Noise and Fluctuations: UPoN 2002: Third International Conference, CP665*, S.M. Bezrukov, Editor. 2002, AIP: Washington DC. p. 305-311.

29. Bryant, S.L., Eixenberger, J.E., Rossland, S., Apsley, H., Hoffmann, C., Shrestha, N., McHugh, M., Punnoose, A., and Fologea, D., *ZnO nanoparticles modulate the ionic transport and voltage regulation of lysenin nanochannels.* Journal of Nanobiotechnology, 2017. **15**(1): p. 90 DOI: 10.1186/s12951-017-0327-9

30. Pustovoit, M.A., Berezhkovskii, A.M., and Bezrukov, S.M., *Analytical theory of hysteresis in ion channels: Two state model.* J. Chem. Phys., 2006. **125**: p. 194907(8)

31. Bryant, S., Shrestha, N., Carnig, P., Kosydar, S., Belzeski, P., Hanna, C., and Fologea, D., *Purinergic control of lysenin's transport and voltage-gating properties.* Purinergic Signalling, 2016: p. 1-11 DOI: 10.1007/s11302-016-9520-9

CHAPTER FIVE: CONCLUSIVE REMARKS AND PERSPECTIVE

Although more than twenty years have passed since the first reports on lysenin's discovery and early investigations on biological activities, its unique features are far from being well-understood. There is no doubt that extended investigations are needed to unveil new biophysical traits, decipher their physiological implications, and enable applications that exploit such unique characteristics.

Lysenin is considered a pore-forming toxin (PFT), and this classification is justified by strong similarities with bacterial and other exotoxins. Lysenin is not a membrane protein in its native environment; it is secreted as a monomer in water-soluble form, and the interaction with target membranes leads to binding, oligomerization, and pore formation, which is typical for PFTs. Lysenin's binding specificity for membranes containing sphingomyelin, and such specificity for non-protein membrane components is also a feature presented by many cytolysins. The oligomeric pore is a beta-barrel spanning the membrane, and the large conducting pathway dissipates the electrochemical gradients, leading to cell death. The large diameter of the pore may accommodate large molecules such as DNA and peptides, and their translocation was exploited with resistive-pulse techniques for single-molecule identification, characterization, and potentially fast sequencing.

The toxin-like behavior of lysenin is completed by numerous additional features commonly shared by ion channels. From the first electrophysiology experiments, lysenin showed a strong regulation by voltage, manifested as a significant decrease of the

macroscopic conductance at positive bias voltages. Interestingly, the voltage-regulation

was abolished when neutral lipids (as opposed to anionic lipids) were used to produce the

support membrane. The voltage regulation feature was thoroughly investigated, and it

was concluded that it originates in voltage-induced gating, which is a salient feature of

voltage-gated ion channels. Another important feature, also characteristic to ion channels,

is the ligand-induced gating. Lysenin channels interact reversibly with numerous

multivalent ions and adjust their conformation and conducting states. This ligand-induced

gating is very distinct from what is typically observed for ion channels because it shows

strong dependency on charge density: a high charge density leads to a complete closing

of the channel, while a lower charge density forces the channels to adopt a stable sub-

conducting state.

Another unusual feature of lysenin channels regarding voltage-induced gating is

the strong hysteresis in conductance, which was observed during excitation with

oscillatory voltage stimuli. Although a few ion channels show such behavior, the time

scale at which lysenin presents history-dependent conductance is much larger, by many

orders, than any ion channel, therefore presenting strong memory capabilities.

The work done in preparation of this thesis added novel investigations on

lysenin's transport properties, unveiling features that not only provide insight into

biological activities but also opportunities for developing specific applications for which

common PFTs or ion channels would be difficult to be used. In our work we performed

electrophysiology experiments in asymmetrical ionic conditions and concluded that

lysenin channels present selectivity, which is another salient feature of ion channels.

Although the permeability ratios measured for various anions and cations are much

smaller than the ones reported for ion channels, our experiments indicate that large, physiologically relevant transmembrane voltages may be attained by introducing concentration gradients of ionic species. However, another important feature with respect to selectivity was deciphered in our work. We exploited the unique feature of lysenin channels to attain a stable sub-conducting state in the presence of divalent metal cations and observed a suppression of selectivity. This is important not only for understanding how a channel may adjust its selectivity and consequently its biological functionality but also providing opportunities to control the transmembrane voltages in natural and artificial systems by modulating the concentrations of multivalent ions by physical or chemical stimuli.

Another intriguing property regarding voltage-induced gating and hysteresis was discovered through our work with lysenin. A prior report indicated that Cu^{2+} ions interact with lysenin channels and forced them to adopt a fully-closed state, similar to the ligand-induced gating elicited by trivalent metals. However, the fully closed state is achieved by lysenin channels undergoing an intermediate sub-conducting step, which is not stable. Prompted by this unique behavior, we extended prior investigations on the effects of multivalent cations on hysteresis by employing Cu^{2+} ions as ligands. The results of our experiments surpassed all anticipation. Very small amounts of Cu^{2+} added to the support electrolyte modulated the hysteretic conductance to such an extent that lysenin channels were arrested in the voltage-induced closed state even when the bias potential returned to zero. This is clearly indicative of strong memory capabilities, which manifest at very large time scales: although technical capabilities limited our measurements to tens of minutes, the asymptotic approach of a steady state leads to the hypothesis that the

memory lasts for much longer times. The original state of the channels (open) may be achieved by a simple reset consisting of a short application of a negative membrane voltage. This history-dependency, bi-stability, and hysteretic behavior strongly suggest that lysenin is a biological memristor operating at low voltages and preserving status information upon eliminating the transmembrane voltage. In the same line of research, we also identified that lysenin channels reconstituted in neutral lipid membranes fully recover their voltage-gating feature and hysteretic behavior.

The new features of lysenin channels uncovered in this work provide opportunities for applications otherwise not possible to develop by employing ion channels or other PFTs. The selective nature and its modulation by multivalent ions may be exploited for developing drug delivery systems consisting of lysenin channels reconstituted in spherical lipid membranes and exquisitely controlled by physical or chemical stimuli. Lysenin provides unique opportunities for bioelectronics and integration with electrically controlled artificial systems. The rectification and negative conductance region may be exploited for development of self-sustained biological oscillators, while the bi-stability and memristive properties are anticipated to lead to the development of logical circuits and solid state – bio interfaces.

APPENDIX A

Experimental Details

A typical experimental setup for investigations of lysenin channels' sensing capabilities and identification of potential mechanisms of interactions leading to adjustments of the ionic currents is depicted in Figure A1.
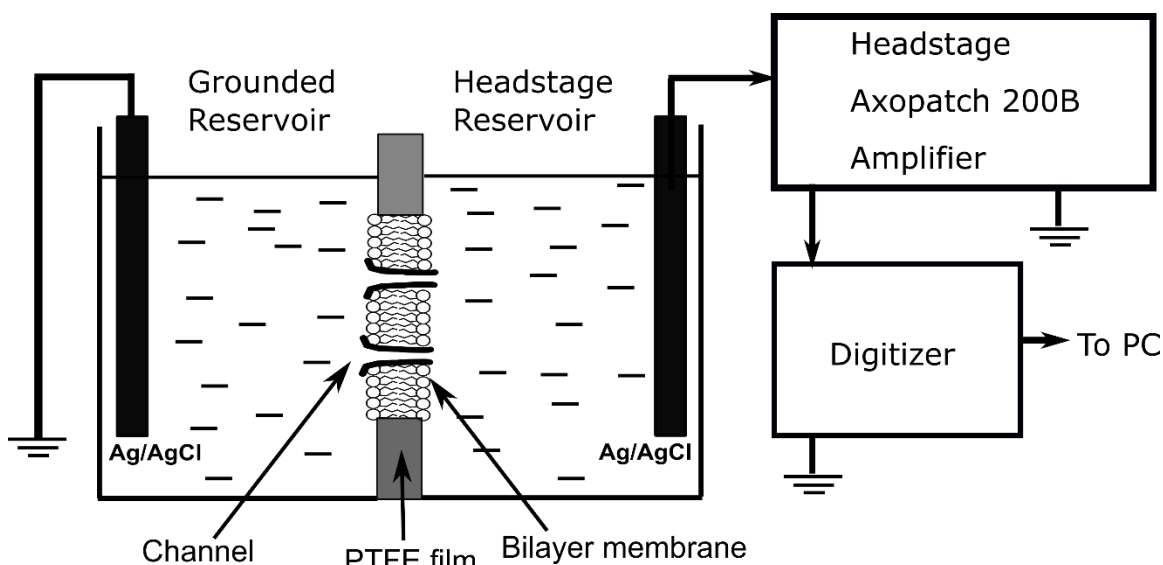

Figure A1.   A typical experimental setup for lysenin channel reconstitution into bilayer lipid membranes and electrical measurements of changes in ionic currents induced by interactions with analytes.

The setup consists of two PTFE reservoirs (each of ~ 1mL volume) separated by a thin PTFE film (120 μm thickness) in which a small central hole (~70 μm diameter) is produced by an electric spark. Each reservoir is filled with an electrolyte solution, and two Ag/AgCl electrodes ensure electrical connections with the electrophysiology amplifier. Reports in the literature for similar setups are not necessarily consistent with defining each reservoir (i.e., cis, or trans), therefore the electrical connections may be used for unequivocal identification (i.e., headstage-connected and ground-connected reservoir, respectively). The bilayer is produced by the painting method, and its formation and integrity are monitored by real time capacitance and conductance

measurements. Once a stable bilayer lipid membrane is achieved, channel reconstitution is performed by addition of small amounts of lysenin monomer to the grounded reservoir while applying a negative voltage to the headstage-connected reservoir (to prevent voltage induced gating). The concentration of lysenin in the reservoir varies from sub-pM to nM, and depends on the monomer source, purity, and targeted number of inserted channels. Macroscopic conductance measurements imply using a large number of channels, while investigations on regulatory mechanisms and molecule translocations require using single channels. When single channels are needed, complete exchange with monomer-free electrolyte solution in the grounded reservoir right after the first insertions may prevent reconstitution of an excessive number of channels into the membrane.

The macroscopic conductance of large populations of inserted lysenin channels before and after analyte additions is estimated from the slope of the linear IV plots recorded in response to voltage ramps within the negative voltage range; the plots may be recorded by using a low sampling rate (i.e., one sample/s) and cut-off frequency of the hardware low-pass filter. Analysis of regulatory mechanisms on single channels and macromolecule translocation experiments require using a high sampling rate (up to 2.5×10^5 samples/s) and cut-off frequency to observe fast changes in ionic currents through individual channels and prevent signal alteration by excessive filtration.
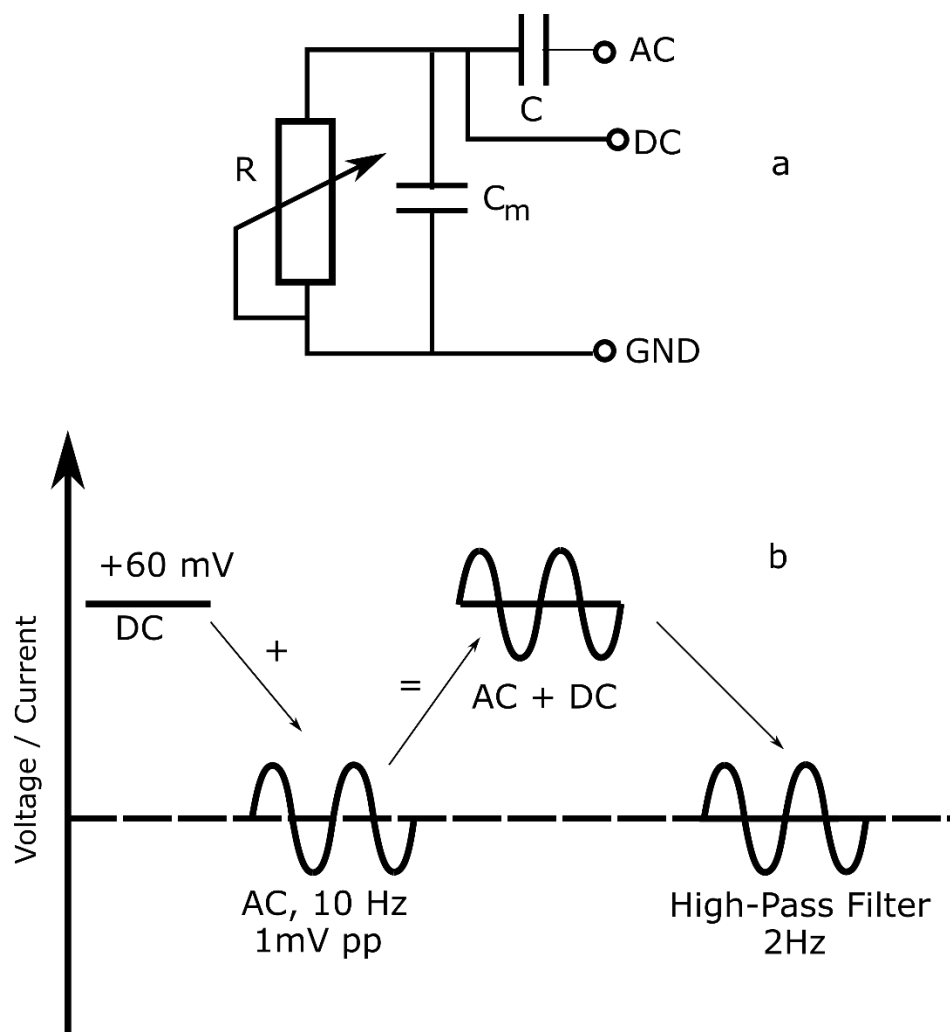
APPENDIX B

Scheme 1

Figure B1. **Diagram of the experimental setup utilized for simultaneous AC/DC application and measurements. a) Simultaneous application of DC and AC (through capacitive coupling) to a membrane characterized by variable resistance R and membrane capacitance C_m. b) The shape of the electrical signals (either voltage or currents) applied or measured through the system. The high-pass filtering of the recorded current suppresses the DC component of the electric signal but maintains the AC contribution.**